

Editor-in-Chief B.E.Paton

Editorial board:

Yu.S.Borisov	V.F.Khorunov
A.Ya.Ishchenko	I.V.Krivtsun
B.V.Khitrovskaya	L.M.Lobanov
V.I.Kyrian	A.A.Mazur
S.I.Kuchuk	Yatsenko
Yu.N.Lankin	I.K.Pokhodnya
V.N.Lipodaev	V.D.Poznyakov
V.I.Makhenko	K.A.Yushchenko
O.K.Nazarenko	A.T.Zelnichenko
I.A.Ryabtsev	

International editorial council:

N.P.Alyoshin	(Russia)
U.Diltey	(Germany)
Guan Qiao	(China)
D. von Hofe	(Germany)
V.I.Lysak	(Russia)
N.I.Nikiforov	(Russia)
B.E.Paton	(Ukraine)
Ya.Pilarczyk	(Poland)
G.A.Turichin	(Russia)
Zhang Yanmin	(China)
A.S.Zubchenko	(Russia)

Promotion group:

V.N.Lipodaev, V.I.Lokteva
A.T.Zelnichenko (exec. director)

Translators:

A.A.Fomin, O.S.Kurochko,
I.N.Kutianova, T.K.Vasilenko

Editor:

N.A.Dmitrieva
Electron gallery:
D.I.Sereda, T.Yu.Snegiryova

Address:

E.O. Paton Electric Welding Institute,
International Association «Welding»,
11, Bozhenko str., 03680, Kyiv, Ukraine
Tel.: (38044) 200 82 77
Fax: (38044) 200 81 45
E-mail: journal@paton.kiev.ua
http://www.nas.gov.ua/pwj
URL: www.rucont.ru

State Registration Certificate
KV 4790 of 09.01.2001

Subscriptions:

\$324, 12 issues per year,
postage and packaging included.
Back issues available.

All rights reserved.
This publication and each of the articles
contained herein are protected by copyright.
Permission to reproduce material contained in
this journal must be obtained in writing from
the Publisher.
Copies of individual articles may be obtained
from the Publisher.

CONTENTS

SCIENTIFIC AND TECHNICAL

- Kharlamov M.Yu., Krivtsun I.V., Korzhik V.N. and Petrov S.V.* Formation of liquid metal film at the tip of wire-anode in plasma-arc spraying 2
- Rymar S.V., Zhernosekov A.M. and Sidorets V.N.* Effect of single-phase power sources of welding arc on electric mains 7
- Shlepakov V.N. and Kotelchuk A.S.* Investigation of thermochemical characteristics of mixtures of dispersed materials by differential thermal analysis methods 13
- Rimsky S.T.* Control of properties of the weld metal by regulating the level of oxidation of the weld pool in gas-shielded welding 16
- Moravetsky S.I.* Hygroscopicity of high-basicity synthetic flux 20

INDUSTRIAL

- Paton B.E., Lobanov L.M. and Volkov V.S.* Transformable structures (Review) 25
- Bogdanovsky V.A., Gawva V.M., Makhlin N.M., Cherednik A.D., Tkachenko A.V., Kudryashev V.B., Kulikov A.P. and Kovalyuk A.V.* Application of automatic orbital welding to fabricate absorbing inserts for spent nuclear fuel storage containers 34
- Yushchenko K.A., Borisov Yu.S., Vojnarovich S.G., Kisliitsa A.N. and Kuzmich-Yanchuk E.K.* Two-layer bio-cermet titanium-hydroxyapatite coating 38
- Makovetskaya O.K.* Organization and topics of R&D in the field of joining technologies conducted by TWI and DVS Association of Researchers (Review) 41
- Index of articles for TPWJ'2011, Nos. 1-12 45
- List of authors 49



FORMATION OF LIQUID METAL FILM AT THE TIP OF WIRE-ANODE IN PLASMA-ARC SPRAYING

M.Yu. KHARLAMOV¹, I.V. KRIVTSUN², V.N. KORZHIK² and S.V. PETROV²

¹V. Dal East-Ukrainian National University, Lugansk, Ukraine

²E.O. Paton Electric Welding Institute, NASU, Kiev, Ukraine

A mathematical model is proposed, describing formation of a molten metal film at the tip of sprayed anode-wire under the conditions of plasma-arc spraying of coatings. Numerical analysis of the influence of spraying mode parameters on the position of molten wire tip relative to plasma jet axis, thickness of liquid interlayer contained on the wire tip, temperature and velocity of metal flow in it was performed.

Keywords: *plasma-arc spraying, coatings, wire-anode, spraying modes, thermal condition, molten metal film, mathematical model*

Stability of the process of plasma-arc wire spraying, as well as formation of specified quality characteristics of coatings, are largely determined by the conditions, under which the concentrated flow of spraying material particles is formed. Parameters of the formed dispersed particles depend chiefly on the intensity of the processes of thermal and gas-dynamic interaction of melting wire-anode with arc plasma flow moving around it. Therefore, detailed study of the above processes, including development of the appropriate mathematical models, is highly important for further progress of plasma-arc spraying technology.

Spraying of wire consumables is not given enough attention in scientific-technical publications, the available work being devoted, mainly to the process of electric-arc metallizing [1–3]. Results obtained in the above studies are not applicable to the process of plasma-arc spraying, as it differs by the location of sprayed wire relative to the arc (the latter form an angle of 70–90°), as well as high values of temperature (up to 30,000 K) and velocity (up to 4000 m/s) of plasma, flowing around the wire [4].

For the conditions of plasma-arc spraying a model was earlier proposed for thermal processes in solid metal wire-anode, fed into the plasma arc behind the plasmatron nozzle tip [5]. This model allows forecasting the temperature field and calculating the molten metal volume depending on the parameters of plasmatron operation mode, wire feed rate and diameter, as well as its position in space relative to the tip of plasma-shaping nozzle and distance from molten wire tip to plasma jet axis. However, the melt zone thickness obtained within this model can differ considerably from that observed in the experiments. The reason for that is the molten metal at the wire tip being under a considerable dynamic impact of the plasma flow that results in just part of the melt being contained at the wire tip, forming a liquid interlayer, and part being carried off into a thin jet — so-called tongue [1].

Here, the molten wire tip takes up such a position relative to plasma jet axis that corresponds to the thickness of liquid interlayer, ensuring a balance of thermal and dynamic impact of plasma on the molten metal. In other words, for a correct determination of the parameters of liquid metal interlayer contained on the sprayed wire tip, as well as distance from the molten wire tip to the plasma jet axis, it is necessary to coordinate the calculations within the thermal model [5] with calculations of gas-dynamic impact of the transverse plasma flow on the molten metal. Development of such a self-consistent model is exactly the objective of this study.

When plotting a mathematical model of formation of molten metal film at the tip of sprayed wire-anode under the conditions of plasma-arc spraying, let us assume that solid metal wire of round cross-section of radius R_w is fed into the plasma arc at constant rate v_w normal to the axis of symmetry of the plasma flow (Figure 1). The arc closes on the wire right end which is the anode. Let us also assume that the melting front is flat (plane $z_b = 0$) and is located normal to the plasma flow axis at distance L_p from it, and the rate of wire melting is equal to its feed rate. Under the impact of the arc anode spot and high-temperature plasma flow moving around the arc, it is heated, and molten metal volume of thickness L_{liq} forms at its tip, that is carried off into a thin jet by plasma flow moving around the arc. Let us assume that the upper part of liquid interlayer contained at the wire tip takes the form of a spherical segment under the impact of the arriving plasma flow, the spherical segment having height L_b and radius R_b of a sphere forming the segment with the center in a point located at distance L_0 from the melting front ($R_b = L_0 + L_b$; $R_b^2 = L_0^2 + R_w^2$) (see Figure 1).

As a result of removal of part of the melt from the wire tip, the conditions of heat balance in it are violated. Tending to an equilibrium condition, the wire will take up such a position relative to plasma jet axis, defined, for instance, by distance $L_p - L_b$, at which the volume of liquid interlayer contained at the



wire tip V_b will correspond to the volume of wire molten metal $V_{liq} = \pi R_w^2 L_{liq}$, i.e. condition $V_b = V_{liq}$ will be fulfilled. A problem is posed to determine wire position, at which the above condition is satisfied at specified parameters of the spraying mode, and the volume of liquid interlayer contained at the wire tip, temperature, as well as molten metal flow, are calculated.

Let us move over to construction of the model of liquid interlayer formation at the wire tip. Thickness L_{liq} and volume V_{liq} of molten metal layer, respectively, depending on the distance from molten wire tip to plasma jet axis $L_p - L_{liq}$ at other assigned spraying mode parameters being equal can be determined from the model of wire thermal condition [5].

To assess the thickness of liquid interlayer contained on the wire tip, let us consider the interaction of two flows – viscous outflow of incompressible liquid (molten metal) along the boundary of wire melting and turbulent flow of arc plasma along the surface of liquid metal boundary with the medium interphase at $z_0 = L_b$ (see Figure 1). Let us assume that the main force, acting on the melt from the side of the plasma flow, is the viscous force. Considering that the melt flow occurs in the following plasma flow, viscous forces on the medium interphase prevail, so that such an approximation can be regarded as quite justified.

A boundary layer [6] forms in the plasma flow in the immediate vicinity of the liquid metal boundary, which is characterized by an abrupt change of the main parameters of the flow in the transverse direction. In particular, plasma velocity changes from its value in the outer flow to the value of the velocity of flowing of liquid wire material on the medium interphase (satisfying the «sticking» condition is assumed).

In view of the turbulent nature of plasma flow [4], several subregions can be singled out in the considered boundary layer [7]. The outer layer is a region of fully developed turbulent flow, its properties being dependent on the flow prehistory. The inner region of the turbulent boundary layer in the general case consists of a viscous underlayer, transition region and region of logarithmic profile of velocity. Universal nature of velocity distribution corresponds to flowing in the inner region, that is the basis for plotting special near-wall functions, connecting the flow parameters with the distance from medium interphase [6, 7].

Considering the smallness of liquid interlayer thickness, flowing of liquid metal in it can be considered to be practically laminar, and a linear dependence of tangential component of velocity can be assumed here [6, 7]:

$$v_{liq}(z_b) = \frac{z_b}{L_b} v_m, \quad (1)$$

where v_m is the melt flow velocity on the medium interphase (at $z_b = L_b$). Value v_m can be connected

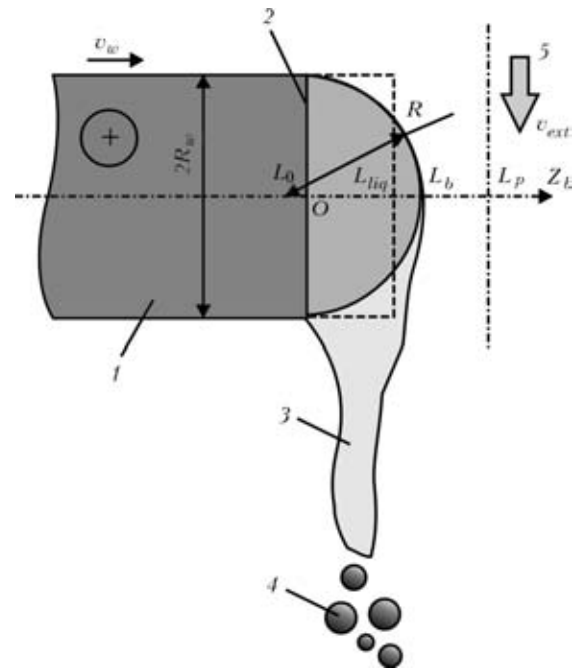


Figure 1. Schematic of liquid interlayer formation at the tip of current-carrying wire in plasma-arc spraying: 1 – current-carrying wire; 2 – fusion boundary; 3 – molten metal jet («tongue»); 4 – sprayed particles; 5 – plasma flow

with parameters of plasma flow moving around the arc, proceeding from the assumption that tangential stresses in the plasma and melt on the medium interphase are equal:

$$\eta_{liq} \frac{\partial v_{liq}}{\partial z_b} \Big|_{L_b} = \eta_p \frac{\partial v_p}{\partial z_b} \Big|_{L_b}, \quad (2)$$

where η_p, η_{liq} are the coefficients of dynamic viscosity of plasma and molten metal of the wire, respectively; $v_p(z_p)$ is the distribution of tangential (relative to melt surface) plasma velocity along axis z_b . To find $v_p(z_p)$ we will apply the logarithmic near-wall function, which is often used at description of flow parameters in near-wall regions [7, 8]. For the flowing around conditions considered by us, this function can be written as follows:

$$v^+ = \frac{1}{\text{Kar}} \ln(Ey^+). \quad (3)$$

Here $v^+ = \bar{v}_p/v^*$ is the dimensionless tangential velocity of plasma; $\bar{v}_p(z_b) = v_p(z_b) - v_m$ is the velocity of plasma flow relative to the melt flow velocity; v^* is the dynamic velocity determined as

$$v^* = \sqrt{\tau_p/\rho_p}, \quad (4)$$

where $\tau_p = \left(\eta_p \frac{\partial u}{\partial r} \right)_{L_b}$ is the friction stress in the plasma

on the flowing surface; ρ_p is the plasma density; $\text{Kar} \approx 0.41$ is Karman constant; E is the constant determining the degree of wall roughness (for smooth wall $E = 8.8$ [7]); y^+ is the dimensionless distance from the interface, determined as $y^+ = \frac{\rho_p(z_b - L_b)}{\eta_p} v^*$.



We will assume that the transition from the melt flowing velocity («sticking» condition) to the velocity of undisturbed plasma flow, which can be determined, for instance, by model [4], occurs in region $0 \leq y^+ < 400$ [8]. Then, based on expression (3) tangential stress in the plasma can be presented as follows:

$$\tau_p(v_m) = \frac{\bar{v}_{ext}^2(v_m)}{\left(\frac{1}{\text{Kar}} \ln(Ey^+)\right)^2} \rho_p = \frac{\bar{v}_{ext}^2(v_m)\rho_p}{396.71}, \quad (5)$$

where $\bar{v}_{ext}(v_m) = v_{ext} - v_m$ is the flowing velocity of undisturbed plasma flow near the wire tip v_{ext} relative to the melt flowing velocity v_m .

As a result, in order to determine the thickness of liquid interlayer L_b , it is necessary to consider the balance of the weight of molten wire material. Considering the made assumption that the molten metal in the upper part of the wire tip takes the shape of a segment of a sphere, consumption of liquid wire material passing through axis z_b normal to the axis of the plasma jet can be determined as

$$G_2 = 2\rho_w \int_0^{L_b} v_{liq}(z_b) \int_0^{y(z_b)} dy dz_b, \quad (6)$$

where $y(z_b) = \sqrt{R_w^2 - 2((R_w^2 - L_b^2)/(2L_b))z_b - z_b^2}$ is the curve of crossing of the segment of a sphere with the above plane; ρ_w is the density of the metal wire. In its turn, proceeding from the conditions of the constancy of the velocities of wire feed and melting, quantity of wire material, melting in a unit of time, and, therefore, crossing section $z_b = 0$, is given by the expression

$$G_1 = \rho_w v_w S_w, \quad (7)$$

where $S_w = \pi R_w^2$ is the wire cross-sectional area.

Then considering that half of the molten wire material comes to the considered half of the segment of a sphere, we will come to the following relationship:

$$G_1/2 = G_2. \quad (8)$$

Substituting expressions (6) and (7) into (8), and considering assumption (1), we obtain the dependence of maximum melt flowing velocity on its interlayer thickness at the wire tip:

$$v_m(L_b) = \frac{S_w}{4} \frac{v_w L_b}{L_b \int_0^{z_b} \int_0^{y(z_b)} dy dz_b}. \quad (9)$$

Now condition (8) can be rewritten as follows:

$$\frac{v_w S_w}{2} = 2 \frac{\tau_p(v_m(L_b))}{\eta_{liq}} \int_0^{L_b} \int_0^{y(z_b)} dy dz_b, \quad (10)$$

whence thickness L_b of liquid interlayer on the wire tip can now be determined. Equation (10) closed by relationships (5) and (9) can be solved by one of the numerical methods of solution of nonlinear equations [9]. This can be done using the simplest method of dichotomy or, considering that the antiderivative of the integrand in (5) and (9) is expressed analytically, Newton iteration method can be applied.

Using the model of thermal processes in the wire [5] for determination of the volume of its molten part V_{liq} , as well as expression (10), on the basis of which the volume of liquid interlayer contained at the wire tip is found:

$$V_b = \pi \int_0^{L_b} [y(z_b)]^2 dz_b, \quad (11)$$

it is possible to determine what position of the molten wire tip relative to plasma jet axis is set at the specified spraying mode. For this purpose, fixing the mode parameters and varying just value L_b , based on model [5] we obtain dependence $V_{liq} = V_{liq}(L_p - L_{liq})$, and based on expressions (10), (11) — dependence $V_b = V_b(L_b)$, and find such a position of the wire at which their equality is achieved. This condition, essentially, is the connecting link between the models of thermal [5] and gas-dynamic interaction of wire with plasma flow moving laterally around it, and it allows determination of the distance, to which the molten wire tip is removed from the plasma flow axis, depending on the values of spraying mode parameters. In its turn, this value is the basis, which can be used to determine using expressions (1), (9), (11) and model [5], the characteristics of the liquid metal contained at the wire tip, including its flowing velocity and temperature. The above characteristics will have a direct influence on the dimensions and temperature of drops separating from the wire tip, and will determine the point of their entering the plasma flow.

Let us conduct numerical analysis of the influence of spraying mode parameters on the characteristics of liquid interlayer, contained at the tip of sprayed wire-anode, as well as spatial position of the latter. Calculations were performed for the conditions of plasma-arc spraying of steel wire, the thermo-physical characteristics of which are taken from [10]. The following parameters of the spraying mode were selected [4]: arc current $I = 160-240$ A, plasma gas (argon) flow rate $G_{Ar} = 1.0-1.5$ m³/h, wire feed rate 6–15 m/min, wire diameter 1.2–1.6 mm. It was assumed that the anode-wire is located at 6.3 mm distance from the plasmatron nozzle tip, normal to the axis of the plasma flow. Distributions of velocity and temperature of undisturbed plasma flow along the wire-anode for various modes of plasmatron operation were calculated in advance based on model [4] and are given in Figure 2.

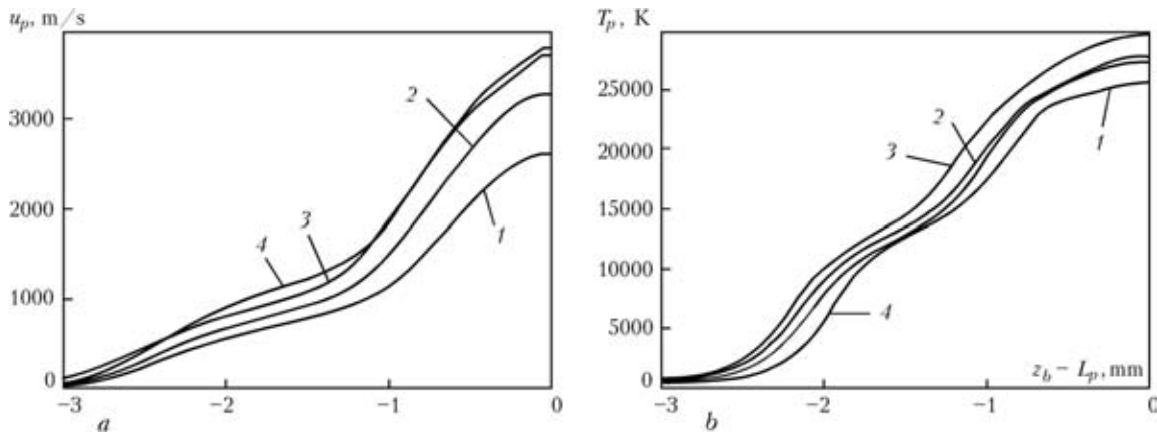


Figure 2. Distribution of axial component of velocity (a) and temperature (b) of arc plasma along anode-wire: 1 – $I = 160$; 2 – 200; 3 – 240 A at $G_{Ar} = 1.0 \text{ m}^3/\text{h}$; 4 – $G_{Ar} = 1.5 \text{ m}^3/\text{h}$ at $I = 200$ A

As is seen from Figure 2, values of plasma velocity and temperature change quite abruptly in the transverse direction relative to plasma jet axis. Therefore, the conditions of viscous and thermal interaction of the plasma flow with wire essentially depend on the position of the molten wire tip relative to the plasma flow axis. The closer to the jet axis, the larger is the thermal flow into the wire, and the more increased are the viscous forces acting on the melt surface, carrying the liquid metal off the wire tip. Therefore, it should be noted that in spraying modes, at which heat propagation in the wire is difficult, its molten tip is located closer to the plasma jet axis. For instance, at increase of the feed rate the region of wire heating and melting become smaller, and the wire comes to the plasma jet axis until the molten metal volume can be contained at its tip. The same situation should be observed also when larger diameter wire is used.

Influence of plasmatron operation mode on the position of the molten wire tip relative to plasma jet axis, as well as thickness of the liquid interlayer contained at the wire tip, can be illustrated in Figure 3. For all the considered modes, the molten wire tip is located at distance 0.1–1.4 mm from the jet axis at interlayer thickness of 0.10–0.15 mm. Increase of arc current leads to increase of plasma velocity and temperature (see Figure 2), convective-conductive and radiation-thermal flows into the wire increasing, as well as the intensity of viscous force acting on liquid metal at the wire tip. As a result, the increased melt volume cannot be contained at the wire tip, and part of it is carried off by the plasma flow, and the wire tip will take a new equilibrium position, farther from the plasma flow axis. At increase of the plasma gas flow rate, the flow velocity rises, temperature profile, however, being more compressed towards the jet axis (see Figure 2, curves 2 and 4). Here, wire melting occurs at wire tip location in near-axis regions of the plasma jet, and increase of the intensity of dynamic interaction of the plasma flow will lead to reduction of the volume of liquid interlayer, contained at the wire tip, and, therefore, also its thickness (see Figure 3).

Molten material of the wire is entrained by the plasma flow, forming a liquid metal jet, which at further flowing separates into individual drops – dispersed particles of the spraying material – under the impact of external and inner disturbing factors. Here, transverse dimensions of the liquid interlayer and melt flowing velocity determine the characteristics of the above jet flowing, and, therefore, also the conditions of drop formation. In its turn, the melt flowing velocity is connected to the quantity of wire material molten in a unit of time, as well as the set thickness

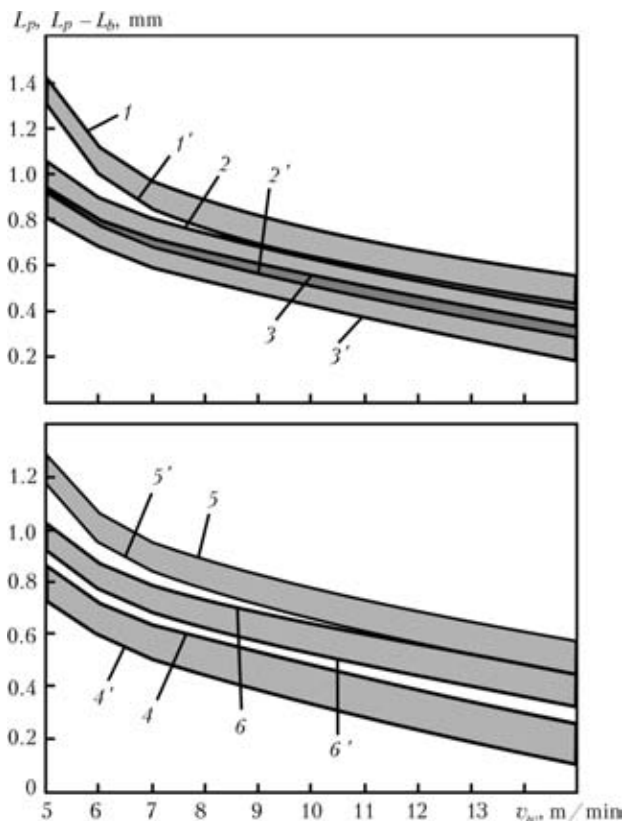


Figure 3. Influence of wire feed rate on distance from wire melting plane L_p (1–6) and distance from molten wire tip $L_p - L_b$ (1'–6') to plasma jet axis at different parameters of the spraying mode: $2R_w = 1.2$ (1; 1'), 1.4 (2; 2'), 1.6 (3; 3') mm at $I = 200$ A, $G_{Ar} = 1.0 \text{ m}^3/\text{h}$; $I = 160$ (4; 4'), 240 (5; 5') A at $2R_w = 1.4$ mm, $G_{Ar} = 1.0 \text{ m}^3/\text{h}$; $G_{Ar} = 1.5 \text{ m}^3/\text{h}$ (6; 6') at $2R_w = 1.4$ mm, $I = 200$ A



Parameters of liquid interlayer contained at the tip of sprayed wire-anode at plasma-arc spraying of coatings

I, A	$G_{Ar}, m^3/h$	$2R_w, mm$	$v_w, m/min$	$L_p - L_b, mm$	L_b, mm	$v_m, m/s$	T, K
200	1.0	1.4	5	1.054	0.113	1.81	2070
			6	0.893	0.117	2.05	1931
			7	0.798	0.127	2.42	1774
			9	0.686	0.129	2.64	1773
			12	0.550	0.133	3.07	1774
		15	0.428	0.141	3.61	1774	
		1.2	9	0.811	0.125	2.10	1775
		1.6	9	0.604	0.131	2.68	1774
160	1.0	1.4	9	0.526	0.140	2.18	1776
240	1.0	1.4	9	0.829	0.118	2.61	1773
200	1.5	1.4	9	0.684	0.109	2.83	1774

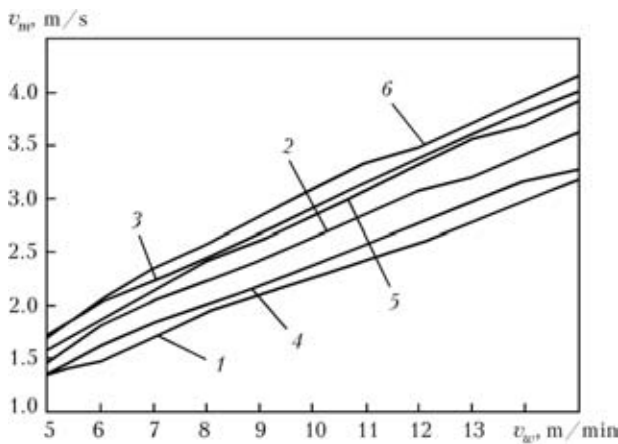


Figure 4. Dependence of melt flow rate in liquid interlayer at the wire tip on its feed rate at different diameters of wire-anode and plasmatron operation modes: $2R_w = 1.2$ (1), 1.4 (2), 1.6 (3) mm at $I = 200 A, G_{Ar} = 1.0 m^3/h$; $I = 160$ (4), 240 (5) A at $2R_w = 1.4 mm, G_{Ar} = 1.0 m^3/h$; $G_{Ar} = 1.5 m^3/h$ (6) at $2R_w = 1.4 mm, I = 200 A$

of the liquid interlayer, that is illustrated, for instance, by dependencies in Figure 4.

Liquid interlayer parameters at plasma-arc spraying are given in the Table. As is seen, for most of the modes, overheating of liquid metal above the melting temperature does not exceed 20 K, as the molten material does not have enough time for any significant overheating and is immediately carried off by the flow from the wire tip. Metal overheating in the liquid interlayer by 200–250 K above the melting point is, as a rule, characteristic for melting modes with low wire feed rates, at which the heat conductivity mechanism has a significant role in heat propagation in the wire.

CONCLUSIONS

1. Mathematical model of thermal condition of wire-anode at plasma-arc spraying of coatings was improved by allowing for gas-dynamic impact on the wire of plasma flow moving around it. Such a self-consistent model allows determination of wire position relative

to plasmatron axis, as well as characteristics of liquid interlayer contained at the wire tip, including its thickness and melt flowing velocity, depending on the spraying mode parameters.

2. Distance, to which the molten wire tip is removed from the plasma flow axis, is determined by the condition of equality of the wire molten part to the volume of liquid metal interlayer that can be contained at the wire tip at plasma flow moving laterally around it, and is equal to 0.1–1.4 mm under the considered conditions at interlayer thickness of 0.10–0.15 mm, depending on the spraying mode parameters.

3. At plasma-arc spraying of coatings metal temperature at the molten wire tip reaches 1780–2100 K, here for most of the spraying modes liquid metal overheating above melting temperature (1773 K) is insignificant, and is not higher than 20 K, as the forming melt is carried by the plasma flow out of the interaction zone, and the total heat content of the wire is not decreased.

1. Korobov, Yu.S. (2004) Estimation of forces affecting the spray metal in electric arc metallizing. *The Paton Welding J.*, **7**, 21–25.
2. Korobov, Yu.S., Boronenkov, V.N. (2003) Kinetics of interaction of sprayed metal with oxygen in electric arc metallizing. *Svarochm. Proizvodstvo*, **7**, 30–36.
3. Vakhalin, V.A., Maslenkov, S.B., Kudinov, V.V. et al. (1981) Process of melting and spraying of electrode material in electric arc metallizing. *Fizika i Khimiya Obrab. Materialov*, **3**, 58–63.
4. Kharlamov, M.Yu., Krivtsun, I.V., Korzhik, V.N. et al. (2007) Mathematical model of arc plasma generated by plasmatron with anode wire. *The Paton Welding J.*, **12**, 9–14.
5. Kharlamov, M.Yu., Krivtsun, I.V., Korzhik, V.N. et al. (2011) Heating and melting of anode wire in plasma arc spraying. *Ibid.*, **5**, 2–7.
6. Lojtsyansky, L.G. (1973) *Mechanics of fluid and gas*. Moscow: Nauka.
7. Volkov, K.N. (2006) Boundary conditions on the wall and mesh dependence of the solution in turbulent flow calculation on unstructured meshes. *Vychislit. Metody i Programirovanie*, **7**(1), 211–223.
8. Wilcox, D.C. (1994) *Turbulence modeling for CFD*. La Canada: DCW Industries.
9. Kalitkin, N.N. (1978) *Numerical methods: Manual*. Moscow: Nauka.
10. Hu, J., Tsai, H.L. (2007) Heat and mass transfer in gas metal arc welding. Pt 2: The metal. *Int. J. Heat and Mass Transfer*, **50**, 808–820.



EFFECT OF SINGLE-PHASE POWER SOURCES OF WELDING ARC ON ELECTRIC MAINS

S.V. RYMAR, A.M. ZHERNOSEKOV and V.N. SIDORETS
E.O. Paton Electric Welding Institute, NASU, Kiev, Ukraine

Harmonic composition of the electric mains in operation of single-phase welding power sources was investigated. It is shown that the welding power sources generate the higher harmonics of current into mains, in particular triplen harmonics, thus deteriorating the quality of electric power. It is recommended to apply the filters of higher harmonics for decreasing the effect of single-phase welding power sources on electric mains.

Keywords: *electric mains, single-phase welding power sources, higher harmonics of current and voltage, coefficient of non-linear distortions of current and voltage*

At the end of the XX century the industrialized countries encountered the problem of growing deterioration of quality of electric power in mains, consisting in distortion of a sinusoidal shape of mains current and voltage, that caused the increase in losses and decrease in safety of electric equipment service. This resulted in growing of amount of equipment with non-linear loads, generating of higher harmonics of current into electric mains.

Single-phase non-linear loads (pulsed power sources, adjustable-frequency electric drives, rectifiers and inverters, systems of automatic control, computer systems of technological process control, TV equipment, office equipment, energy-saving lamps, etc.) lead due to their large quantity to increase in value of coefficient of total non-linear (harmonics) current distortion [1] up to THD_I of 90–140 %, especially due to generation of a zero sequence (the 3rd one and harmonics, multiple by it up to 80 %) [2].

Single-phase non-linear loads deteriorate electromagnetic compatibility that can lead to non-reliable operation and failure of electric and electron equipment [1, 2], burn-out of lighting devices, corrosion of earthing elements, quick ageing of insulation, overheating of rotors and wear of bearings of electric motors. Due to prevailing of the 3rd harmonic and harmonics, multiple by it, in the mains, the reverse rotation of asynchronous electric motors and burning of insulation of neutral wires up to their ignition at current exceeding in a neutral wire above a design level may occur.

Higher harmonics of current increase also the total value of coefficient of total non-linear (harmonic) voltage distortion of mains up to THD_U of 7 % and higher.

The European and national standard documents, determining the parameters of quality of single-phase mains, do not specify the levels of coefficient of non-linear distortions of current, but limiting the absolute

values of current of definite harmonics. In Ukraine the standard is valid only for single-phase mains with current of not more than 16 A per phase [3]. In the North America [4] and EU countries the THD_I levels are standardized for three-phase mains. Therefore, it is possible to predict the appearance of standardized documents, limiting the THD_I levels also in single-phase mains.

The values of coefficient of non-linear distortions of voltage are considered acceptable, which reach 3 % for individual non-linear loads, while the allowable value was defined as 5 % for combined loads of the mains [4]. The national standardized documents [3] allow value of $THD_U = 8$ %, at which the sinusoidal voltage of mains is already greatly distorted.

To reduce the effect of higher harmonics of current is possible by using the filters of higher harmonics of current, which decrease their level in the mains.

Single-phase welding equipment for electric arc supply, being a non-linear load, welding rectifiers and inverters generate also the powerful higher harmonics of current. Therefore, each year the decrease of level of current harmonics in operation of welding equipment becomes more and more actual. It is especially urgent for promotion of national welding technologies and equipment into industrialized countries.

The aim of the present work is to study the effect of operation of typical single-phase welding power sources on electric mains and issue of recommendations for decreasing the higher harmonics of current, generating by them. The article is the continuation of work [5], in which the welding power sources operating at three-phase electric mains were considered.

Such single-phase power sources for welding arc supply were considered, which were connected to AC mains of 50 Hz frequency, representing the single-phase non-linear loads in the welding manufacturing:

- industrial single-phase welding transformer STSh-250 (transformer for welding current of up to 250 A) with a developed transverse magnetic leakage fluxes and a magnetic shunt, containing a device for stabilization of welding arc burning [6–8]. It is serially manufactured by the Pilot Plant of Welding Equipment of the E.O. Paton Electric Welding Insti-



tute and designed for manual arc welding with AC stick electrodes. The presence of device for stabilization of welding arc burning allows also realizing welding with DC electrodes;

- single-phase welding power source VDU-125 with a capacitor voltage multiplier (universal arc rectifier for welding current of up to 125 A). It consists of a welding transformer with developed yoke magnetic leakage fluxes and capacitor voltage multiplier with a bridge diode circuit of rectification [9, 10]. The voltage multiplier provides the improved initial ignition of welding arc, ignition in transition of current through zero and stability of its burning. It was designed and manufactured at the E.O. Paton Electric Welding Institute and also at the Institute of Electrodynamics of the NASU in small batches. The power source has a discrete adjustment of welding current and designed for manual arc welding with AC stick electrodes;

- single-phase welding power source VDU-201 with a capacitor voltage multiplier and thyristor adjustment of welding current (for welding current of up to 200 A). It consists of a welding transformer with yoke magnetic leakage fluxes with a bridge thyristor circuit of rectification, parallel-connected auxiliary diode bridge rectifier and phase-shifting reactor to provide the continuous welding current in operation of thyristors. It was designed at the E.O. Paton Electric Welding Institute and manufactured by the Lithuanian enterprise «Relema» (Vilnius) and designed for manual arc welding with AC and DC stick electrodes;

- industrial single-phase thyristor inverter power source VDI-200, manufactured by the Pilot Plant of Welding Equipment of the E.O. Paton Electric Welding Institute and designed for manual arc welding of low-carbon and alloyed steels with AC and DC stick electrodes.

As a measuring unit, an analyzer of quality of electric mains (single phase) Chauvin Arnoux C.A. 8230 (France) was used, allowing obtaining time dependencies of current and voltage with their typical values (maximum and minimum; full, active and reactive power, etc.), as well as spectra of harmonics up to maximum number of harmonic $h_{\max} = 50$.

Let us consider the operation with mains of welding transformer STSh-250, containing a device for stabilization of welding arc burning.

Figure 1, *a* shows dependencies of relative instantaneous values of current i^* and voltage u^* in mains on time t in operation of welding transformer, obtained in welding of stainless steel 12Kh18N10T with stick electrode OZL-8 of 3 mm diameter at 90 A welding current. Values i^* and u^* refer to their highest amplitude values: $i^* = i/|I_m|$ and $u^* = u/|U_m|$, where $I_m = 80.8$ A, $U_m = -313.2$ V, selected from technical characteristic, where highest «+» and lowest «-» are

the amplitude values of voltage and current for periods I_{m+} , I_{m-} , U_{m+} , U_{m-} , obtained during experiment.

Shape of curves of current and voltage is negligibly differed from sinusoidal one. The superposition of a short-time pulse, corresponding to a stabilizer pulse, and also a small bend of current curve during transition through zero were noted.

Figure 1, *b* shows diagram of harmonic components h of current $I_{h\%}$ and voltage $U_{h\%}$ from effective value of current and voltage of the 1st main harmonic, taken as 100 %: $I_{h\%} = I_{h\%}/I_1 \cdot 100$ %, $U_{h\%} = U_{h\%}/U_1 \cdot 100$ %. Values of numbers of harmonics are limited by number 27 for improving the diagram visualization.

It is seen from diagram that during the welding transformer operation the 3rd harmonic of current, equal to 15.3 % of the 1st one, and the 5th, being 2.3 %, are clearly seen in mains, while the rest uneven harmonics of current do not exceed 1 %. Uneven numbers of harmonics of voltage, reaching more than 1 % of the 1st harmonic, have the following values: the 3rd — 2.5, the 5th — 1.3, the 9th — 1 %. There is also a constant component of current of 10.9 % and even harmonics of current (the 2nd — 2.8, the 4th — 2.4 %). The constant component and even harmonics of voltage are negligibly expressed.

Coefficients of non-linear distortions of current and voltage of transformer STSh-250 [1] are $\text{THD}_I = 15.9$ and $\text{THD}_U = 3.1$ %.

K-factor, determining how much the incremental losses in electric equipment and conductors of electric mains are increased as compared with the fact if only the 1st main harmonic of current was passing in equipment and mains, is equal to 1.38.

Incremental losses are caused by eddy currents, passing in current-carrying parts and conductors of electric mains. The eddy currents themselves are due to magnetic leakage fluxes, passing through the current-carrying parts and conductors.

Thus, the incremental losses in mains and equipment during operation of welding transformer being considered at the given type of its load are increased by 1.38 times. The Table gives the main parameters of operation of the welding transformer at the type of load being considered.

When varying the welding conditions, these values can vary within the range of 13–24 %, and the coefficient THD_U — within 2.5–3.5 %. These results confirm the theoretical analysis of harmonic composition of alternating current of arc [11], which is supplied from the welding transformer.

The welding transformer STSh-250 generates not very high harmonic components of current into supply mains, though they can show negative effect on operation of equipment connected to the mains. Value of THD_U is also not high. The shown characteristics are also typical to other types of single-phase welding transformers.



Main parameters of mains in operation of welding arc power sources

Parameter	STSh-250	VDU-125	VDU-201	VDU-200
I_{m+} , A	80.8	30.2	61.2	59.5
U_{m+} , V	310.6	304.5	312.2	312.9
I_{m-} , A	-74.3	-33.3	-54.7	-59.6
U_{m-} , V	-313.2	-304.3	-315.1	-313.1
I , A	41.0	23.8	26.1	36.8
U , V	221.0	210.6	220.1	221.5
S , V·A	9895.9	5008.3	5202.2	8282.5
P , W	2787.2	3701.6	2543.6	6130.1
Q , var	9495.2	3373.6	4537.9	5569.6
k_p	0.282	0.739	0.489	0.740
$\cos \varphi$	0.280	0.764	0.530	0.980
$\text{tg } \varphi$	3.376	0.816	1.573	-0.129
THD _I , %	15.983	16.879	41.165	86.366
THD _U , %	3.110	2.256	3.624	5.957
K	1.383	1.309	3.233	7.259

Notes. 1. Here I , U – effective values of current and voltage; S , P , Q – full, active and reactive (can include distortion power in the presence of harmonics) powers; k_p – coefficient of power, equal to ratio of active and full power P/S ; $\cos \varphi$ – coefficient of phase shifting between current and voltage. 2. Formulae for calculation of parameters are given in work [5].

Figure 2, *a* shows time dependencies of relative values of current and voltage in mains during operation of welding power source VDU-125. Characteristics were recorded during welding with 3 mm diameter stick electrodes ANO-22 at 120 A welding current. The highest amplitude values of current and voltage during experiment were the following: $I_m = -33.3$ A, $U_m = 304.5$ V. After current transition through zero a low disturbance is superposed on sinusoidal current, caused by operation of voltage multiplier. The shape of voltage is very close to sinusoidal.

Figure 2, *b* shows diagram of harmonic components of effective value of current and voltage. It is seen from this diagram that during operation of power source the 3rd harmonic of current, equal to 15.6 % of the 1st harmonic, and the 5th, equal to 4.6 %, are well expressed in supply mains. The rest uneven harmonics of current do not exceed 1 %. The uneven numbers of harmonics of voltage, having more than 1 % of the 1st harmonic, have the following values: the 3rd – 1.6, the 5th – 1.1 %. The constant component of current is equal to 3.7 %. Even harmonics of current are as follows: the 2nd – 4.0, the 4th – 1.1 %. The constant component and even harmonics of voltage are negligibly expressed.

The coefficients are equal to THD_I = 16.9, THD_U = 2.2 %. K -factor reaches 1.31.

Welding power source VDU-125 has acceptable values of THD_I and THD_U. Incremental losses in

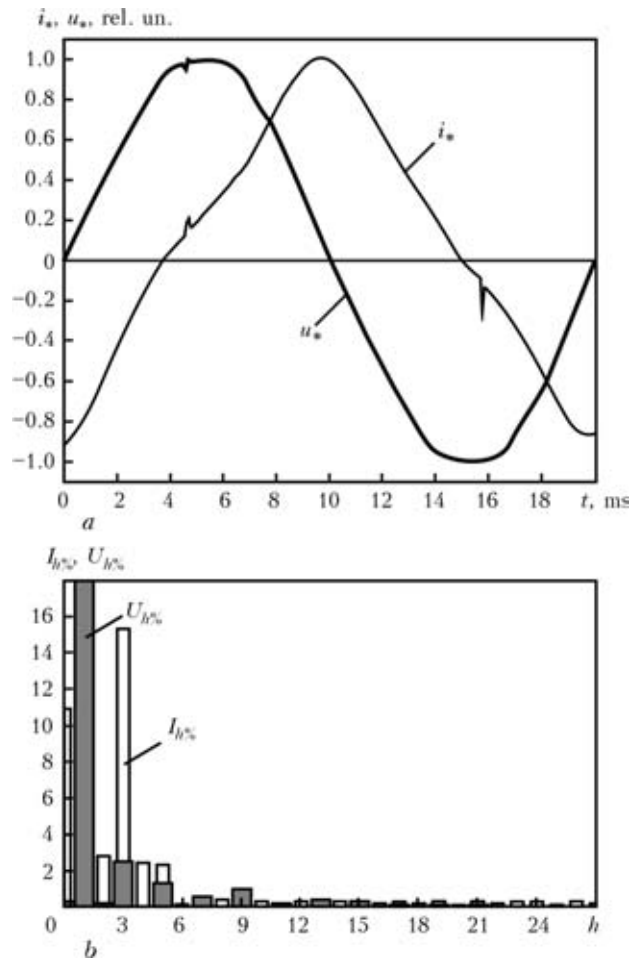


Figure 1. Dependence of current and voltage on time in supply mains of industrial single-phase welding transformer STSh-250 with device for stabilization of welding arc burning (*a*), and harmonic composition of mains current and voltage (*b*)

mains and equipment during operation of power source at the mentioned type of load are 1.3 times increased.

When varying the welding conditions, the values given in the Table, are changed, here THD_I will be 8.7–20.8, THD_U – 2.2–2.8 %.

These characteristics are typical of all types of welding power sources with a capacitor multiplier of voltage, different of types of welding transformers, manufactured as VDU-140, VDU-160 and VDU-180 and designed at the E.O. Paton Electric Welding Institute.

Figure 3, *a* shows time dependencies of relative values of current and voltage in supply mains during operation of welding power source VDU-201. The highest amplitude values of current and voltage are as follows: $I_m = 61.2$ A, $U_m = -315.1$ V. Experiments were performed in welding with 3 mm diameter stick electrode ANO-22 at 90 A welding current. A current pulse of high amplitude at commutation of thyristors was superposed on a basic sinusoidal current of low amplitude, which was provided by a phase-shifting reactor. Sinusoid of voltage had only a negligible distortion just after maximum value.

Figure 3, *b* shows harmonic composition of current and voltage at the input of welding power source. In

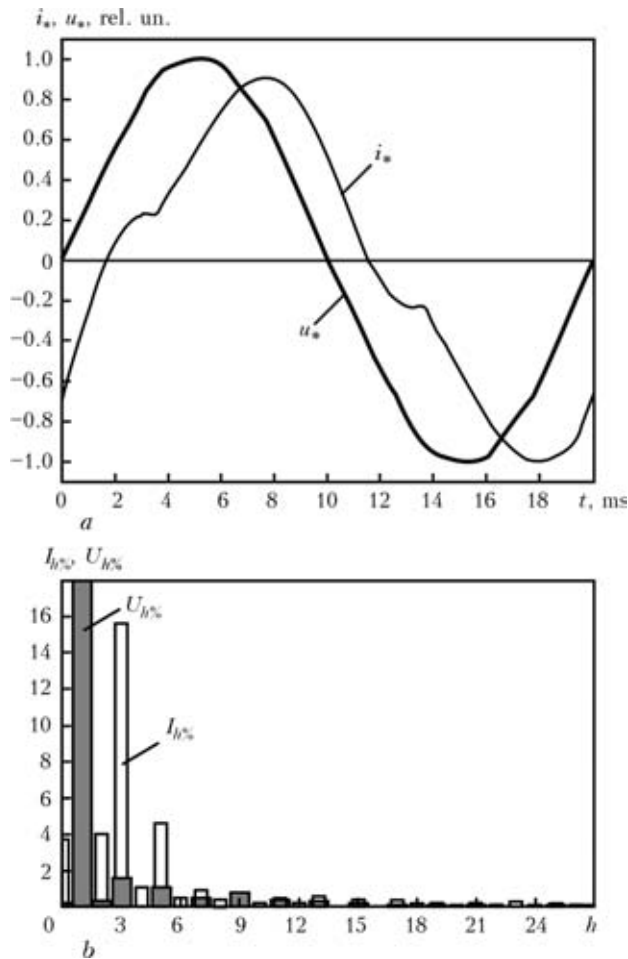


Figure 2. Dependence of current and voltage on time in supply mains of single-phase welding power source VDU-125 with capacitor multiplier of voltage (a), and harmonic composition of mains current and voltage (b)

the power source mains the 3rd harmonic of current, equal to 37.7 % of the 1st harmonic, the 5th – 6.8, the 7th – 6.1, the 9th – 2.5, the 11th – 1.1, the 13th – 1.0 and 19th – 1.1 % are expressed, the rest uneven harmonics of current did not exceed 1 %. Uneven numbers of harmonics of voltage of more than 1 % of the 1st harmonic had the following values: the 3rd – 2.5, the 5th – 1.6 and the 13th – 1.4 %. Expressed are the constant component of current (6.8 %) and its even harmonics (the 2nd – 4.5, the 4th – 7.7, the 6th – 7.9, the 8th – 5.0 and the 10th – 2.4 %). The constant component and even harmonics of voltage are negligibly expressed.

The coefficients of non-linear distortions of current and voltage of power source VDU-201 have the following values: $THD_I = 41.2$, $THD_U = 3.6$ %, $K = 3.2$. In this power source the value of coefficient THD_I is high. In addition, high harmonic components of current, which are also important, generate into mains.

Incremental losses in mains and equipment during the operation of power source at the mentioned type of load are increased by more than 3 times.

The Table shows main parameters of power source operation at the given type of load. In case of varying the welding condition these values are changed, here

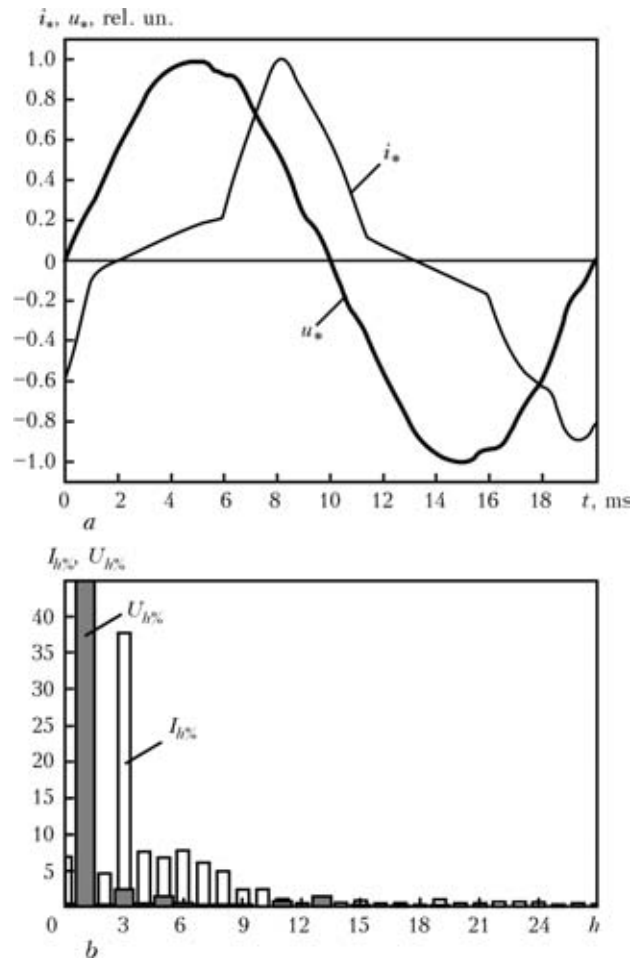


Figure 3. Dependence of current and voltage on time in supply mains of single-phase welding power source VDU-201 with capacitor multiplier of voltage (a), and harmonic composition of mains current and voltage (b)

the coefficient THD_I will be 9.5–46.5 %, and the coefficient THD_U – 1.8–3.9 %.

Figure 4, a shows time dependencies of relative values of current and voltage in mains during operation of welding inverter VDI-200. The highest amplitude values of current and voltage in experiment were equal to $I_m = -59.6$ A, $U_m = -313.1$ V.

Figure 4, b shows harmonic composition of current in mains line and linear voltage at the input of welding power source during welding of low-alloy steel St3 with 5 mm diameter electrodes UONI-13/55 at 200 A welding current.

In mains of power source almost all uneven harmonics of current are expressed, in particular the 3rd current harmonic, equal to 75.1 % of the 1st harmonic, the 5th – 39.5, the 7th – 10.5, the 9th – 8.3, the 11th – 7.4, the 13th – 1.2, the 15th – 3.1, the 17th – 2.4, the 21st – 1.9, the 27th – 1.1 %. The uneven numbers of harmonics of voltage of more than 1 % of the 1st harmonic have the following values: the 3rd – 5.2, the 5th – 2.2, the 7th – 1.4 %. The constant component of current and voltage is absent. Even harmonics of current are negligibly expressed.

The coefficients of non-linear distortions of current and voltage of power source VDI-200 are as follows: $THD_I = 86.4$ %, $THD_U = 5.9$ %, $K = 7.2$.



The curve of current represents the clearly expressed pulse on the background of almost zero values at the rest extension of a semi-period, the value of coefficient THD_I is rather high for power source VDI-200. Moreover, very wide spectrum of harmonic components of current generates into mains. The curve of voltage, though being like a sinusoid, has cuts in the region of extremums, therefore, the amplitudes of harmonic components of voltage are also high. This shape of curve of voltage can lead to false operation of devices of continuous supply, connected to the same mains, which are connected in case of lowering the amplitude value of mains voltage.

Incremental losses in mains and equipment during operation of power sources at the given type of load are increased by more than 7 times. The Table shows main parameters of operation of power source VDI-200 at the given type of load. Negative value $\text{tg } \varphi$ proves that inverter power source is an active-capacitive load for the mains.

When varying the welding condition these values are changed, here the coefficient $THD_I = 82.0\text{--}121.5\%$, and the coefficient $THD_U = 2.8\text{--}6.7\%$.

By analyzing the given data, it is possible to make a conclusion that to improve the quality of electric power and to reduce the level of higher harmonics of current and voltage, generated by welding equipment, it is rational in a number of cases to apply filters of higher harmonics of current. Here, the welding power sources, except providing the required technological characteristics, will have a good electromagnetic compatibility, and also reduce the incremental losses in mains wires and equipment connected to the mains.

It is necessary to note the positive properties of transformer power sources of arc, which except technological effectiveness, safety and low cost, have a negligible effect on the mains. Welding transformers and power sources, manufactured on their base, provide the adjustment of welding current by transformer itself [12] (without electron unit of current adjustment). This is due to the fact that the welding transformer has an increased leakage inductance to provide a steep-falling external characteristic [12, 13], and this promotes the decrease in higher harmonics of current. The capacitors of voltage multiplier and welding transformer with developed magnetic leakage fluxes form something like an inner filter of higher harmonics of current of power source. However, the higher harmonics of current themselves (in absolute values) are rather high, therefore, the application of filters of higher harmonics is desirable for the single-phase welding transformers and power sources manufactured on their base. In this connection, the transformer power sources of welding arc are characterized, in spite of their increased mass, by many positive properties. They should be also developed and improved in future, for example, together with capacitor multipliers of voltage, which greatly decrease the mass of

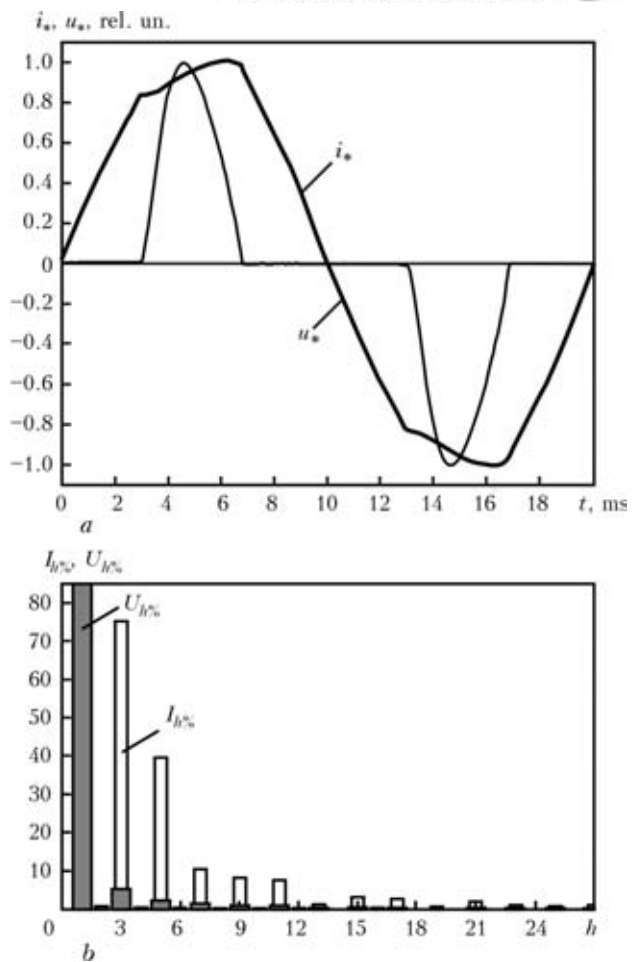


Figure 4. Dependence of current and voltage on time in supply mains of single-phase transformer inverter power source VDI-200 (a), and harmonic composition of mains current and voltage (b)

transformer and consumed power in mains, or with devices of stabilization of welding arc burning, whose application gives an opportunity to use DC electrodes in welding.

Unlike the welding transformers, the power sources, comprising the electron control circuits, generate much more harmonics of current, it particularly concerns the welding inverters. In spite of advantages (small mass, guarantee of preset shape of external characteristic, high value of $\cos \varphi$, etc.) the welding inverters generate the widest spectrum of harmonic components of current into mains and distort greatly the sinusoidal curve of current and voltage, therefore, in this case the obligatory application of filters of higher harmonics of current is required. The similar conclusions were made also by the Chinese researchers [14].

The single-phase welding power sources for mains, unlike the three-phase ones, load significantly the neutral wire, not designed for high loads, with higher harmonics of current of zero sequence. Therefore, except the resonance inductive-capacitive filters of higher harmonics of current [15], it is necessary to apply the autotransformer filters of currents of zero sequence [16, 17], used for three-phase four-wire mains. In addition these filters are balancing the mains. They can be connected in parallel with mains



at the entrance into enterprise or building or several filters can be used along the length of the mains. In some cases it is rational to apply devices of compensation of reactive power simultaneously with single-phase welding power sources, in which the decreased value of power factor $\cos \varphi$ was observed. In our case these are power sources STSh-250 and VDU-201.

Recommended filters do not almost generate the reactive power, which affects negatively the operation of mains, into the mains and are characterized by improved safety in operation in «non-quality» mains, thus providing the reduction of coefficient THD_I down to 5–15 % in single-phase mains.

The E.O. Paton Electric Welding Institute has a large experience in development of methods of calculation of mains parameters and devices for suppression of higher harmonics of current required for their filtering.

CONCLUSIONS

1. It is shown that the single-phase welding power sources generate higher harmonics of current into the mains, thus deteriorating the quality of electric power. Generation of the 3rd harmonic and harmonics, multiple by it, present a particular hazard.

2. Total value of coefficient THD_I during operation of power sources is 8.7–121.5 %, and coefficient THD_U is equal to 2.2–6.7 %, that proves a poor electromagnetic comparability of single-phase welding supply sources.

3. It was found that the coefficient, accounting for the increase in incremental losses from eddy currents in equipment and mains (K -factor), was equal to 1.3–7.3, that gives no opportunity to refer adequately all the single-phase power sources to the category of energy-saving ones.

4. Rationality and in some cases the necessity were defined for application of filters of higher harmonics of current and filters of current of zero sequence together with single-phase sources of arc supply, reducing the coefficient THD_I to 5–15 %. The application of devices for compensation of reactive power are required for some power sources.

5. It was established that the single-phase transformer power sources (welding transformers with developed magnetic leakage fluxes) and welding power sources (without electron adjustment of current),

manufactured on their base, require the obligatory applying of filters of higher harmonics of current.

6. It is shown that the widest spectrum of higher harmonics of current is generated by single-phase welding inverters, distorting most of all the sinusoidal shape of current and voltage of the mains, therefore the obligatory application of filters of higher harmonics of current is required.

1. Paice, D.A. (1995) *Power electronic converter harmonics. Multipulse methods for clean power*. New York: IEEE Press.
2. Pentegov, I.V., Volkov, I.V., Levin, M. (2002) Devices of attenuation of higher harmonics of current. In: *Technical electrodynamics: Subject Issue on Problems of Current Electrical Engineering*. Pt 1. Kyiv: IED.
3. *DSTU IEZ 61000-3-2:2004*: Electromagnetic compatibility. Pt 3-2: Norms. Norms for emission of harmonics of current (at input current force of equipment of not more than 16 A per phase). Kyiv: Derzhspozhyvstandart Ukrainy.
4. (1992) *IEEE Recommended practices and requirements for harmonic control in electrical power systems*: IEEE Standard 519-1992. New York: IEEE Standard Board.
5. Rymar, S.V., Zhernosekov, A.M., Sydorets, V.N. (2011) Influence of welding power supplies on three-phase mains. *The Paton Welding J.*, **10**, 40–45.
6. Zaruba, I.I., Dymenko, V.V. (1992) Multioperator power supplies for AC welding. In: *Transact. on New Welding Power Supplies*. Kiev: PWI.
7. Pentegov, I.V., Dymenko, V.V., Sklifos, V.V. (1994) Welding power supplies with pulse ignition of arc. *Avtomatich. Svarka*, **7/8**, 36–39.
8. Paton, B.E., Zaruba, I.I., Dymenko, V.V. et al. (2007) *Welding power supplies with pulse stabilization of arc burning*. Kiev: Ekotekhnologiya.
9. Pentegov, I.V., Latansky, V.P., Sklifos, V.V. (1992) Small-size power supplies with improved energy data. In: *Transact. on New Welding Power Supplies*. Kiev: PWI.
10. Pentegov, I.V., Rymar, S.V., Latansky, V.P. (2000) Prospects of development of new types of transformers for manual arc welding. *Visnyk PryazovDTU*, **10**, 217–223.
11. Sidorets, V.N., Kunkin, D.D., Moskovich, G.N. (2011) Harmonic analysis of alternative current of electric welding arc. In: *Technical electrodynamics: Subject Issue on Power Electronics and Power Efficiency*. Pt 1. Kyiv: IED.
12. Paton, B.E., Lebedev, V.K. (1966) *Electric equipment for arc and slag welding*. Moscow: Mashinostroenie.
13. (1974) *Technology of fusion electric arc welding of metals and alloys*. Ed. by B.E. Paton. Moscow: Mashinostroenie.
14. Xiao, J.-G., Xing, M.-Z., Xiong, G. et al. (2009) Suppression technology of electromagnetic disturbance for IGBT inverter welder. *Electric Welding Machine*, **39(12)**, 39–42.
15. Volkov, I.V., Kurilchuk, M.N., Pentegov, I.V. et al. (2005) Improvement in quality of industrial enterprises mains using filters of higher harmonics of current. *Visnyk PryazovDTU*, **2(15)**, 15–19.
16. Shidlovsky, A.K., Kuznetsov, V.G. (1985) *Improvement in quality of energy in electric mains*. Kiev: Naukova Dumka.
17. Pentegov, I.V., Volkov, I.V., Rymar, S.V. et al. *Three-phase filter of harmonics of current of zero sequence of autotransformer type*. Pat. 88912 C2 Ukraine. Int. Cl. H01F27/24. Publ. 10.12.2009.



INVESTIGATION OF THERMOCHEMICAL CHARACTERISTICS OF MIXTURES OF DISPERSED MATERIALS BY DIFFERENTIAL THERMAL ANALYSIS METHODS*

V.N. SHLEPAKOV and A.S. KOTELCHUK

E.O. Paton Electric Welding Institute, NASU, Kiev, Ukraine

It is shown that formation of melts as early as at a stage of heating of the powder core up to melting of the sheath of a flux-cored wire and evolution of the gaseous products (H_2O , CO_2 , SiF_4) determine shielding functions of an electrode material and exert a substantial effect on the course of metal to gas interaction reactions at the drop and pool stages. Temperature ranges of thermochemical reactions accompanying the heating process overlap, and their thermal effects superimpose on one another, thus stimulating development of some processes and slowing down the other ones. Control of these reactions by varying composition of a mixture allows regulation of the rate of melting of the core to achieve favourable characteristics of melting of the flux-cored wire and transfer of the electrode metal into the weld pool.

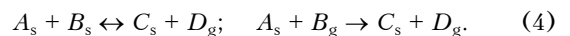
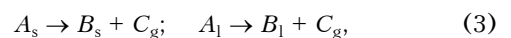
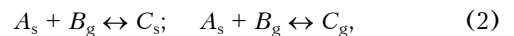
Keywords: *electric arc welding, flux-cored wire, core composition, thermochemical processes, thermal analysis, thermogravimetry, differential scanning calorimetry*

The flux-cored wire sheath or electrode rod is heated during welding primarily due to the heat released by the electric current flow and heat of the active spot of the welding arc. In this case a temperature field close to the quasi-steady one is formed at the extension (region of the wire ranging from the contact tube or holder to the arc) [1–3]. As shown by the earlier calculations [3], the electrode rod or flux-cored wire sheath can be heated at the extension to a temperature above 1000 °C. The powder composite of the wire core or electrode covering at a high melting rate is heated mostly due to the heat transferred from the arc and, to a lesser degree, from the rod or sheath. As thermal conductivity of the powder composite is dozens of times lower than that of metal, at high melting rates the heat transferred to the electrode wire tip from the arc propagates to a considerably smaller distance [3]. This allows the flux-cored wire core or electrode covering to be modelled as an infinite-length cylinder (solid or hollow) heated from the surface (external or internal) and tip to make corresponding calculations [1, 3]. However, practical application of the calculations for estimation of the extent of the reactions developing in the powder composite is hampered by the need to find relationships and coefficients that are also determined by the extent of development of the reactions. Therefore, physical modelling is a well justified approach for experimental estimation of development of the processes of evaporation, dissociation,

thermal destruction and oxidation of components of the flux-cored wire core or electrode covering, which accompany heating and melting of the powder composites during welding [4–6].

The above processes can be successfully studied by the methods and procedures of thermal analysis of powder materials and composites: differential thermal analysis, thermogravimetric (TG) analysis, differential thermogravimetric analysis and differential scanning calorimetry (DSC) [1, 2, 5, 6]. These methods of thermal analysis are supplemented by mass-spectral analysis of the gas phase formed in heating and melting of the materials investigated.

Investigation procedure. Complex thermal analysis for the solid, liquid and gas phases allows investigation of reactions of the following types (the «prime» mark means allotropic transformation):



Equations (1) through (4) are well suited to describe the processes of evaporation, oxidation, dissociation and reduction, as well as other phase transformations characteristic of the welding processes [1, 2]. Investigations of such processes were carried out by using thermoanalyser TGA/DSC Q600 STD (TA Instruments, USA) combined with mass-spectrometer VG ProLab (Thermo Scientific Fisher, Great Britain) (Figure 1). Thermoanalyser TGA/DSC Q600 STD is an analytical instrument allowing simultaneous investigations by the DSC and TG methods. It is used to measure the heat flow and mass variations that accompany phase transformations and reactions in the

* Based on the paper presented at the VI International Conference on Welding Consumables of the CIS Countries «Welding Consumables. Development. Technology. Production. Quality. Competitiveness» (Krasnodar, 2011), P. 91–97.

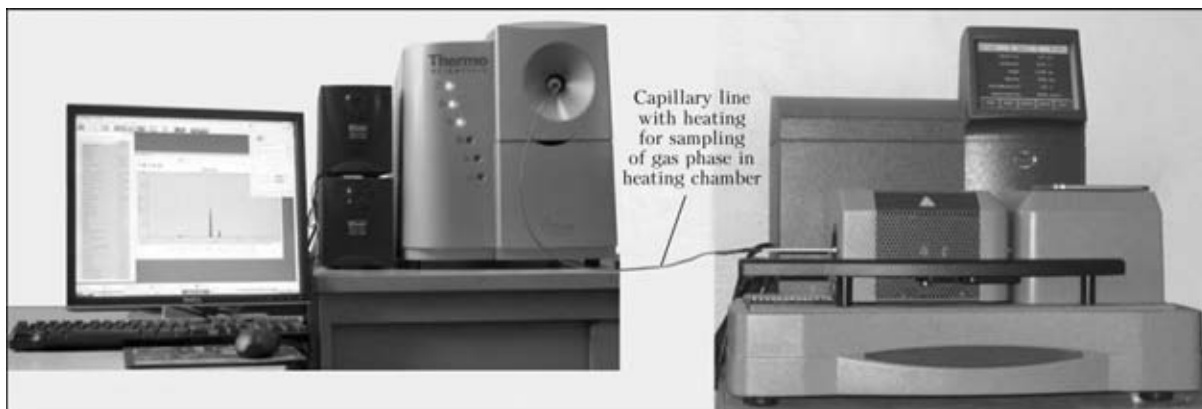


Figure 1. Thermoanalyser TGA/DSC Q600 STD (to the right) combined with mass-spectrometer VG ProLab (to the left) for monitoring and analysis of gas phase composition in heating chamber

materials investigated. The data obtained enable distinguishing the endothermic and exothermic processes that do not lead to changes in mass (e.g. melting and solidification) from the processes of interaction with the gas phase that cause a change in mass of a sample (e.g. dissociation or oxidation). Simultaneous calorimetric and thermogravimetric analyses of the same sample make it possible to decrease the experimental and sampling errors.

Specifications of thermoanalyser TGA/DSC Q600 STD, as well as of the employed crucibles, scales, heating chamber and purging gases are given below [7]:

Thermocouples	platinum-platinum + 13 % rhodium, type R
Temperature range for investigations, °C	5–1500
Heating rate, °C/min	up to 100 (to 1000 °C) up to 25 (to 1500 °C)
Type of crucibles	platinum, ceramic (Al ₂ O ₃)
Capacity of crucibles	platinum: 40 and 110 µl aluminium oxide: 40 and 90 µl
Accuracy of measurements of heat flow (DSC) for pure metals, %	±2
Frequency of measurements of heat flow (DSC) for pure metals, %	±2
Accuracy of measurements of temperature for pure metals, °C	±1
Frequency of measurements of temperature for pure metals, °C	±0.5
Sensitivity to temperature difference (DTA), %	0.001 (200–1300)
Sensitivity in determination of mass, µg	0.1
Mass measurement accuracy, %	±1
Primary purging gases	He, N ₂ , air, Ar
Primary purging gas flow rate, ml/min	20–1000
Secondary purging gases	O ₂ , air, CO, CO ₂ , N ₂ , He, Ar
Secondary purging gas flow rate, ml/min	10–100

The secondary purging system is intended to provide the low concentration of a reagent gas fed to the chamber with a sample. The gas flow rate is set by the control computer and adjusted by the flow meter, which also provides a switch-over of gases [7].

Experimental investigations by using the thermoanalyser are carried out by one common scheme, which includes selection of modes and signals for registration, setting of gas flow rates for primary and secondary purging, setting of temperature conditions

for an experiment, selection and mounting of empty crucibles on arms of microscales, calibration of a mass signal, weighing of the required amount of a sample, closing of the heating chamber, starting up of the experiment, removal of the sample remainders after the experiment, and processing and analysis of the data obtained. Most of the operations are performed by using control software of the external control computer. To achieve the required accuracy, the instrument is preliminarily calibrated by the signals of mass, temperature, heat flow and difference in temperatures of the sample and standard.

Composition of the gas phase in the thermoanalyser heating chamber is monitored by using quadrupole mass-spectrometer VG ProLab, the system of which is designed to analyse gases under a pressure close to the atmospheric one (from 100 to 1500 mbar) and a low flow rate (not higher than 20 ml/min) [8]. Sampling of gas is done by using a quartz capillary line with heating. The frequency of analysis of samples is up to 1 ms, the mass of fixed ions being up to 300 amu. The mass-spectrometer comprises a closed contamination-resistant ion source, the sensitivity of which is not lower than 5·10⁻⁵ A/Torr (for nitrogen using the Faraday detector). The limit of detection by using the Faraday detector is not lower than 10⁻⁵, and that by using the electronic multiplier is not lower than 10⁻⁶ [8]. The software package for control of the mass-spectrometer and processing of its data contains the library of spectra to ensure quality analysis of an unknown composition of the gas phase.

Investigation of thermochemical processes in heating and melting of mixtures by an example of compositions of flux-cored wire cores. Objects for our investigations were powder composites, the compositions of which corresponded to two types of self-shielding flux-cored wires: having cores of the fluoride-oxide (system MgO–BaF₂–LiF) and carbonate-fluorite (CaCO₃–CaF₂–Li₂O·TiO₂–CaO·SiO₂) types with the oxidising and alloying system on the Al–Mn–Ni–Zr base. Properties of such composites were studied on samples with a mass of 20.0±0.2 mg placed

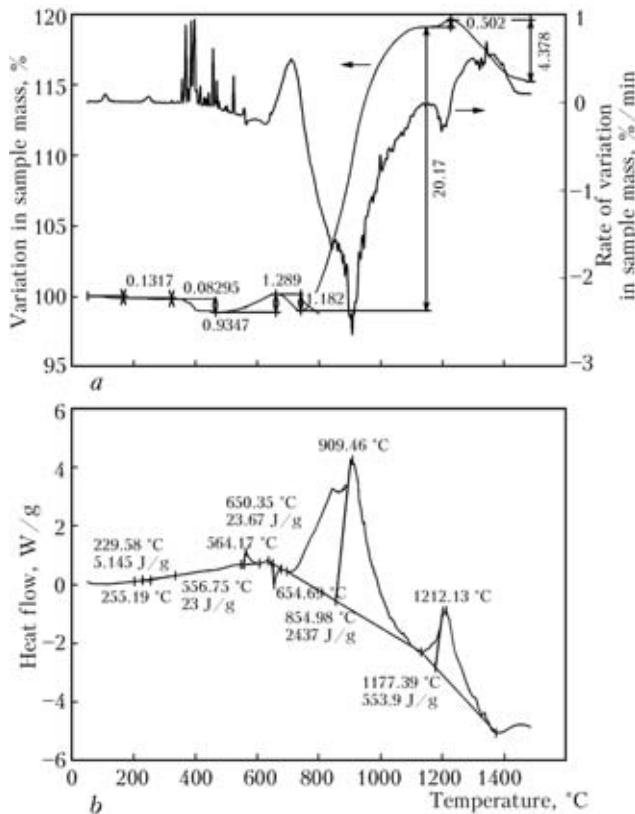


Figure 2. Results of analysis of a sample of flux-cored wire charge of the carbonate-fluorite type by the TG (a) and DSC (b) methods

in aluminium oxide crucibles during dynamic heating to 1500 °C in air at its flow rate of 100 ml/min.

Figure 2, a shows typical results of TG analysis of the flux-cored wire charge of the carbonate-fluorite type containing calcium, magnesium and sodium carbonates, as well as sodium hexafluorosilicate. Characteristic ranges of removal of absorbed moisture at a temperature of approximately up to 150 °C, thermal dissociation of sodium hexafluorosilicate to evolve SiF₄ in a temperature range of 380–450 °C and that of carbonates (700–1450 °C) to evolve CO₂ can be seen in the sample mass variation curve. Evolution of the said gases was confirmed by mass-spectral monitoring of composition of the gas phase in the heating chamber. At a temperature above 450 °C the processes of thermal destruction to evolve gaseous products were superimposed by a growth of mass of a sample due to development of oxidation of the iron powder, ferroalloys and alloying components. Upon reaching a temperature of 700 °C the increase in mass of the sample was replaced by its decrease, and the intensity of current of the carbon dioxide ions increased in the mass spectrometer, this evidencing the intensification of thermal destruction of the carbonates.

Figure 2, b shows results of analysis of the same charge sample by the DSC method and calculations of the total thermal effects of the overlapping reactions. The process of heating of the carbonate-fluorite type mixtures was accompanied by the exothermic effects of a low intensity in a temperature range of

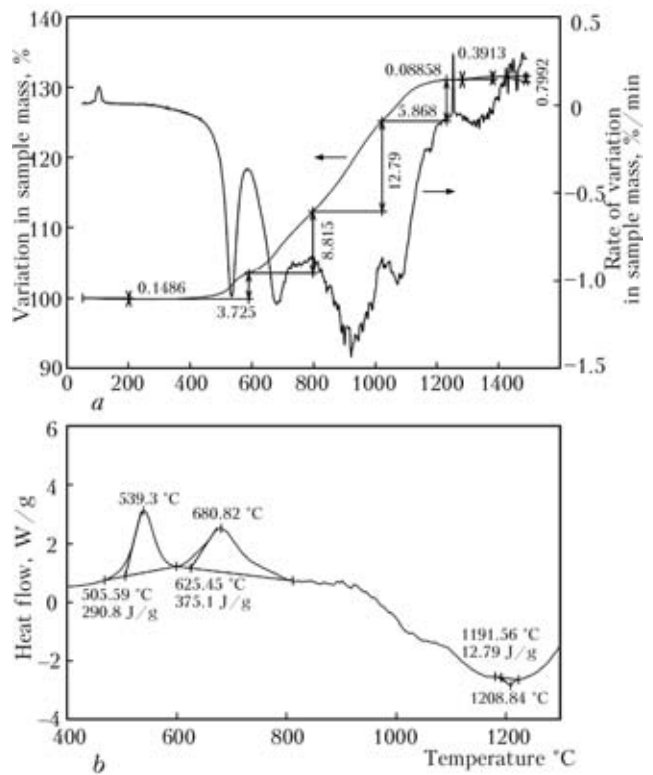


Figure 3. Results of analysis of a sample of flux-cored wire charge of the oxide-fluoride type by the TG (a) and DSC (b) methods

600–800 °C. Further heating was accompanied by alternation of the exothermic and endothermic effects, from which it is possible to determine the simultaneous course of the processes of destruction of mineral components and oxidation of metallic components. Concerning self-shielding flux-cored wires of the carbonate-fluorite type, the experimental investigations, the results of which are presented in study [9], made it possible to establish that the highest efficiency of the gas shielding is provided by using compositions of the core for which the gas evolution processes extend from 400 °C to the melting temperature of steel. In other words, the strongest gas shielding is formed in welding using wires with the cores that generate shielding gases at all stages of their heating and melting.

Figure 3, a shows typical results obtained by the method of TG analysis of the flux-cored wire charge of the oxide-fluoride type containing aluminium-base master alloys (in particular, Al-Li and Al-Mg master alloys), and Figure 3, b shows results of analysis of the same sample by the DSC method and calculation of the total thermal effects of the reactions.

The process of heating of the flux-cored wire charge of the oxide-fluoride type was characterised by the exothermic effects at temperatures of about 600 and 800 °C, as well as by a much higher intensity compared to the wire charge of the carbonate-fluorite type, which were accompanied by increase in mass of a sample and decrease in the content of oxygen in the gas phase of the heating chamber, this being indicative of the processes of oxidation of the aluminium and magnesium powders, iron powder and ferroalloys. The slag



melt was formed at a temperature close to 1200 °C. This was accompanied by a marked exothermic effect reaching its maximum at the said temperature.

Discussion of results and conclusions. Investigations of physical-chemical properties of powder materials and their mixtures modelling the flux-cored wire core, which were carried out by the methods of complex thermal analysis and mass-spectroscopy of the gas phase in dynamic heating from 30 to 1500 °C, make it possible to establish the temperature ranges, extent of development and consumption of heat for the reactions of thermal destructions to evolve gases, oxidation of components, and melting of mixtures to form the primary melt of the metal and slag phases. Formation of the melts as early as at a stage of heating of the powder core up to melting of the wire sheath and evolution of the gaseous products (H₂O, CO₂, SiF₄) determine shielding functions of the electrode material and exert a substantial impact on the course of the metal to gas interaction reactions at the drop and pool stages. Temperature ranges of the thermochemical reactions (endothermic processes of removal of moisture, destruction and melting, and exothermic processes of oxidation and complex formation) accompanying the heating process overlap, and their thermal effects superimpose on one another, thus stimulating development of some processes and slowing down of the other ones. Therefore, control of these reactions

by varying composition of a mixture allows regulation of the rate of melting of the core to achieve favourable characteristics of melting of the flux-cored wire and transfer of the electrode metal to the weld pool. Values of the heat flow in heating of powder composites enable estimation of the consumption of heat for their heating and melting, allowing for the mutual effect of the exothermic and endothermic reactions occurring in the material investigated.

1. Pokhodnya, I.K., Suptel, A.M., Shlepakov, V.N. (1972) *Flux-cored wire welding*. Kiev: Naukova Dumka.
2. Pokhodnya, I.K., Yavdoshchin, I.R., Paltsevich, A.P. et al. (2004) *Metallurgy of arc welding: interaction of metal with gases*. Ed. by I.K. Pokhodnya. Kiev: Naukova Dumka.
3. Erokhin, A.A. (1973) *Principles of fusion welding. Physical-chemical mechanisms*. Moscow: Nauka.
4. Killing, R. (1980) Welding with self-shielded wires – the mechanism of shielding and droplet transfer. *Metal Constr.*, 12(9), 433–436.
5. Shlepakov, V.N. (1990) *Kinetics of processes of interaction between metal and gases in flux-cored wire welding*. Kiev: Naukova Dumka.
6. Shlepakov, V.N., Suprun, S.A., Kotelchuk, A.S. (1987) Kinetics of gas generation in flux-cored wire welding. *IIW Doc. XII-1046-87*.
7. (2003) *Combined DSC-TGA Q600: User's manual*. Moscow: Intertech Corp.
8. (2008) Prolab: Operation manual. *Thermo Sci., Ion Path*, Issue 7, July.
9. Shlepakov, V.N., Suprun, S.A., Kotelchuk, A.S. (1990) Estimating of the characteristics of flux-cored wire welding under the wind flow effect. In: *Proc. of Int. Conf. on Welding under Extreme Conditions* (Helsinki, Sept. 4–5, 1989). Oxford; New York: Pergamon Press, 171–179.

CONTROL OF PROPERTIES OF THE WELD METAL BY REGULATING THE LEVEL OF OXIDATION OF THE WELD POOL IN GAS-SHIELDED WELDING

S.T. RIMSKY

E.O. Paton Electric Welding Institute, NASU, Kiev, Ukraine

Activity of oxygen dissolved in the weld pool metal was determined directly in the process of welding of low-alloy steel in the oxidising shielding gas atmosphere by using the electrochemical method. Prediction of mechanical properties of the weld metal depending on the activity of oxygen in molten metal and welding heat input was substantiated.

Keywords: arc welding, consumable electrode, oxidising shielding gases, weld pool, electrochemical method, oxygen activity, heat input, weld metal, structure and mechanical properties

Structure and properties of the weld metal on low-alloy steels are known to depend to a considerable degree on its oxygen content [1, 2]. Oxygen contained in molten metal of the drops and weld pool in arc welding of steel in oxidising shielding gases may be in different states: in a dissolved or chemically combined state in the form of suspended particles of oxides and complex inclusions. Metal-soluble oxygen [O]_s or oxygen activity a_o determines the course of the processes of deoxidation, refining and secondary oxidation and af-

fects the final composition of the weld metal, its structure formation and properties.

The methods applied in practice for analysis of the oxygen content of the weld metal allow evaluation of its total concentration, i.e. the total content of oxygen [O]_t, both active and combined into chemical compounds. It takes several hours to perform this operation, including sampling, preparation of a sample, its transportation to a laboratory and analysis by the vacuum melting method.

At the same time, large-scale metallurgy uses to an increasing extent the method of evaluation of the activity of oxygen in iron-based melts, which consists in measuring the electromotive force (emf) generated in a concentration cell based on solid oxide electrolyte

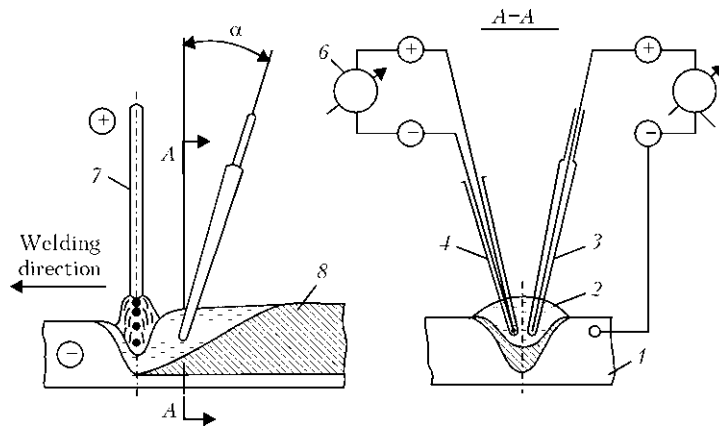


Figure 1. Schematic diagram of express monitoring of oxygen activity in weld pool metal: 1 – base metal; 2 – weld pool; 3 – oxidation sensor; 4 – thermocouple; 5, 6 – measuring instruments; 7 – welding electrode; 8 – weld ($\alpha = 15\text{--}20^\circ$ – angle of inclination of sensor and thermocouple)

[3]. An important feature of this method is that the oxide phase forming in molten metal as a result of its oxidation does not affect the level of the generated emf and, hence, the activity of oxygen in metal. Therefore, the measurements can be performed without any preliminary holding of sensor in the melt, which is usually applied to stabilise processes occurring in the galvanic cell circuit, this being of high importance for investigation of short-time fast processes taking place in the weld pool. The measured values of the oxygen activity range from 0.0001 to 0.2 wt.% [4].

The soluble oxygen content can be determined by the electrochemical method within 15–20 s by immersing the oxygen galvanic cell into the weld pool [5, 6]. Oxygen activity a_o (this directly measurable value is taken as a criterion of oxidation of the weld pool metal) and total oxygen content $[O]_t$ of the weld are the mutually complementary values, as their difference $\Delta[O] = [O]_t - a_o$ characterises the content of oxygen combined into chemical compounds, i.e. the content of oxide and complex inclusions in the metal [6].

Participating in metallurgical reactions during fusion welding, oxygen may have both positive and negative effect on the technological strength [7, 8], sensitivity to formation of pores [8] and mechanical properties of the welds [9], depending on its concentration in the melt.

The purpose of this study was to analyse mechanical properties and structure of the weld metal depending on the variations of the activity of oxygen in the weld pool metal directly in the process of welding of low-carbon steel in the oxidising shielding gas atmosphere.

The data on the content of soluble oxygen in the melt were obtained by using the electrochemical method. Figure 1 shows schematic diagram of the express method used to monitor oxygen activity a_o in the weld pool metal by measuring the emf generated in an oxygen concentration galvanic cell based on solid electrolyte. For this the use was made of a commercially produced oxidation sensor made from Y_2O_3 -stabilised ZrO_2 and comprising the Mo– MoO_2 reference electrode, which was immersed into a low-tem-

perature zone of the weld pool to a depth of 4–6 mm. The distance between the sensor, thermocouple and arc was 10–12 mm. The local measurement of temperature of the weld pool metal was made with tungsten-rhenium thermocouple VR 5/20. Digital voltmeters with a voltage measurement range of zero to 1000 mV were used to fix the emf induced in the sensor and thermocouple.

The oxygen activity was determined from the measured values of emf in the galvanic cell and temperature of the weld pool metal [4]:

$$\lg a_o = 2.685 - \frac{10.086E + 5661}{T},$$

where E is the emf generated in the concentration cell circuit, mV; and T is the temperature of the weld pool, K.

Experimental V-groove butt joints on steel VSt3sp (killed) were welded at a reverse polarity current by using 2 mm diameter wire Sv-08G2S in the CO_2 and $Ar + 20\% CO_2$ gas mixture atmospheres. Variations in oxygen activity a_o in the weld pool metal were studied depending on the arc voltage in a range of 28 to 36 V at fixed values of the welding current: 400, 450 and 500 A, and at welding heat input g/v ranging from 5 to 35 kJ/cm. Measured results are given in Figures 2 and 3.

As seen from Figure 2, in case of welding in the $Ar + 20\% CO_2$ mixture, oxygen activity a_o in the weld pool metal linearly increases with growth of the arc voltage, this being most pronounced at a current of 400 A. The sensitivity of a_o to variations in the arc voltage decreases with increase of the welding current. In welding at a current of 500 A, the oxygen activity remains almost unchanged over the entire range of the tested values of the arc voltage. The range of the welding conditions was determined, in which a change of the main process parameters (I_w , U_a , v_w) caused no substantial changes in the oxygen activity, i.e. the level of oxidation of molten metal, at the fixed compositions of the shielding gas and welding current. It can be seen from Figure 3 that with increase of welding



Mechanical properties of metal of the welds made in oxidising shielding gases on steel VSt3sp depending on the welding heat input and oxygen activity in the weld pool

Shielding gas	g/v , kJ/cm	$[O]_t$, wt. %	a_o , wt. %	$\Delta[O]$, wt. %	$\sigma_{0.2}$, MPa	σ_t , MPa	δ_5 , %	ψ , %	KCV, J/cm ² , at T , °C		
									+20	-20	-40
CO ₂	18.4	0.054	0.0056	0.0484	350	420	26.5	55.2	120	60	32
	28.8	0.061	0.0063	0.0547	335	380	25.2	53.4	98	42	16
Ar + 20 % CO ₂	18.4	0.035	0.0034	0.0316	384	530	33.0	66.0	165	115	55
	28.8	0.046	0.0040	0.0420	353	465	29.3	58.6	136	91	43

Note. Given are the values averaged over the results of tests of three to five specimens.

heat input g/v the level of oxidation of the weld pool metal first grows almost linearly, then this growth slows down, and in a range of welding conditions with a heat input above 20 kJ/cm the value of a_o remains almost constant. This regularity shows up when welding is performed in the CO₂ and Ar + 20 % CO₂ gas mixture atmospheres having a different oxidising ability. This character of dependence of the oxygen activity on the welding parameters is attributable, first of all, to increase in the base metal content of the weld pool, as well as to increase in the content of iron vapours in the arc atmosphere causing decrease in a partial pressure of the oxidising gases and, hence, absorption of oxygen by the electrode metal drops.

Further investigations allowed evaluation of the effect of welding heat input on the oxygen activity in the melt, as well as of mechanical properties of the welds made on steel VSt3sp in the CO₂ and Ar + 20 % CO₂ gas mixture atmospheres (Table). The data of the Table show that the a_o values grow with increase in the oxidising ability of the shielding atmosphere. However, they are an order of magnitude lower than total oxygen content $[O]_t$ of the weld metal determined by the vacuum melting method.

Structure of metal of the experimental welds was examined by using the optical and electron microscopes, and character of the $\gamma \rightarrow \alpha$ transformation of

this metal under conditions of continuous cooling was studied by using the high-sensitivity dilatometry instruments combined with the «Ala-Too» unit for high-temperature metallography. The Pt-Pt-10 % Rh thermocouple was employed for precise measurement of temperature. The dilatometer was evacuated to a pressure of $2 \cdot 10^{-4}$ Torr and then filled up with high-purity argon to prevent oxidation or decarburisation of samples. To investigate the effect of oxygen on peculiarities of decomposition of austenite in the weld metal, the samples were heated to a temperature of 1250 °C and held for 2 min at this temperature providing the identical grain sizes. Cooling from 800 to 500 °C was performed at a rate of 5 °C/s. The temperature versus time of elongation of a sample was recorded during this thermal cycle simulating the welding conditions by using a specially calibrated potentiometer KSP-4.

It was established that high values of impact toughness of the weld metal and a maximal amount of acicular ferrite in structure of the weld metal can be achieved at the content of combined oxygen $\Delta[O]$ in the weld ranging from 0.015 to 0.045 % (Figure 4, a) and at the following contents of alloying elements and impurities, wt. %: 0.08–0.11 C, 0.40–0.55 Si, 1.2–1.5 Mn, 0.015–

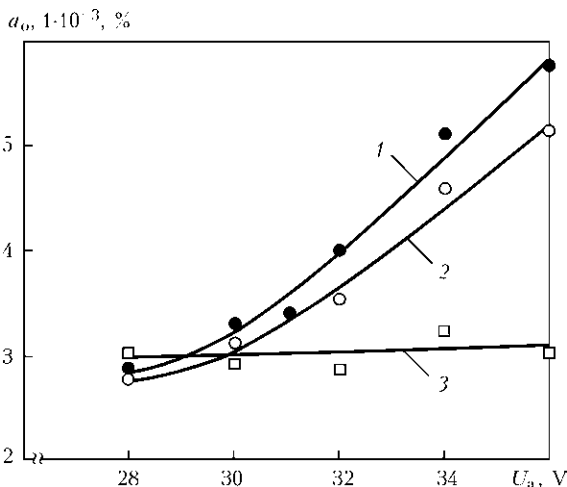


Figure 2. Variations in oxygen activity a_o in weld pool metal depending on the arc voltage in welding of steel in Ar + 20 % CO₂ gas mixture: 1 – $I_w = 400$; 2 – 450; 3 – 500 A

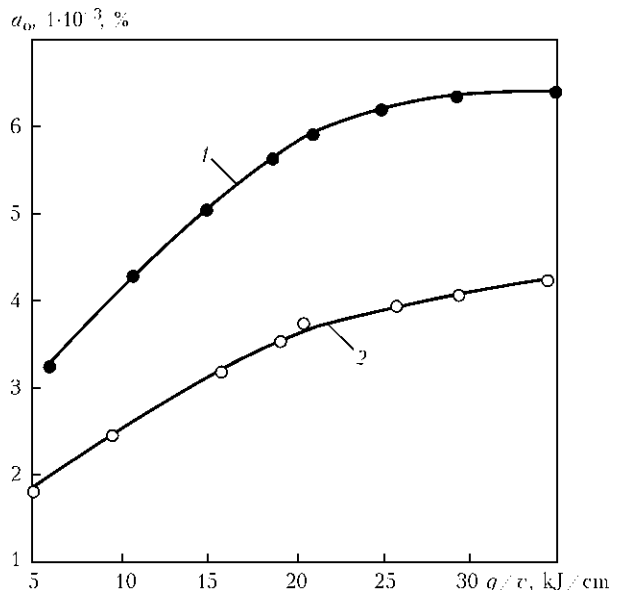


Figure 3. Variations in oxygen activity a_o in weld pool metal depending on the heat input in welding of steel in oxidising shielding gases: 1 – CO₂; 2 – Ar + 20 % CO₂

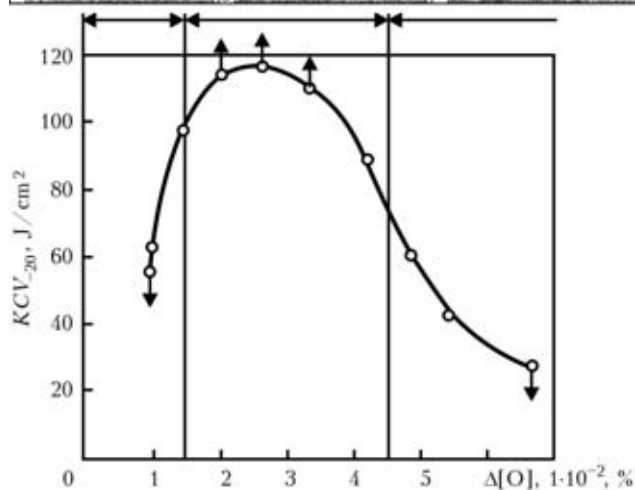
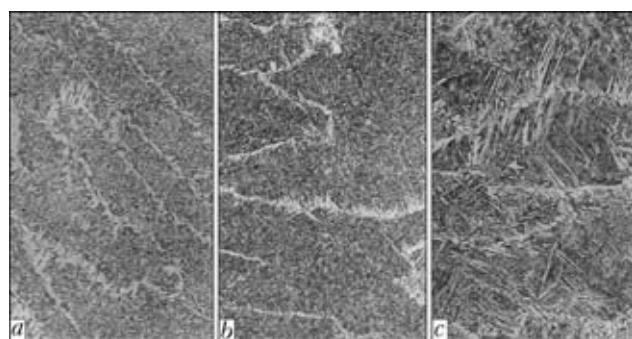


Figure 4. Effect of oxygen combined into chemical compounds, $\Delta[\text{O}]$, on impact toughness and microstructure ($\times 200$) of metal of the welds made in oxidising shielding gases: *a* – structure of acicular ferrite with bainite regions; *b* – structure with predominant acicular ferrite; *c* – grain-boundary ferrite and lamellar precipitates of Widmanstatten ferrite

0.020 S and P. Deviations of the oxygen concentration to higher or lower values from the said ranges were accompanied by decrease in the amount of acicular ferrite in structure of the weld metal.

The $\gamma \rightarrow \alpha$ transformation in the weld metal with a high oxygen content (0.06–0.07 %) occurred at higher temperatures of 720 to 680 °C, this being 20–30 °C higher than in the welds with the 0.045 % or lower oxygen content. Lowering of the transformation beginning temperature decelerated diffusion processes in the pearlitic transformation region. As a result, the major portion of austenite undergoes transformations by the shear mechanism to form finely dispersed acicular ferrite. It was found out that at an oxygen content of 0.015 to 0.045 % the structure of the weld metal contained 75–80 % of acicular ferrite (Figure 4, *b*). Electron microscopic examinations showed that the formed acicular phase was not bainite, as there were no characteristic precipitates of the carbide phase at the needle edges (Figure 5). The matrix surrounding a growing ferrite needle featured an increased density of dislocations.

Fine oxide particles with a size of less than 0.1 μm present in metal were nuclei of the ferrite phase in the bulk of austenitic grains, which was confirmed by the results of electron microscopic examinations (see

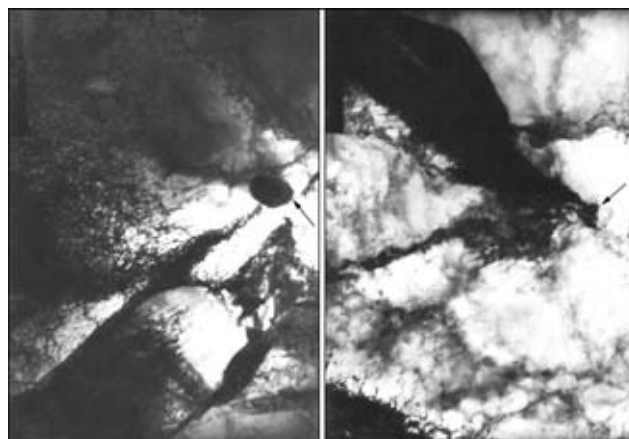


Figure 5. Microstructure ($\times 13,200$) of acicular ferrite in metal of the welds made in Ar + 20 % CO_2 mixture (arrows indicate to oxide inclusions connected to edge regions of ferrite needles)

Figure 5). Decrease in the acicular ferrite content of the welds with an oxygen concentration of less than 0.015 % (see Figure 4, *a*) can be explained by decrease in the quantity of the oxide particles, i.e. quantity of the ferritic phase nucleation centres. Depending on their quantity and size, such particles favour formation of this or other morphology of the ferritic phase [1] affecting the fine metal structure and, hence, its sensitivity to brittle fracture.

Therefore, the quantitative data on the activity of oxygen in molten metal of the weld pool do not only make it possible to explain the phenomena taking place during welding, but also, which is more important, allow the scientifically substantiated planning of this or other effect. In particular, such data are extremely important for development of the schemes of alloying of new welding wires, selection of the optimal shielding gas–wire combinations, development of the technologies for welding of steels, and more reliable prediction of mechanical properties of the welds.

1. Cochrane, R.C., Kirkwood, P.R. (1979) The effect of oxygen on weld metal microstructure. In: *Proc. of Int. Conf. on Trends in Steels and Consumables for Welding* (London, 14–16 Nov. 1978). Cambridge: TWI, 103–122.
2. Kulikov, I.S. (1975) *Deoxidation of metals*. Moscow: Metallurgiya.
3. Yavojsky, V.I., Vishkarev, A.F., Luzgin, V.P. et al. (1975) *Express analysis of oxygen content of steel*. Moscow: Metallurgiya.
4. Luzgin, V.P., Yavojsky, V.I. (1983) *Gases in steel and quality of metal*. Moscow: Metallurgiya.
5. Rimsky, S.T., Svetsinsky, V.G., Bondarenko, T.P. et al. (1988) *Method of determination of activity of elements in melt*. USSR author's cert. 1491161. Int. Cl. G 01 N 27/46. Prior. 22.12.1986. Publ. 1988.
6. Svetsinsky, V.G., Bondarenko, T.P., Rimsky, S.T. et al. (1988) Determination of activity of oxygen in molten metal in gas-shielded welding of steel. *Avtomatich. Svarka*, **2**, 73.
7. Rimsky, S.T., Svetsinsky, V.G. (1977) Effect of composition of oxidizing argon mixture on solidification crack resistance of weld on steel VSt3sp. *Ibid.*, **10**, 48–52, 54.
8. Pidgaetsky, V.V. (1970) *Pores, inclusions and cracks in welds*. Kyiv: Tekhnika.
9. Svetsinsky, V.G., Rimsky, S.T., Petrov, Yu.N. (1974) Peculiarities of fine structure of gas-shielded welds. *Avtomatich. Svarka*, **8**, 5–8.



HYGROSCOPICITY OF HIGH-BASICITY SYNTHETIC FLUX

S.I. MORAVETSKY

E.O. Paton Electric Welding Institute, NASU, Kiev, Ukraine

It was experimentally found that hygroscopicity of synthetic acid fluxes is at the same that of standard fused fluxes. Hygroscopicity of the synthetic fluxes grows not less than 10 times with increase in their basicity from 0.8 to 2.4. This probably is caused by the presence of a free lime which forms in the synthetic flux as a result of the solid-phase reaction between magnesium oxide and calcium fluoride in flux sintering. The thermodynamic calculation results and experimental data confirm the above assumption.

Keywords: *welding flux, oxide-fluoride system, basicity, hygroscopicity, phase composition, solid-phase chemical reaction*

Development of welding fluxes obtained by means of a solid-phase synthesis of initial charge components and mechanical refinement of fused product per granules [1] is an important result of investigations, carried out in the E.O. Paton Electric Welding Institute.

Deterioration of welding-technological properties of the fluxes can be caused by increase of their basicity. Indicated tendency was also noted for a synthetic flux. Thus, some degradation of forming capability of the flux, tarnish of a weld surface, and in some cases, appearance of single pores were found after relatively short soaking of SFT-6 flux (TU PWI 839–93) with $B_{IIW} = 2.4$ basicity under humid atmospheric conditions during surfacing of low alloy heat-resistant steel. These drawbacks were eliminated after repeated baking of such a flux at 550–600 °C for 2 h. Soaking in humid atmosphere of the low-basicity synthetic fluxes, for example, pilot flux SF-1 ($B_{IIW} = 0.8$) does not result in notable degradation of welding-technological properties. It can be assumed, therefore, that the synthetic fluxes, like others, obtain higher hygroscopicity with increase of basicity.

The aim of the present work lies in experimental determination of hygroscopicity of SFT-6 type syn-

thetic fluxes of MgO–CaF₂–Al₂O₃–SiO₂ system and reasons of its increase at basicity rise. Hygroscopicity of the standard fluxes of other types (agglomerated, fused vitreous fluxes and fused honeycombed ones), as well as low basicity of the synthetic flux, was determined for comparative assessment.

The charge components from Table 1 were selected for manufacture of the synthetic fluxes (objects of investigation of this study). A gravimetric method was used for determination of hygroscopicity of the fluxes.

Several forms of moisture differing by type and energy of bonding between the atoms of hydrogen, oxygen and flux material [2] can be, symbolically, distinguished in the fluxes. Temperature of thermal desorption of the moisture from the flux is determined by value of indicated energy. Most of chemically bound moisture (around 80 %) in the fused fluxes granulated by pouring of a melt in a water refers to high-temperature form and is removed at temperature values of 800–1000 °C [2]. There is no high-temperature form of the moisture in the fluxes having no exposure of «wet» granulation.

Content of moisture in the fluxes is determined by standard method [3] allowing setting general (gross) moisture emission from the flux in the temperature interval from 20 to 1000 °C. However, the hygroscopicity of fluxes is to be evaluated considering the

Table 1. Some charge materials used for production of the synthetic fluxes

Charge materials	Main component of the material	Grade	Normative document (GOST)
Periclase fused powder for steel-making production (magnesite)	MgO	PPK-88	24862–81
Fluor-spar lump concentrate (fluorite)	CaF ₂	FKS-95A	4421–73
Alumina	Al ₂ O ₃	GK	6912–87
Feldspar for electrode coatings	NaK[AlSi ₃ O ₈]	PShM	4422–73
Glass breakage*	Na ₂ O–CaO–6SiO ₂	–	–
Quartz sand	SiO ₂	PB-150-1	22551–77
Manganese ore concentrate for electrode coating	MnO	–	4418–75
Metallic manganese	Mn	Mn95	6008–90
Calcium quicklime	CaO	Grade 1	9179–77
Crystalline foundry graphite	C	GL-1	5279–74

* Powder material, product of soda-lime glass milling being a spoilage and wastes of production of houseware and ornamental glass products according to GOST 24315–80 and(or) flat glass according to GOST 111–2001.

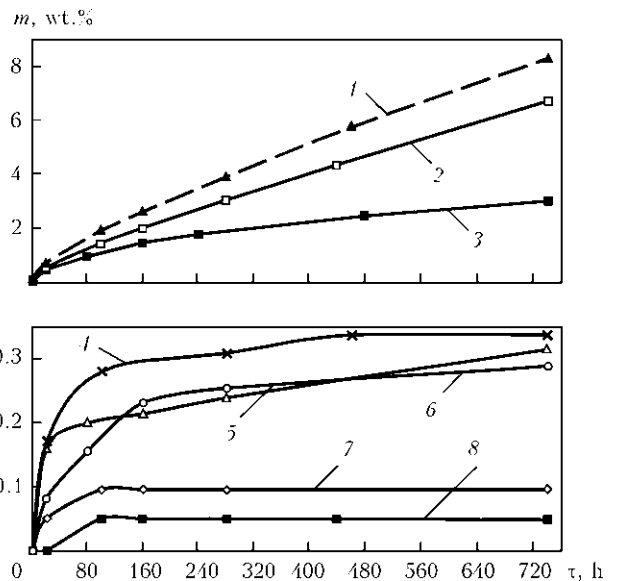


stated task, i.e. their capability to water absorption after repeated baking and at further soaking in the atmosphere. The fluxes, significantly differing by method of manufacture and, therefore, containing constantly unknown amount of the moisture of different forms, were the objects of investigation. In consideration of mentioned above application of the method, described in [3], will inevitably lead to obtaining of the numerical results which are difficult for interpretation and reasonable comparison without performance of large number of additional experiments. The moisture, absorbed by the fluxes in the course of this experiment, in each case would be an undetermined item in a level of its gross emission, determined by the method given in [3]. At the same time, soaking of small portions (samples) of the fluxes in the atmosphere with given relative humidity and determining increase of their mass by means of weighting before and after soaking as, for example, in study [4], allow more easily evaluating the flux hygroscopicity.

Baking of agglomerated flux OK 10.63 at 300 °C during 2 h was carried out before the experiment (recommendation of the manufacturer – ESAB, Sweden). Fused AN-43, AN-67B, AN-66 and synthetic SF-1 fluxes were baked at 400 °C for 2 h and fluxes AN-22M and SFT-6 were treated at 570 °C for 2 h (taking into account the general recommendations of operation [5]). Initial weighting of the samples of indicated fluxes of 30–80 g weight was performed immediately after baking and cooling to temperature close to room one. Then, the samples were put in the atmosphere, created in a tightly closed exiccator with water on a bottom, and soak at 20–25 °C. Thickness of layer of the fluxes in the samples was equal 12–15 mm. Size of the flux grains made 0.63–2 mm. The samples were weighted using an analytical balance and set of weights of the 4th class of accuracy according to GOST 7328–61. Results of the experiments are shown in the Figure and Table 2. They give the values of the basicity calculated on IIW formulae [6] using the average weight fractions of components on data of corresponding normative documents. It follows from the Figure that the hygroscopicity of synthetic flux SFT-6 (curve 2) only 19 % lower than that of agglomerated flux OK 10.63 (curve 1) during 744 h of soaking.

Further, the following changes were introduced in a standard production technology of the high-basicity synthetic flux: heating and cooling of sintered charge with furnace, increase of maximum sintering temperature from 1050 to 1160 °C and duration of soaking at maximum temperature from 1 to 2 h. Hygroscopicity of the high-basicity synthetic flux of basic composition, sintered on changed technology (Table 2, flux B1; Figure 1, curve 3), was 2.2 times lower than in flux SFT-6. However, hygroscopicity of the synthetic flux at that remains significantly higher than that of the most hygroscopic from the fused fluxes, i.e. honeycombed flux of AN-66 grade. Hygroscopicity of the low-basicity synthetic flux SF-1 is comparable with that of the fused ones.

It should be noted that the general (gross) level of absorption of different forms of the moisture by



Kinetics of absorption of the moisture by welding fluxes: 1 – OK 10.63; 2 – SFT-6; 3 – B1; 4 – AN-66; 5 – AN-22M; 6 – SF-1; 7 – AN-67B; 8 – AN-43 (*m* – relative increase of weight)

flux is characterized by specific values of weight increase of the samples. Portion of the moisture, absorbed by surface of grains and pores, and being removed at temperature from 20 to 200 °C makes only 5 % in the fused fluxes of AN 348A type. 15 % of total amount of the moisture, which should, apparently, be referred to sorbed and zeolite forms, is removed in 20–600 °C interval. The main amount of the moisture is removed from flux at heating above 800 °C and refers to chemically bound form of hydroxyl group type [2]. Only application of special methods of the investigation can provide accurate ratio in distribution of different forms of the moisture, absorbed by the synthetic fluxes. At the same time, portion of the moisture, absorbed by surface of the grains and micropores of the synthetic fluxes, is supposed to have the same order that in the fused ones. Elimination of appearance of zeolites in the synthetic flux due to significant difference of the conditions of their natural and industrial synthesis [7] from the conditions of synthetic flux sintering [1] is also to be considered. Therefore, it is assumed for the future that portion of the sorbed moisture is neglected due to its small

Table 2. Hygroscopicity of the fluxes of different types

Flux grade	Flux type	Flux basicity B_{IIW}	Hygroscopicity*, wt. %
OK 10.63	Agglomerated	2.56	8.4
SFT-6	Synthetic	2.40	6.8
B1	Same	2.40	3.08
AN-66	Honeycombed fused	0.97	0.34
AN-22M	Vitreous fused	1.35	0.32
SF-1	Synthetic	0.80	0.29
AN-67B	Vitreous fused	1.04	0.097
AN-43	Same	1.12	0.050

*Hygroscopicity during of soaking in humid atmosphere for 774 h.



amount and all moisture, absorbed by the synthetic flux, is referred to chemically-bound form.

Thus, rapid (10–23 times) increase of hygroscopicity of the synthetic flux was promoted by a change of component composition and basicity, represented in Table 3. It was supposed based on these data and taking into account specified remarks that appearance of the compounds having tendency to hydration in a finished flux and causing a rise of the flux susceptibility to moisture absorption (similar to silicate-lump in the agglomerated fluxes) was contributed by such a change of component composition. In this connection an investigation of phase composition of SFT-6 flux was of interest.

X-ray phase analysis of SFT-6 flux carried using DRON-UM1 diffractometer in monochromatic CuK_{α} irradiation by step-by-step scanning method (accelerating voltage 35 kV, current 25 mA) allowed determining the main components of its phase composition, i.e. fluorite CaF_2 , alumomagnesite spinel $MgO \cdot Al_2O_3$, forsterite $2MgO \cdot SiO_2$, cuspidine $3CaO \cdot 2SiO_2 \cdot CaF_2$ and free MgO . Small and trace amounts of diopside $CaO \cdot MgO \cdot 2SiO_2$, pseudo-wollastonite $\alpha-CaO \cdot SiO_2$ and other compounds are present in the flux. Nomenclature of the main components in SF-1 flux composition (for which the same analysis was performed [1]) does not correspond with the given one and includes nepheline $\beta-Na_2O \cdot Al_2O_3 \cdot 2SiO_2$, enstatite $MgO \cdot SiO_2$, andalusite $Al_2O_3 \cdot SiO_2$, braunite $MnO \cdot SiO_2$, wollastonite $\beta-CaO \cdot SiO_2$ and diopside.

Study of the compounds of SFT-6 flux being responsible for its high hygroscopicity will be carried out in the experimental way. For this a sintering of the simplified model charges consisting of fluorides and oxides is to be performed. The latter are taken in a compatible mole proportion corresponding to known minerals. Ratio of weight fraction of the fluoride to sum weight fraction of the oxides made 2:3 in the charge that is typical for the fluxes with high content of CaF_2 . An output of the investigated compound is supposed to be maximum at such ratios and presence

of the necessary thermodynamic conditions. At the same time a reproduction of all peculiarities of solid-phase reactions between the components, which are stipulated by the presence of large amount of CaF_2 , will be possible. Table 4 shows component composition of the charge. Charge materials given in Table 1 were used.

Granulated material with the same grain size as in earlier tested fluxes was obtained from the sintered charges by means of mechanical refinement and sieving. Further, hygroscopicity of the obtained granulated products was evaluated using indicated gravimetric method. Limit of the maximum soaking in humid atmosphere for all the samples made 336 h. Hygroscopicity of the separate charge components after their heat treatment using mode of sintering of model charges (maximum temperature 1125 °C; time of heating up to maximum temperature – 2 h; duration of soaking at maximum temperature – 2 h, heating and cooling with the furnace) was also determined taking into account the possibility of existence of real compounds of the unreacted components in a free state (for example, MgO , CaF_2) in the fluxes.

Table 4 shows a relative increase of weight of the samples characterizing hygroscopicity of the sintered products. It was stated that hygroscopicity of phases of SFT-6 flux lies in the ranges from 0.07 for fluorite up to 0.50 wt.% for sintered mixture of fluorite + forsterite. It was noted that the hygroscopicity of a pure MgO (superpure according TU 6-09-2807-78) is an order higher than of fired magnesite. However, if theoretically decide that all magnesite in SFT-6 flux charge was chemically inert during sintering as well as obtained properties of pure MgO then its contribution in the increase of flux weight would make $0.31 \cdot 2.6 = 0.81$ %. This is significantly lower of particularly registered hygroscopicity of SFT-6 flux under any conditions of sintering (2.0–3.5 wt.% during 336 h). It followed from these data that the sum contribution of mineral components of the SFT-6 synthetic flux cannot be an explanation of its increased

Table 3. Influence of component composition, basicity and parameters of sintering of the synthetic fluxes on their hygroscopicity*

Flux grade	Weight fraction of components, %								Peculiarities of sintering	B_{IIW}	Hygroscopicity, wt. %
	Magnesite	Fluorite	Alumina	Feldspar	Glass breakage	Manganese ore	Metallic manganese	Graphite			
SF-1	5	15	20	–	50	10	–	–	Setting of a charge in the furnace, heated up to 950 °C, soaking at that temperature for 1 h, air cooling	0.8	0.29
SFT-6	31	26.25	16	23	–	–	1.75	2	Setting of a charge in the furnace, heated up to 1050 °C, soaking at that temperature for 1 h, air cooling	2.4	6.80
B1	31	26.25	16	23	–	–	1.75	2	Soaking of a charge at maximum temperature 1160 °C during 2 h, heating and cooling with furnace	2.4	3.08

*Compared are the values of the hygroscopicity during soaking in humid atmosphere for 744 h.



Table 4. Composition and hygroscopicity of the sintered model charges

Charge grade	Fraction of components, wt. %								<i>m</i> [*] , wt. %
	Fluorite	Manganese oxide	Magnesite	Alumina	Lime	Feldspar	Quartz sand	Other components	
Flux basic composition									
SFT-6	26.25	–	31.0	16.0	–	23.0	–	Graphite 2.0; Mn 1.75	3.50
B1	26.25	–	31.0	16.0	–	23.0	–	Same	2.05
Charge with fluorite + alumomagnesite spinel MgO·Al ₂ O ₃									
FSh	41.0	–	18.0	41.0	–	–	–	–	0.22
FSh-1**	36.9	–	16.2	36.9	–	10.0	–	–	0.21
Fluorite + forsterite 2MgO·SiO ₂									
FF	39.77	–	35.28	–	–	–	24.95	–	0.50
Fluorite + diopside CaO·MgO·2SiO ₂									
FD	39.0	–	12.0	–	17.0	–	32.0	–	0.47
Fluorite + wollastonite CaO·SiO ₂									
FV	40.0	–	–	–	29.0	–	31.0	–	0.13
Cuspidine 3CaO·2SiO ₂ ·CaF ₂									
K	21.3	–	–	–	45.9	–	32.8	–	0.17
Fluosilicates with excessive and insufficient content of feldspar									
FS1	31.0	–	–	–	–	69.0	–	–	0.11
FS2	43.0	7.4	–	–	–	49.6	–	–	0.04
Fluorite + magnesite CaF ₂ ·MgO									
FM	65.0	–	35.0	–	–	–	–	–	1.46
Charge components (lime, chemically pure MgO, alumina, magnesite, fluorite, feldspar)									
I	–	–	–	–	100	–	–	–	30.10
MgO	–	100	–	–	–	–	–	–	2.60
G	–	–	–	100	–	–	–	–	0.83
M	–	–	100	–	–	–	–	–	0.21
F	100	–	–	–	–	–	–	–	0.07
PSh	–	–	–	–	–	100	–	–	0.04

*Relative increase in weight of the granulated product samples for the period of soaking in humid atmosphere for 336 h. **Charge with feldspar addition for improvement of sintering.

hygroscopicity. However, experimental data of [8] allowed assuming that a contribution of free lime CaO in composition of the finished flux creates the increased hygroscopicity of SFT-6 flux.

As shown in [8], free lime can be an intermediate product of chemical reaction between the CaF₂, oxides and silicate-lump with formation and decay of complex oxyfluoride due to effect of anion redistribution mechanism between the calcium and magnesium during heating of a multicomponent charge of the agglomerated flux with excessive content of the acid oxides. Further, the lime appeared in such a flux is consumed for formation of anorthite mineral.

If possible intermediate reactions for formation of the magnesium and calcium oxyfluorides are omitted then a process of lime formation can be represented by more simple reaction



An equilibrium constant of such a reaction can be interpreted as

$$k_{\text{eq}} = (a_{\text{CaO}} \cdot a_{\text{MgF}_2}) / (a_{\text{CaF}_2} \cdot a_{\text{MgO}}), \quad (2)$$

where *a* is an activity of agents, indicated in the indices.

Temperature dependence of the equilibrium constant of this reaction can be calculated using an exact method of L.P. Vladimirov and reference value of variables [9]. Taking into account formulae (2) the obtained calculated values lg *k*_{eq} from –3.027 up to –2.414 at temperatures from 800 to 1127 °C, respectively, indicate the appearance of several percents of products of reaction (1) in MgO_(s)–CaF_{2(s)} system after its continuous soaking at 1125 °C. Specified reaction has a tendency to intensify with temperature rise.

A model charge consisting of MgO and CaF₂ in 1:1 mole ratio was sintered for checking the possibility of formation of the free lime in reaction (1). Hygroscopicity of the sintered product made 1.46 wt. % during 336 h of soaking that, respectively, 7 and 21 times higher than in magnesite and fluorite, sintered individually (see Table 3). Obtained result indicates that a phase appears in the process of sintering in MgO_(s)–



CaF_{2(s)} system, the hygroscopicity of which significantly higher than in the initial components. Hygroscopicity of the lime after heat treatment in the mode of sintering of model charge was also evaluated and made 30.1 % during 336 h of soaking in the exiccator. This result has a good agreement with theoretical ratio of the molar masses of quicklime (CaO) and slaked lime (Ca(OH)₂). The latter is higher of the first by 32.12 %.

Content of the free lime in the product can be approximately evaluated taking into account additivity of the hygroscopicity m_{Σ} of the sintered product of MgO_(s)-CaF_{2(s)} system as a result of contribution of all phases of this product and allowing that indicated sintered product has no other agents except for the initial chemical agents and products of reaction (1). For this it is also assumed that the hygroscopicities of fluorite m_f and manganese fluoride m_{MgF_2} are equal. Union of magnesite, fluorite and MgF₂ in the sintered product is considered as one agent the hygroscopicity m_0 of which consists of contributions of magnesite m_m and fluorite m_f accepted considering their weight fractions in the initial charge:

$$\begin{aligned} m_0 &= 0.65m_f + 0.35m_m = \\ &= 0.65 \cdot 0.07 + 0.35 \cdot 0.21 = 0.119 \%. \end{aligned}$$

If hygroscopicity of the lime m_l is known than its mass fraction x_l in the sintered product of MgO_(s)-CaF_{2(s)} system can be easily determined from the following equation relatively to x_l :

$$m_{\Sigma} = x_l m_l + (1 - x_l) m_0. \quad (3)$$

The calculation using expression (3) showed that content of the free lime in the sintered product of MgO_(s)-CaF_{2(s)} system makes 4.47 wt.%.

Such minerals as alumina spinel MgO·Al₂O₃, calcium aluminate CaO·Al₂O₃ and CaO·2Al₂O₃ etc. are thermodynamically very stable compounds in a wide temperature interval. Therefore, increase of temperature provides beginning of their formation at achievement of sufficient diffusion mobility of the atoms of the initial components. Many factors (lattice defectiveness, presence of additions and moisture of constitution in the components, appearance of liquid and gas phases in salt-oxide systems) promote mineral formation under real conditions reducing temperature of beginning of the solid-phase reactions. For example, formation of spinel from commercially pure and naturally humid components becomes already apparent at 700–800 °C and that for forsterite makes 900 °C [10]. As a result the basic oxides and fluorite dominate over the acid oxides in the charge of sintered flux and the latter, probably, completely or mostly will be consumed for formation of complex oxides and oxyfluorides to the moment when the oxide system achieves its maximum temperature. On the contrary the fluorite and magnesite will remain in excess. The lime formed according to reaction (1) at temperature, approximately, 700–1000 °C, under these conditions reacts with, for example, Al₂O₃ forming the calcium aluminates. However, after free Al₂O₃ has been exhausted the lime, appearing during soaking at maxi-

imum temperature, cannot be quickly bound in the minerals.

Hygroscopicity of the high-basicity synthetic flux (see the Figure and Table 1) is reduced with the increase of temperature of sintering and duration of soaking at maximum temperature. Reduction of a content of the free lime due to processes of mutual dissolution of the components at high temperatures, as well as reaction of CaO with the initial chemical compounds with formation of more complex secondary minerals [10], can, probably, explain such dependence. However, speed of these processes, apparently, is not enough for complete binding of the lime, formed according to reaction (1). Therefore, increased hygroscopicity of the finished high-basicity synthetic flux of MgO-CaF₂-Al₂O₃-SiO₂ system is caused by remains of some amount of the free CaO.

CONCLUSIONS

1. It was shown that hygroscopicity of the flux increases 10–23 times and become comparable with hygroscopicity of the agglomerated flux with rise of basicity of the synthetic flux from 0.8 to 2.4 times. The latter is provided by simultaneous rise of weight fractions of magnesite and fluorite in its composition.

2. It was determined that the presence of the free lime, forming as a result of chemical reaction between CaF₂ and MgO taking place in MgO-CaF₂-Al₂O₃-SiO₂ system at high (approximately 1100 °C) temperature and absence of the acid oxides in a free form which could effectively bound the lime in the minerals, in composition of the synthetic flux can be the reason of high hygroscopicity of the synthetic fluxes of MgO-CaF₂-Al₂O₃-SiO₂ system.

3. It was stated that hygroscopicity of the high-basicity synthetic fluxes can be significantly increased by rise of sintering temperature and duration of soaking at this temperature. However, their hygroscopicity is significantly higher than in fused ones.

1. Kasatkin, B.S., Tsaryuk, A.K., Vakhnin, Yu.N. et al. (1994) Synthetic welding fluxes, fabrication and fields of application. *Avtomatich. Svarka*, **3**, 62–66.
2. Goncharov, I.A., Paltsevich, A.P., Tokarev, V.S. et al. (2001) About the form of hydrogen existence in welding fused fluxes. *The Paton Welding J.*, **4**, 27–30.
3. GOST 22974.14–90: Welding fused fluxes. Procedure for determination of humidity content. Moscow: Standart.
4. Kuzmenko, V.G., Guzej, V.I. (2004) Hydration of fluxes with a locally changed chemical composition of grains. *The Paton Welding J.*, **6**, 41–43.
5. Potapov, N.N. (1979) *Principles of flux selection in welding of steels*. Moscow: Mashinostroenie.
6. Galinich, V.I., Sokolsky, V.E., Kazimirov, V.P. et al. (1991) Basicity of fused fluxes and possibility of its experimental determination. *Avtomatich. Svarka*, **5**, 35–37.
7. Eremin, N.I. Nonmetallic mineral products. <http://web.ru/db/msg.html?mid=1172887&uri=glava10.htm>
8. Sokolsky, V.E., Roik, A.I., Davidenko, A.O. et al. (2010) On phase transformations in agglomerated flux of salt-oxide slag system at heating. *The Paton Welding J.*, **12**, 9–14.
9. Vladimirov, L.P. (1970) *Thermodynamic calculations of equilibrium of metallurgical reactions*. Moscow: Metallurgiya.
10. Budnikov, P.P., Ginstling, A.M. (1965) *Reactions in mixtures of solids*. Moscow: Gosstrojizdat.

TRANSFORMABLE STRUCTURES (Review)

B.E. PATON, L.M. LOBANOV and V.S. VOLKOV

E.O. Paton Electric Welding Institute, NASU, Kiev, Ukraine

The paper deals with the main classes of transformable structures, which are shells of soft and rigid type. The main problems are outlined, which greatly reduce the range of application of such structures in modern engineering. Technical solutions, allowing optimization of functional properties of transformable shell structures, are suggested.

Keywords: *transformable structures, load-carrying shells, transformable shells*

Searching for a compromise between the need to create shell-type structures with the required parameters and possibility of their further transportation to the operation site involves addressing a wide range of engineering tasks, accompanied by upgrading of the currently available technologies and work performance in difficult-of-access places. The main problem consists in the complexity of realization in the intended structure operation site of the time- and labour-consuming process of its fabrication. On the other hand, development of engineering determines the need for shells of ever greater volume and overall dimensions, range of application of which is limited either by the absence of the respective transportation means, or their extremely high cost. The above conditions require application of special class of structures, capable of changing their geometrical dimensions in a broad range at practically unchanged mechanical properties of the material of the shell — transformable structures (TS).

The urgency of the work on TS development is due not only to appearance of new non-standard engineering tasks, requiring a search for new decisions of the respective level. A common case is that of «shell-in-shell», when upgrading or replacement of large-sized tanks in limited technological space (for instance, a compartment of an all-welded ship hull) is required.

Known is a number of TS applications, in which the transformation process is applied to solve an independent engineering task or obtain new physical properties of the object, namely excess buoyancy, rigidity, reflectivity, etc., that can be achieved in the case, when TS functional and technological characteristics meet the requirements made of its prototype.

Experience of practical application of engineering facilities of this class allows outlining the main problems, elimination of which is capable of essentially widening the sphere of TS application in engineering. Solution of these problems is reduced to ensuring multiple reproducibility of geometrical parameters, leak-proofness and stability of strength characteristics of the transformed shell.

Load-carrying shells taking the load at sufficient rigidity have the greatest applied importance. Their capability of considerable elastic displacements can be regarded as undesirable consequence of the small thickness and flatness of the shell, associated with geometrical non-linearity and loss of stability. This is exactly the property, however, which is the basis for the technology of changing the form of the shells, combining the advantages of enclosing and load-carrying structures.

In most of the cases the known TS can be conditionally regarded as bodies of shell type, which are divided into three main classes: load-carrying soft; based on transformable frame; and rigid. By the type of transformation TS are divided into structures transformed by application of excess pressure in the inner volume, and through mechanical transformation of the load-carrying frame, in particular with application of shape-memory materials. By their functional characteristics TS can be also conditionally divided into leak-proof and non leak-proof.

PWI developed a separate class of TS, which belong to hard shells and which are capable of combining the characteristics inherent to different types of transformable shells [1]. Technology of changing the form of thin-walled metal shells, to which V.M. Balitsky contributed greatly, was developed on the basis of the method of isometric bending of surfaces and combines the main advantages of the considered TS classes:

- possibility of continuous transformation of structures without application of auxiliary technological operations;
- absence of the need to maintain in the inner volume the excess pressure, used only during transformation;
- leak-proofness of the transformable shells, achieved by application of the technology of butt welding;
- absence of the need for a load-carrying frame;
- high values of transformation coefficient K_t ;
- structure compactness before form change.

Developed methods of shell structure form change with preservation of topologically equivalent surface allowed creating a wide range of TS based on spatial bodies of revolution — spheres, ellipsoid, etc. Their fabrication technology is based on the methods of com-

binatorial geometry, and in most of the cases practical solution of the problem is realized by substitution of the surface by a family of equivalent polygons sequentially assembled by bending along the mating lines up to mutual superposition with formation of a compact pack.

The most promising in terms of effectiveness of working space utilization and convenience in manufacturing of initial billets are structures, the form of which is close to the cylindrical or conical shape [2].

Design-technological solution of TS of a cylindrical type is based on the principle of transformation of a hyperboloid fold into a shell of uniform circular cross-section. Hyperboloid fold is a complex polyhedral surface, determined by two kinds of edges, which are rectilinear generatrices of two coaxial one-sheet hyperboloids. At certain geometrical relationships such a fold is mobile in the axial direction, and can be folded compactly until its panels and edges touch each other. Owing to isometricity of the surfaces of the fold and cylinder, the stacked fold can be transformed into a cylindrical shell by pressure, created inside the volume enclosed by this shell. Here, rotation of one of the cylindrical bases relative to the other, fold form change and bending of rectilinear edges along a cylindrical surface take place. Degree of fold opening depends on the level of forming pressure, at joining of several folds along the edges a multisection hyperboloid fold can be obtained, in which each of the sections is an independent transformed element.

Figure 1 shows a transformable cylindrical shell, obtained by mating of two hyperboloid folds. Different orientation of the edges relative to the bases of cylindrical billets allows making right-hand and left-hand folds.

In unidirectional multisection systems the angle of reciprocal rotation rises in proportion to their number. The rotation, which is highly undesirable in most of the cases of potential application of cylindrical TS

(for instance, docking chambers, which cannot have any deplanation or circular displacement of docking units), can be prevented at equal quantity of right and left folds.

The main disadvantages of cylindrical TS include labour-consuming technology of forming hyperboloid folds, requiring development of complex special equipment for each typesize of the end item. It was established experimentally that the optimum result in fold formation can be achieved only in a certain range of relationships $0.3 \leq H/D \leq 0.6$, where H is the height of the transformable part of the shell, D is the diameter of the shell-billet.

In most of the cases preference is given to well-established technology of TS fabrication by forming corrugated discs from thin-walled conical billets, which allows development of structures of a broad range of typesizes and parameters.

Similar to the considered case of structures of a cylindrical shape, technology of manufacturing TS of a conical type is based on the method of isometric transformation of the surface, which envisages the possibility of shell bending without material tension or compression [3]. The technology consists in changing the form of the billet (closed conical truncated shell) into a disc with multiple circular corrugations. Initial height of the cone decreases to a value, corresponding to the depth of a groove of the forming matrix.

Metal discs with circular corrugations widely used in instrument-making mostly have small dimensions and shallow corrugations. Such membranes are usually made by stamping that is unacceptable for items with deep circular corrugations at a relatively small pitch.

As the entire billet surface is deformed simultaneously, this requires a technological process with powerful pressing equipment; stamping of membranes with considerable corrugation depth cannot be per-

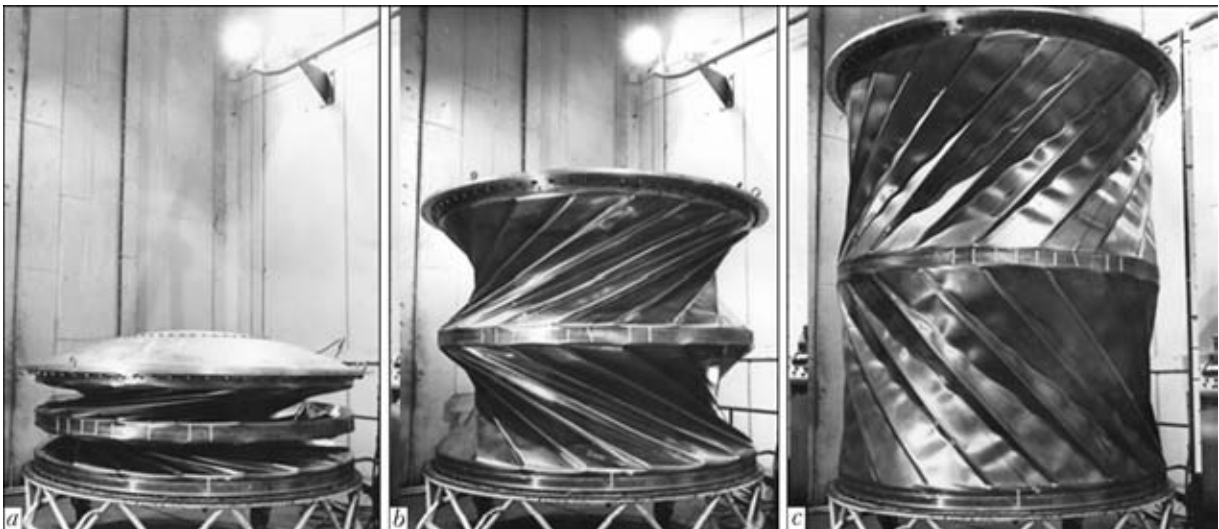


Figure 1. Transformable cylindrical two-section shell (material – 12Kh18N10T steel 1 mm thick and 2000 mm in diameter) at intermediate stages of transformation (*a*, *b*) and in the deployed condition (*c*) ($K_t = 10$)

formed in a single-step process, and a set of dies with smoothly increasing impression depth is required.

In addition, billet material undergoes considerable (up to 50 %) plastic deformations, causing work hardening and increasing its hardness. Restoration of billet ductility requires interoperational annealing, surface cleaning to remove scale, etc.

Considering the above factors, the most acceptable technology of form change of a conical billet can be regarded to be rotation extrusion by forming roller on die mold, reproducing the calculated geometry of the final corrugated disc. Technology allows forming discs of the diameter from several tens of centimeters up to several millimeters. After sealing the discs on the large and small base of initial cone, their reverse transformation into a conical shell can be performed by creating excess pressure in the inner volume. Here circular corrugations caused by local tension of material at forming and increasing the structure radial rigidity, are preserved on the shell surface.

The required number of individual corrugated discs can be joined by welding along the large and small bases into one structure, which takes the shape of a multicone shell of the required dimensions and configuration after transformation. Application of multicone shells is promising in the aerospace field, as load-carrying rods, docking modules and transfer tunnels, additional functional volumes or containers for used materials [1].

Figure 2 shows a multicone shell of a periodic profile, consisting of transformable corrugated discs (1), and general view of leak-proof TS after expansion (2), which can be accepted in development of large-sized space structures [2]. Shell diameter can be up to 4000 mm with 40 m^3 and greater volume that allows such structures to be used as accumulator tanks and storages for bulk and liquid substances [3]. Figure 3 shows a large-sized TS, used as accumulator tank in the system of self-contained water supply.

In the world practice the first TS to become accepted were load-carrying transformable soft shells,



Figure 2. TS of a periodic profile (material – VT1-0 titanium 0.15 mm thick), consisting of 11 basic conical shells [2]: 1 – structure in the compact folded state; 2 – deployed structure

which were used in construction, in development of flying and space vehicles. Their improvement promoted appearance of new materials, combining high strength with resistance to aggressive environmental factors and small specific weight.

Pneumatic structures based on air-borne coverings, in which the functions of the frame are fulfilled by load-carrying pneumobottles, became accepted in building industry. The greatest functionality is characteristic for soft shells with double transformation (Figure 4): first step of volume transformation is designed for creation of basic elements of the load-carrying structure, and the second step – for creation of technological space of the required configuration on their base.

Development of polymer and composite materials on their base over the recent decades promoted emergence of a new subclass of engineering facilities, which were called air-supported structures. The load-carrying shell is fixed in the working position by maintain-

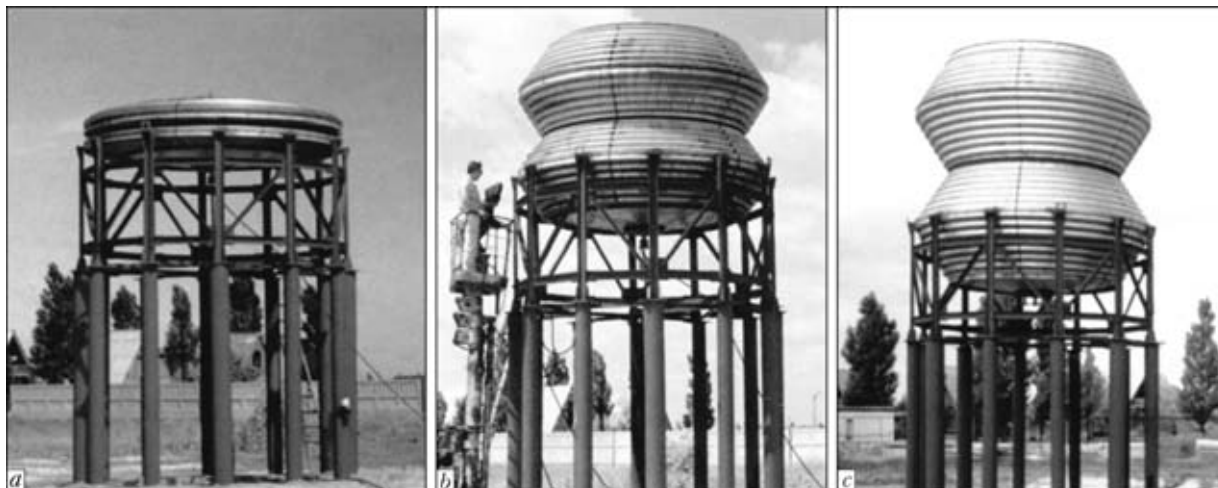


Figure 3. Large-sized TS from four conical shells (material – 08Kh18N10T steel of 2.5 mm thickness, 3800 mm diameter, 4500 mm height, 40 m^3 volume) [3]: a – initial; b – intermediate; c – final stage of transformation

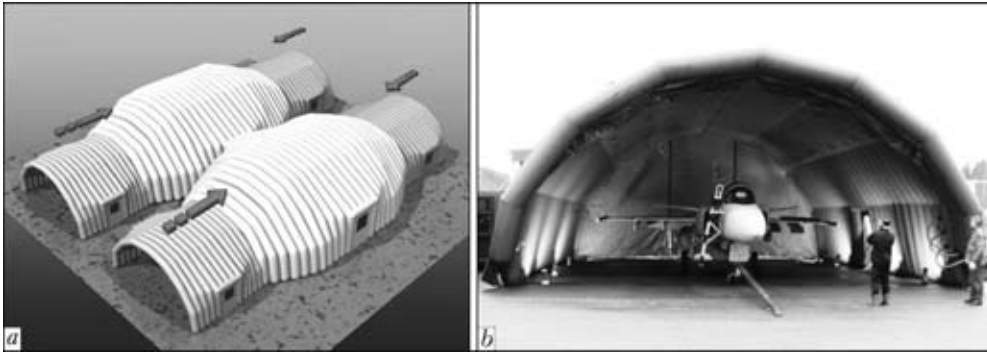


Figure 4. Air-borne structures of hangar type based on pneumobottles, designed for application as mobile living quarters and storage premises (a: arrows show direction of reverse transformation) and for sheltering airplanes in Swedish Airforce (b) [4]



Figure 5. Variants of configuration of air-supported structures of Vingida Company, Finland-Lithania [5]

ing in the service volume a slight excess pressure, not exceeding the level of normal barometric fluctuations. Soft shell from reinforced light-tight PVC fabric is hermetically fastened on the strip footing, the perimeter of which can be equal to hundreds of meters (Figure 5).

Variant of air-supported structure of radar station radome [6], made from reinforcing material of vectran type, is shown in Figure 6. Shell of 36 m diameter, 39 m height and about 8 t weight is capable of opposing wind loads, corresponding to wind velocities of more than 200 km/h without impairing the radar performance.

Application of load-carrying soft shells became one of the first successful solutions on lowering the weight of artificial Earth satellites. In particular, the USA implemented the projects of launching to near-earth

orbit three research satellites and a series of commercial satellites, which represent various types of soft transformable shells. The US Naval Research Laboratory is planning the launch of a spherical research satellite, constructed on the base of a transformable frame [7]. Because of special features of the considered structures operation under the conditions of open space highly important is development of shell materials, characterized by specified properties.

Figure 7 gives the general view of a satellite with a spherical shell from synthetic polyether fibre – (mylar) – with metalized coating.

In 2009 NASA Langley Research Center (NASA LaRC) conducted a successful experiment on launching and retrieval of a lander built by ILC Dover on



Figure 6. Air-supported structure of radome on ILC Dover testing platform in the Gulf of Mexico [6]



Figure 7. PAGEOS observation satellite with 56 kg mass and 31 m diameter of the shell [8]

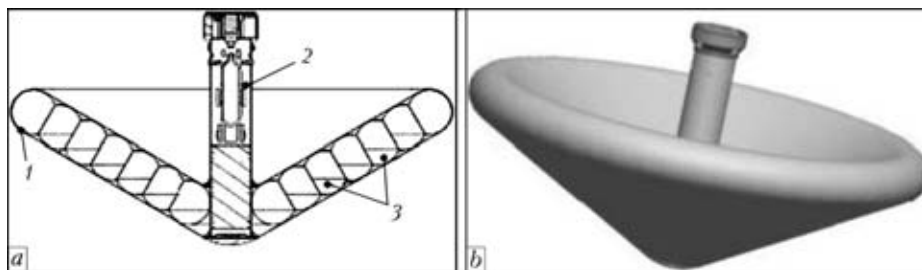


Figure 8. Schematic of a transformable lander (*a*: 1 – protective Kevlar shell; 2 – rigid central part of the structure with boosting system; 3 – toroidal load-carrying pneumobottles), and general view of the vehicle (*b*) [9]

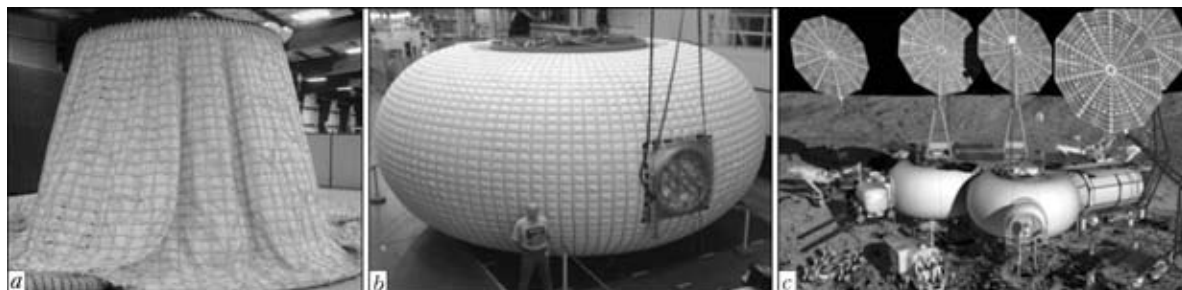


Figure 9. Torroidal Lunar Habitat: *a* – folded condition; *b* – completely deployed condition; *c* – project of NASA manned lunar outpost, constructed on the base of Torroidal Lunar Habitat [6]



Figure 10. Stages of X-Hab module transformation [6]

the base of elastic transformable shell. The vehicle was designed as a pneumatic structure with airborne covering and frame from load-carrying pneumobottles (Figure 8).

At the altitude of 211 km a kevlar shell laid into a cylindrical pack of 0.4 m diameter expanded at excess pressure up to 3 m diameter and returned to dense atmospheric layers. The experiment demonstrated the ability of structures of this class to resist pressures and temperatures, arising at passage through atmospheric layers at hypersonic velocities, while preserving the structural integrity and aerodynamic stability of the shell [9].

Joint efforts of ILC Dover and NASA on designing habitable long-term lunar outposts resulted in development of a prototype of a Toroidal Lunar Habitat, which is a transformable air-supported structure from vectran, reinforced by kevlar fibres, and rigid cylinder base for accommodation of power equipment (Figure 9).

Within NASA «Constellation» program ILC Dover developed new X-Hab Lunar Habitats, which are hybrid structures based on two metal semi-spherical shells, connected by soft cylindrical transfer tunnel of variable length with transformation coefficient, i.e.

ratio of determining parameters in the initial and transformed conditions, $K_t = 10-12$ [6]. Figure 10 gives the stages of transformation of the structure at NASA LaRC.

In all probability, wide acceptance of load-carrying soft shells in space environment may be prevented by a rising contamination of the near – Earth space. The above structures operated in low orbits, practically free from the remnants of used space vehicles,

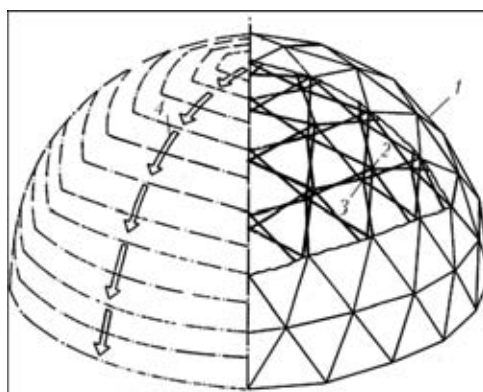


Figure 11. Schematic of a collapsible structure [10]: 1 – spherical structure; 2, 3 – pinning points; 4 – folding direction

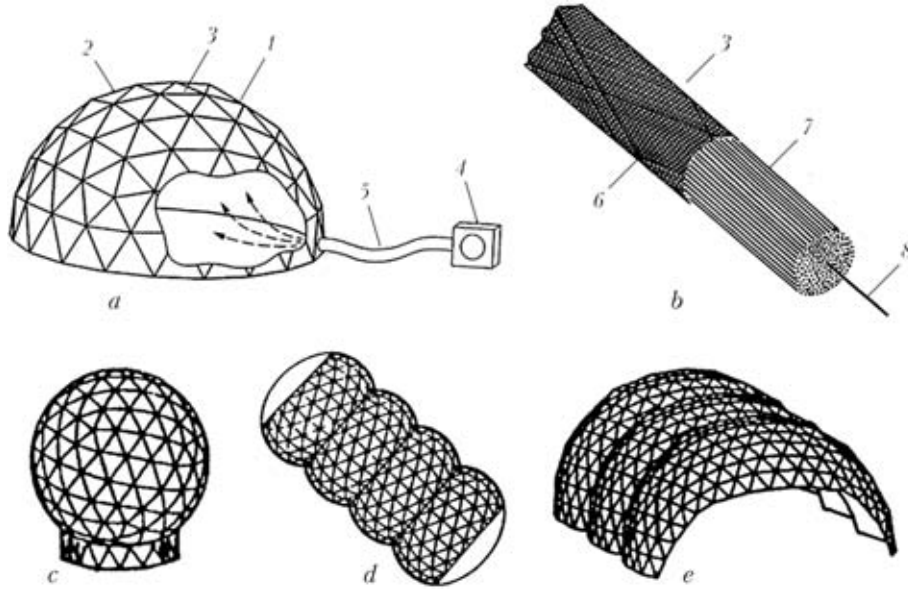


Figure 12. Schematic of an inflatable structure with variable rigidity of the shell [11]: *a* – variant of technology application for formation of sealed semi-spherical shell; *b* – element with variable rigidity; *c-e* – possible configurations of structures developed by this technology; 1 – transformable structure; 2 – shell outer covering from mylar or kapton; 3 – elements of variable rigidity; 4 – compressor; 5 – discharge duct; 6 – element outer covering; 7 – bundle of thermoplastic fibre; 8 – heating element

and their collision with extra-terrestrial hard particles could only be of random nature.

Stationary space stations are fitted with following and orbit correction system for protection from collision with small objects; none-the-less repair and replacement of outer shell elements is included into the mandatory routine maintenance.

The obvious advantage of load-carrying soft shells consists in their capability of unlimited number of direct and reverse transformations, compactness in the folded condition and low specific weight of the structure. Coefficient of transformation K_t can reach 25–30. Their main disadvantages are absence of sufficient rigidity, need for continuous maintenance of excess pressure in the inner volume, low stability of shell material against temperature variations, ultraviolet radiation, wind load, etc.

Construction of soft shells based on load-carrying transformable frame has two main objectives: make the transformation process a single-step one, and create a frame, the configuration of which only slightly affects the structure coefficient of transformation. In

a folding structure (Figure 11), pinning points 2 and 3 of load-carrying cane elements of the frame have sliding connections; forces arising in them are consecutively transferred to adjacent nodes in direction 4. As a result, frame transformation proceeds in the direction of reduction of its horizontal section.

Searching for means to ensure the geometrical stability of the frame promoted emergence of structures with variable rigidity of the shell, in which application of the load-carrying base is combined with transformation using excess pressure.

Figure 12 shows the transformable shells, which are fixed in the open position using elements based on thermoplastic fibre. Element heating and their subsequent cooling lead to rigid fixation of softened fibres in the position, determined by configuration of individual frame sections.

The main disadvantage of elements with variable rigidity is the impossibility of multiple transformation of structures on their base – a characteristic property of soft shells. An alternative solution was introduction of geometrically stable load-carrying structures of complex spatial configuration, close to spherical shell.

Various variants of so-called Hoberman sphere became widely accepted, where the load-carrying frame was developed using computer simulation technologies.

Figure 13 gives the schematic of PERCS satellite, transported to orbit in the folded compact condition [12]. PERCS project can be regarded as a successful application of the technology of transformation of a shell, the leak-proofness of which is not necessary; the object belongs to the class of passive satellites and is not fitted with any hardware.

Over the recent years attempts have been made of testing shell-type transformable habitable structures

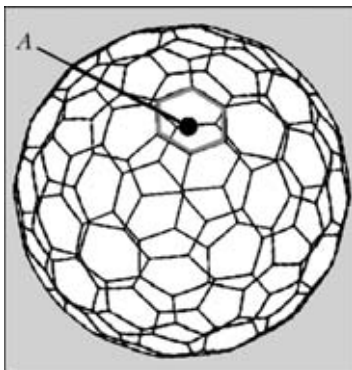


Figure 13. Diagram of PERCS satellite – a transformable sphere formed by movably connected panels *A* [13] of 1.25 m diameter in the initial condition and 10.3 m in the transformed condition

out of terrestrial atmosphere. None of the announced projects, however, has been so far realized in it is full scope. In 2006–2007 Bigelow Aerospace, USA, launched to 500 km orbit the first two prototypes of habitable space stations, which are soft leak-proof multilayer shells of 150 mm thickness supported on a frame (Figure 14). After transformation by inducing excess pressure in the inner volume, module diameter increases up to 2.54 m at unchanged length [14]. At considerable specific weight of the rigid metal frame and low coefficient of transformation, the module structures lack the main advantages of flexible shells, but have the decisive advantages when being launched by rocket-carriers with a relatively small section of the transportation compartment.

Modern materials with new properties allow creating space TS, in which the transformation coefficient K_t can reach 10. However, the problem of combining these parameters with sufficient strength and leak-proofness of the shells is still unsolved. In particular, the structures of vacuum-tight shells of Genesis modules are capable of providing transformation coefficients $K_t \approx 1.6$, which under the terrestrial conditions are acceptable only at transformation of the volume of some laboratory and measuring devices, or future structures, in which parallel problems of optimization of weight-dimensional and strength characteristics are solved.

Transformation of the volume of individual elements of instruments is widely used in laboratory and measuring instrumentation, in components of piping systems, and in special stop valves, in particular tubular condensers — torroidal shells with a circular or close to circular shape of the meridian, capable of undergoing slight elastic deformations. Bellows — thin-walled tubes with circular corrugations, in most of the cases made from nonferrous metal alloys and alloyed steels, became widely accepted.

In bellows structures K_t is determined by the features of shell profile, capable of compression only within the intercorrugation spaces. Bellows are leak-proof, and can be subjected to multiple shape changes under the impact of varying pressure, but they have a special feature — loss of axial stability at inner pressure, while not having sufficient bending rigidity.

Comparative analysis of currently-available TS classes leads to the conclusion that combination of technologically acceptable strength characteristics of the shell with considerable transformation coefficients at simultaneous leak-proofness is only achievable in rigid load-carrying shells, among which conical and multicone transformable structures are the optimum variant owing to simplicity of technology. None-the-less, functional qualities of this class of TS are limited by lack of well-established algorithm of multiple form change, while absence of invariance of embodiments requires development of a versatile calculation procedure of determination of basic geometrical parameters.

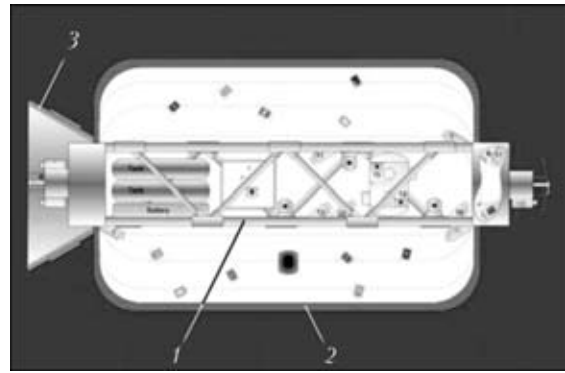


Figure 14. Genesis space module I/II [14] (1363 kg weight, 4.4 m length in the transformation condition, diameter before transformation 1.6, after transformation — 2.54 m): 1 — rigid metal frame, carrying life support systems of the module; 2 — transformable shell; 3 — docking assembly

One of the main approaches to optimization of rigid transformable shell design, allowing an essential expansion of their applications, is creation of a two-layer structure, in which the consequences of possible depressurizing can be prevented owing to duplication of the outer wall.

It was experimentally established that the process realized mainly at the expense of material bending deformation also allows performing simultaneous form change of several billets of equal geometry. Further assembly and welding of basic elements in TS are performed on circumferential load-carrying elements (frame-rings), fulfilling the functions of a jig at alignment of basic element edges, of backing during the welding process and of load-carrying element taking technological and service loads (Figure 15, *b*). Tightness of contact of two-layer shell edges is ensured by a specially developed device, which allows tying basic elements along TS axis.

After sealing the produced discs around the large and small base of initial cone, their reverse transformation into a conical shell is performed by inducing excess pressure in the inner volume. After final transformation the shell surface preserves the characteristic circumferential corrugations, caused by local tension of material in the tips of technological edges at form change and increasing the radial rigidity of the produced structure.

The purpose of the experiment with test two-layer shell consisted in determination of the influence of duplicating wall on the nature of transformation and degree of increase of excess pressure, required for structure transformation. Figure 15 gives the model of two-stage shell structure in the compact and deployed condition. The shell was fitted with a pressure gage with $0.01 \cdot 10^4$ Pa division value. At smooth increase of pressure opening of a two-layer corrugated disc proceeded in stages, starting with larger diameter corrugations and ending by smaller ones, inner shell deformation causing increase of excess pressure in the interwall space, and, consequently — opening of the outer shell.



Figure 15. Model of a two-stage transformable conical shell (material – VT1-0 titanium 0.15 mm thick): *a* – compact condition; *b* – deployed condition; *c* – axial sections of load-carrying elements (frame rings) *I* and *II*; *C, D* – load-carrying and auxiliary frame rings; *F* – shell bottom; *G* – transformable conical shells

After achievement of maximum pressure value for the current diameter, the corrugation deployed jump-like, pressure decreasing abruptly, because of increase of the shell inner volume; the process was repeated right up to complete transformation of TS to the calculated dimensions. Pressure required for complete transformation of the two-layer shell was equal to $P_2 = 22.1 \cdot 10^4$ Pa, and for single-layer shell with similar parameters $P_1 = (9.32-9.51) \cdot 10^4$ Pa. Thus, the

duplicating wall required more than two times increase of technological pressure of transformation.

During transformation of the truncated cone into a corrugated disc and subsequent reverse transformation precise geometrical dependencies between the angle of conicity, length of cone generatrix and corrugated disc parameters are ensured, that allows simulation of the technological operations and double-shell TS components with high precision. Results obtained during the experiment allow making the conclusion about the possibility of development of extended two-stage structures, similar to the currently available multicone TS of periodical profile.

Future tasks of application of multicone TS as extendable systems and case parts of orbital space module are related to the need for their subsequent recovery, requiring optimization of the mechanism of reverse transformation with preservation of initial geometry. The capability of transformable rigid shells for multiple reproducibility of stable geometrical dimensions is in keeping with the bases of the method of regular isometric transformation. However, the real metal shell after the first repeated cycle of transformation develops wave-like deformations in the inter-corrugation spaces, which are indicative of the local loss of stability (Figure 16).

During the conducted experiment a rarefaction of approximately $P = -9.32 \cdot 10^4$ Pa was induced in the model inner cavity by a vacuum pump, that corresponds to reverse value of pressure that is required for deployment of the initial corrugated disc. Within the complete transformation cycle of 33 s duration, a complete restoration of the initial shape of a two-stage shell with local deformations in the vicinity of edge tip was noted. At subsequent cycles an increase of local deformation and combining of their localization zones was noted, which leads to overall loss of structure stability.

One of the possible variants of the change of transformation technology for realization of multiple form change of the shell can be reduction of the rounding-off radius of matrix edge tips, increasing the rigidity of residual circumferential corrugations. Here, the zones of maximum elasto-plastic deformations are localized

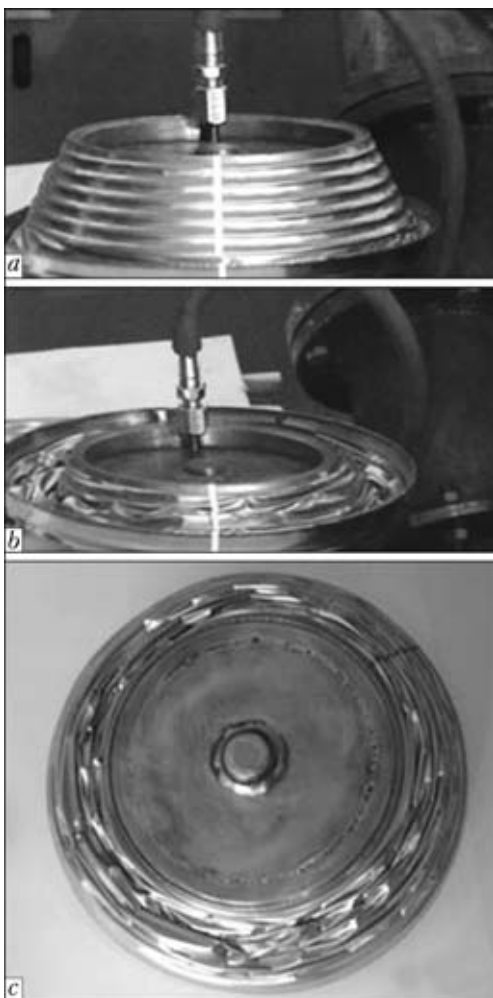


Figure 16. Reverse transformation of conical shell with sinusoidal profile of the generatrix (material – titanium VT1-0 0.15 mm thick): *a* – intermediate stage of transformation; *b* – full reverse transformation of the shell; *c* – shell appearance after complete reverse transformation

in the vicinities of the corrugation tips, and the sinusoidal profile of the conical generatrix becomes close to the shape of piecewise-broken curve, corresponding to the initial mathematical model of mirror reflection of a truncated conical surface.

Figure 17, *a* and *b*, shows the stages of reverse transformation of a model of conical TS with piecewise-broken profile of the generatrix, and configuration, corresponding to the shell, shown in Figure 16. After complete restoration of the initial shape no deformations were noted, and no zones of local loss of stability were found at three subsequent cycles. Figures 16, *c* and 17, *c* show the appearance of conical TS with sinusoidal and piecewise-broken profiles of the generatrix after complete reverse transformation. In Figure 16, *c* one can see an abrupt distortion of the shell surface in the form of multiple fractures of intercorrugation spaces, and the shell in Figure 17, *c* has completely preserved its initial geometrical dimensions.

Conducted experiments on model samples are indicative of the possibility of repeated transformation of TS with structural elements of conical type and development of two-stage TS.

Analysis of various TS classes showed that they are becoming ever wider accepted in building industry and aerospace engineering. TS developed at PWI on the base of rigid load-carrying shells are promising for application under various conditions of mounting and service, including extreme conditions.

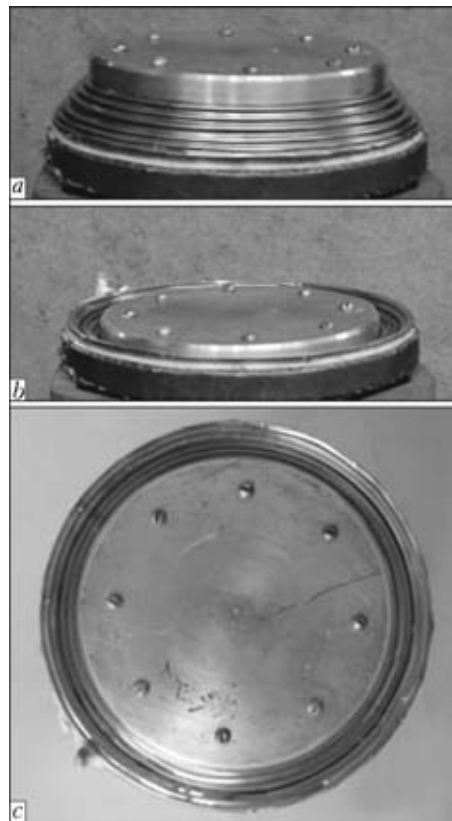


Figure 17. Reverse transformation of conical shell with piecewise-broken profile of the generatrix (material – titanium VT1-0 0.15 mm thick): *a* – intermediate stage of transformation; *b* – full reverse transformation of the shell; *c* – appearance of the shell after full reverse transformation

- (2003) *Space: technologies, materials, structures*. Ed. by B.E. Paton. Taylor&Francis, 447–495.
- Paton, B.E., Lapchinsky, V.F. (1997) *Welding and related technologies in space*. Cambridge Int. Sci. Publ., 88–105.
- Paton, B.E., Lobanov, L.M., Samilov, V.N. et al. (2006) Design and features of fabrication technology of a large-sized transformable shell structure. *The Paton Welding J.*, 7, 2–10.
- Inflatable structures. www.lindstrandusa.com
- Air-supported structures. www.vingida.ru
- Air-supported installations for military purposes. www.ilcdoover.com
- Bernhardt, A., Siefring, C.L., Thomason, J.F. et al. (2008) The design and applications of a versatile HF radar calibration target in low-earth orbit. *Radio Sci.*, 8, 11–21.
- Description of PAGEOS project. www.nssdc.gsfc.nasa.gov
- Hughes, S.J., Dillman, R.A., Starr, B.R. et al. (2010) Inflatable Re-entry vehicle experiment (IRVE) design overview. In: *Proc. of 18th AIAA Conf. and Seminar on Aerodynamic Decelerator Systems Technology* (Munich, Germany, May 23–26, 2010), 52–58.
- Zeigler, Th.R. *Collapsible self-supporting structures a panels and nud therefor*. Pat. 4290244 USA. Int. Cl. E04 B1/32. Publ. 22.09.1981.
- Sallee, B.T. *Rigidizable inflatable structure*. Pat. 5579609 USA. Int. Cl. B64699/00. Publ. 12.03.1996.
- Self-opening satellite PERCS. www.hoberman.com
- Hoberman, C. *Folding covering panels for expanding structures*. Pat. 6834465 USA. Int. Cl. E04 B1/344. Publ. 28.12.2004.
- Module Genesis II. www.bigelow aerospace.com

INTERNATIONAL CONFERENCE «TI-2012 IN CIS»

April 22–25, 2012

Kazan, Russia

A meeting of the Board of Directors of OJSC «Interstate Association «Titan» was held on November, 18, 2011 in FGUP VIAM, Moscow. Current business of the Association was addressed, and a decision was taken on conducting the next Annual International Conference «Ti-2012 in CIS» from April 22 till 25, 2012 in Kazan.

APPLICATION OF AUTOMATIC ORBITAL WELDING TO FABRICATE ABSORBING INSERTS FOR SPENT NUCLEAR FUEL STORAGE CONTAINERS

V.A. BOGDANOVSKY¹, V.M. GAVVA¹, N.M. MAKHLIN¹, A.D. CHEREDNIK¹, A.V. TKACHENKO¹,
V.B. KUDRYASHEV², A.P. KULIKOV² and A.V. KOVALYUK²

¹E.O. Paton Electric Welding Institute, NASU, Kiev, Ukraine

²Separated Structural Unit «Atomenergomash» of State Enterprise

«National Nuclear Energy Generating Company ENERGOATOM», Kiev, Ukraine

Considered is application of automatic orbital TIG welding for production of tight butt-lock joints on absorbing elements, which are the base of absorbing inserts of spent nuclear fuel storage containers. Results of optimisation of the TIG welding technology and ranges of optimal parameters for making of such joints are presented. The commercial unit designed for welding of the lock joints on the absorbing elements and the results of its test operation are described.

Keywords: automatic orbital welding, absorbing inserts, nuclear power plants, butt-lock joints, technological rig, nuclear safety

In compliance with requirements for nuclear safety of water-moderated reactors (WWER type) of power generating units operating at nuclear power plants (NPP), to maintain the required level of subcriticality the fuel assemblies (FA) are fitted with absorbing rods of the control and protection system (AR CPS). The same principle of securing the nuclear safety is used for storage of the spent nuclear fuel. According to this principle, under conditions of normal operation and in design accidents the value of the neutron multiplication factor should not exceed 0.95 [1–3].

One of the methods for securing the nuclear safety of charges of ventilated storing containers for dry storage of the spent nuclear fuel (VSC DSSNF) is fitting up of spent FA with absorbing inserts (AI), which are used along with spent AR CPS and compensate for deficit of the latter.

The absorbing insert used in VSC DSSNF of the Zaporozhie NPP, which was developed by the National Science Centre «Karkov Institute of Physics and Technology» (NSC KhIPT), consists of a cross-arm and 18 absorbing elements (AE). The AI cross-arm serves for simultaneous transportation of the AEs and their ranging during transportation and technological operations. The AEs are intended for placement of an absorbing material in guide channels of spent FA. AE

is analogue of AR CPS in design, shape, overall and setting-out dimensions.

AE consists of a shell (Figure 1) filled up with vibrocompacted boron carbide powder, weighting material, tip, cone (cap) and plugs. The shell is manufactured from a pipe with a diameter of 8.2 mm and wall thickness of 0.6 mm made from austenitic chrome-nickel steel 08Kh18N10T or 12Kh18N10T, tip and cone (rod of the same steel).

According to the AI manufacture technology developed and applied by NSC KhIPT, the sealing butt-lock joints between the shell of AE and its tip and cone are made by the roll butt TIG welding method, in which the workpiece is rotated about its axis at a welding speed, while the torch with tungsten electrode is in a fixed spatial position. The shell is welded to the cone in argon, and to the tip – in a controlled atmosphere (helium) [4]. Specialised units ASTE-7 and SA-281 developed by the Research and Development Institute of Construction Technology (NIKIMT) (Moscow) are used for the welding process [5].

This technology provides the required quality of the welded joints on AE, which is proved by the experience of manufacture of the AIs and their application in VSC DSSNF of the Zaporozhie NPP. At the same time, increase in output of AE caused by the emerging growth of the demand for AI is limited to a certain degree by peculiarities of operation of the durable roll butt welding units, their functional possibilities and level of the end productivity, difficulties in upgrading of this equipment or its replacement by the new one. Also, the noted peculiarities of the equipment employed hamper upgrading of some components of the AE technological manufacture cycle.

One of the possible ways of improving the existing AI manufacturing technology is the technology for sealing of the butt-lock joints on AE by the method of orbital position butt TIG welding, as well as the

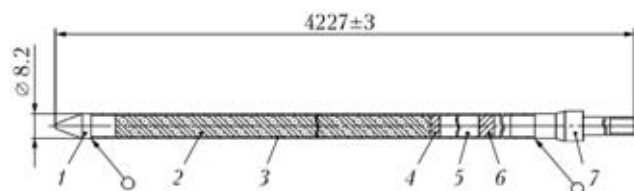


Figure 1. Schematic of absorbing element: 1 – cone (cap); 2 – filling material (boron carbide powder); 3 – shell; 4, 5 – plugs; 6 – weighting material; 7 – tip

equipment used to implement this process, which were developed by the E.O. Paton Electric Welding Institute (PWI) in collaboration with Separated Structural Unit «Atomenergomash» of State Enterprise «National Nuclear Energy Generating Company ENERGOATOM».

The technology for TIG welding of the shell of AE to its tip and cone was optimised by using automatic device ADTs 627 U3.1 for orbital position butt welding of pipelines, which was developed by PWI and is commercially produced now.

Specifications of automatic device ADTs 627.U3.1

Range of diameters of pipes welded, mm	8–24
Minimal inter-pipe distance, mm	60
Limits of regulation of welding current, A:	
lower, not more than	8
higher, not less than	260
Limits of regulation of arc voltage, V	8–24
Maximal deviation of welding current from the preset value at mains voltage fluctuations not above the rated value and length variations not above ± 2.0 mm from the preset value, %	± 2
Accuracy of maintaining of the preset value of arc voltage, V, not worse than	± 0.20
Limits of regulation of rotation speed of welding head chuck, rpm	0.3–12.0
Rated diameter of tungsten electrode (grades VL, VI or VT), mm	1.6
Rated radial displacement of torch, mm	15
Maximal displacement of torch across a joint, mm	± 1
Quantity of arc passes	1–4

Device ADTs 627 U3.1 provides implementation of two types of operations («Setting Up» and «Welding»), two types of control («Manual» and «Automatic»), and the preset cycles of welding in a continuous mode, step-pulse mode or at the modulated current. The device comprises chopper-type multifunctional power source ITs 616 U3.1 for TIG welding, controller unit (control system) ITs 616.20.00.000, remote control panel (operator's panel) ITs 616.30.00.000, welding head ADTs 627.03.00.000 and collector ADTs 625.07.00.000.

Optimisation of the technology for welding of the butt-lock joints on AE was based on the results and recommendations of the earlier studies [6, 7], which had identified the following peculiarities of TIG welding of thin-walled parts without filler wire:

- key factors affecting the quality of the welded joints include a character of variations in heat and energy input during welding, shape of the tip and state of the working surface of tungsten electrode, and state of the surface of the base metal;
- main parameters of TIG welding without filler wire are welding current, arc voltage, welding speed and inert gas flow rate, the proportion of the values of which should correspond to the range of welding parameters determined by the calculation-experimental method that ensures the high quality of the welds [8];
- compared to butt joints, the overlap types of the welded joints (which include the butt-lock joints on AE) are less sensitive to instability of the welding parameters, but to make such joints it is necessary to

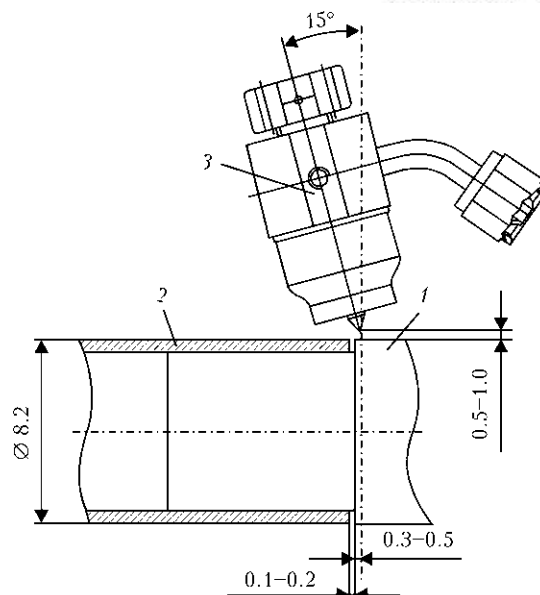


Figure 2. Schematic of fit-up of the butt-lock joint on absorbing element: 1 – cone (tip); 2 – shell; 3 – torch with tungsten electrode

displace the electrode to some distance (up to 0.5 mm) from the joining line and incline it to an angle of 15° towards a higher heat removal [7] (Figure 2).

Experimental joints on AE samples (mockups) were made to determine the ranges of optimal parameters of TIG welding of the butt-lock joints between the AE shell, cone and tip. The samples were prepared for welding by trimming edges of the shell mockups (pieces of the 8.2 mm diameter pipe of steel 08Kh18N10T) and degreasing these mockups, cones and tips. The joints were assembled for welding following the scheme shown in Figure 2 by providing the tight fit (d10) of the cone or tip on the shell.

The shell to cone welding was performed in argon by varying the following process parameters: welding current – 25, 28, 30, 32 and 35 A, arc voltage – 9 to 11 V at an arc length ranging from 0.5 to 1.5 mm, welding speed – 11.5 to 13.5 m/h (7.64 to 8.97 rpm), time of gradual increase of the current – 0.5 to 1.5 s, time of heating (time interval between the moment of the end of gradual increase of the current and that of the beginning of rotation of the arc) – 1.0 to 1.5 s, time of gradual decrease of the welding current at the final stage of the welding process (welding up of crater) – 1.0 to 2.5 s, and inert gas flow rate – 5 to 8 l/min.

The shell was welded to tip in helium based on the arc characteristics stipulated by its thermal- and electrophysical properties. In this case the welding current was 16, 18, 20, 22 and 25 A, arc voltage – 18.0–21.5 V at the arc length of 0.5–1.5 mm, time of gradual decrease of the welding current (welding up of crater) – 1.0–3.5 s, values of the other welding parameters being varied within the limits accepted for experimental welding of the AE shell to cone in argon atmosphere.

The quality of the experimental joints was assessed by visual and measuring control, metallographic ex-

Main parameters of TIG welding of joints on absorbing elements

Parameter	Shell-cone	Shell-tip
Grade of 1.6 mm diameter tungsten electrode	EVI-1, EVI-2, EVI-3, EVI-15 and EVI-20 acc. to GOST 23949-80, or «Abicor Binzel» WT-20, WR-2 and WR-2D	
Shielding gas	Argon acc. to GOST 10157-79	Helium acc. to TU 51-940-80
Welding current, A	30.0±1.2	20.0±1.0
Arc voltage, V	9-10	19-20
Arc length, mm	0.5-1.0	
Welding speed (rotation speed of welding head chuck), m/h (rpm)	12.0±0.4 (7.98±0.27)	13.0±0.45 (8.63±0.30)
Time of gradual increase of welding current, s	1.0±0.1	
Heating time interval, s	0.75±0.05	
Time of gradual decrease of welding current (welding up of crater), s	2.0±0.1	3.0±0.1
Shielding gas flow rate, l/min	5.9-7.1	4.9-6.1
Time of preliminary purging of welding zone with shielding gas (time interval «gas before welding»), s, not less than	5-10	
Time of purging of welding zone with shielding gas at final stage of welding cycle (time interval «gas after welding»), s, not less than	10-20	

aminations, intercrystalline corrosion (ICC) resistance tests and leakage tests. The visual and measuring control was carried out in compliance with requirements of the standards in force in the industry [9] by using a micrometer, as well as a magnifying glass and binocular microscope (e.g. MVS-9) with the $\times(8-10)$ magnification. The metallography was done on the macrosections cut out from the resulting welded joints by using a metallurgical microscope with the $\times(50-100)$ magnification to determine the penetration depth, defects in the weld metal (non-metallic inclusions, pores, wormholes and lacks of fusion), structure of the weld and HAZ metal, and austenite grain sizes. The ICC resistance tests of the weld and HAZ metal were conducted by the AMU method according to GOST 6032-89. The leakage tests were conducted by using a mass-spectrometer and helium leak detector PTI-10 by the vacuum chamber method in compliance

with the requirements and procedures specified in the operating regulatory-technical documents [10].

Welding of several series of the experimental joints between the AE shell, cone and tip, comprehensive inspection of the quality of these joints and analysis of the obtained results allowed a conclusion that to ensure the consistent high quality of the butt-lock joints on AE the main TIG welding parameters should correspond to those indicated in the Table.

Results of the experimental and technological development efforts made by PWI for optimisation of the technology for TIG welding of the sealing butt-lock joints on EA proved the expediency of commercial application of this technology for mass production of both AI for VSC DSSNF and (in the future) AR CPS for FA of the WWER type reactors.

The special technological rig, the schematic of which is shown in Figure 3, was developed and manufactured to implement TIG welding of sealing joints

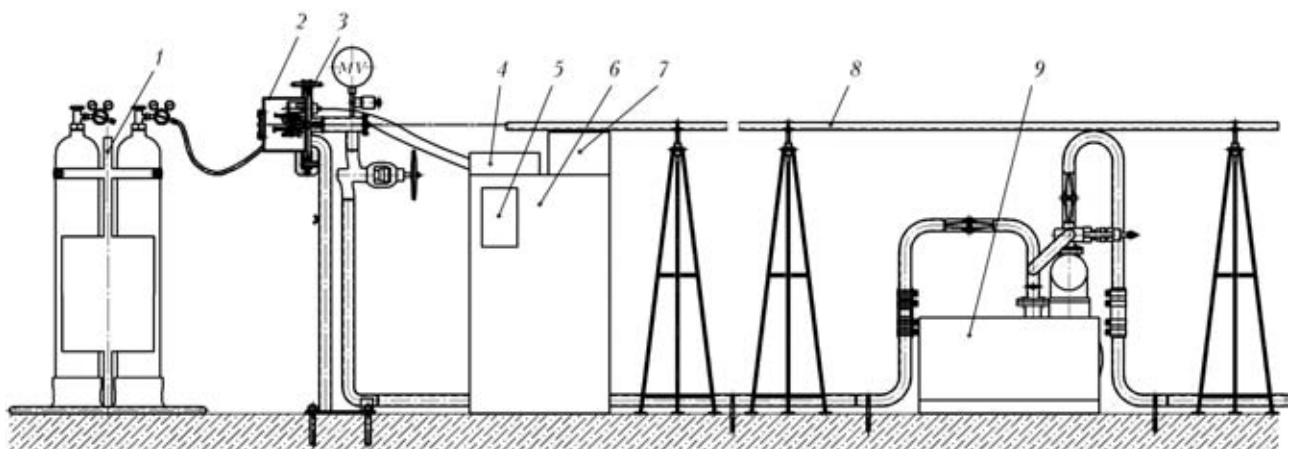


Figure 3. Schematic of the rig for TIG welding of butt-lock joints on AE: 1 – gas bottle rack; 2 – welding chamber; 3 – welding head ADTs 627.03.00.000; 4 – collector ADTs 625.07.00.000; 5 – remote control panel ITs 616.30.00.000; 6 – power source ITs 616.U3.1; 7 – controller unit ITs 616.20.00.000; 8 – cradle; 9 – vacuum valve unit

on AE and similar parts commercially fabricated by «Atomenergomash».

The rig comprises all components of ADTs 627 U3.1 for orbital position butt TIG welding, a welding chamber, vacuum valve unit, guide cradle and gas bottle rack.

The chamber (see Figure 3) with the welding head rigidly fixed inside it provides:

- repeatability and, if necessary, adjustment, fixation of the spatial position and alignment of the butt-lock joints on AE prepared for welding with respect to tungsten electrode of the torch mounted on the welding head chuck;
- free access to the welding head and adjustors of spatial position of the torch with the tungsten electrode, thus facilitating maintenance of the head without its removal from the chamber;
- electric insulation of the current and gas supply lines of the welding torch and control circuits of its rotator with respect to the chamber casing, weldment and other non-current-conducting components of the rig;
- meeting the leak tightness requirements in evacuation of the internal volume of the chamber for subsequent creation of the controlled atmosphere in it by filling it with helium and maintaining the excess pressure at a level of (1.96 ± 0.2) kPa;
- possibility of observation of the course of the welding process through a viewing window.

The general view of the chamber is shown in Figure 4.

The valve unit (see Figure 3) is intended for evacuation of the internal volume of the chamber with rarefaction to a level of not less than 1.33 Pa.

The cradle is a guide support for placement of an absorbing element to be welded in the rig. It protects the AE shell from deformation and mechanical damage during preparatory and final operations, and during welding of the sealing joints on AE.

Testing of the PWI technology for TIG welding of sealing joints on AEs under industrial conditions of «Atomenergomash» showed that the use of the rig (see Figure 3) does not only provide the consistent high quality of the welded joints on AEs, but also leads to some decrease in labour intensiveness and to reduction of duration of the setting up operations preceding the welding process (compared to the existing roll butt welding technology), and simplifies training of welders and attending personnel. The test results served as forcible arguments in favour of arrangement of the specialised sector for commercial fabrication of absorbing elements at «Atomenergomash». Technological fitting of this sector and its productivity with one rig used for welding allow producing up to 1200 AEs a year. The equipment of the sector was used to fabricate an experimental batch of AEs, the samples of which were subjected to comprehensive tests (including by the destructive testing methods) at NSC KhIPT. These tests proved a full correspondence of the quality of the joints on AEs made by the orbital TIG welding technology to the requirements of the standards. Also, it was established that the butt-lock joints on AEs made by the orbital TIG welding technology are identical in their penetration depth, struc-

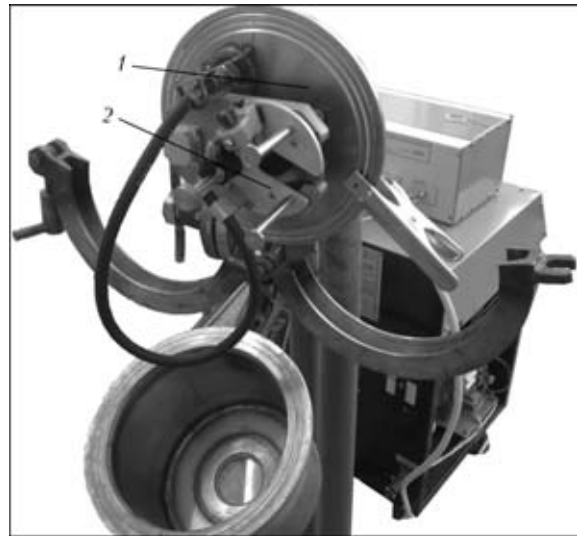


Figure 4. General view of chamber (1) and welding head ADTs 627.03.00.000 (2)

ture of the weld and HAZ metal, austenite grain sizes and mechanical strength to those made by the existing roll butt welding technology.

CONCLUSIONS

1. The developed technology for TIG welding of overlap joints on different-thickness small-diameter bodies of revolution by using automatic orbital welding devices of the ADTs 627 U3.1 type provides the high-quality butt-lock joints on AEs and similar parts.

2. Commercial application of the developed TIG welding technology and corresponding technological equipment will allow manufacturing AIs, AR CPS and similar parts in volumes that meet the nuclear power generation needs.

1. *PN AE G-14-029-91*: Safety rules in storage and transportation of nuclear fuel at nuclear power objects (Gosatomnadzor SSSR). Moscow: Energoatomizdat.
2. *NP 306.2.105-2004*: Principles of securing safety of intermediate dry type storages. Kyiv: Derzhatomregulyuvannya.
3. (2007) *Technical regulations concerning containers for storage and burial of radioactive wastes*: Resolution of the Cabinet of Ministry of Ukraine 939 of 18.07.2007.
4. (1999) *Studies of the technology for fabrication and development of the program for mastering and production of AR CPS in Ukraine*: Report of NTK YaTTs NNTs KhFTI. Kharkov.
5. (1985) *Welding equipment*: Catalogue. Ed. by A.A. Kurkumeli. Moscow: TsNIIatominform.
6. Ishchenko, Yu.S. (2002) Physico-technological principles of weld formation in arc welding. In: *Welding in nuclear industry and power engineering*: Transact. of NIKIMT, Vol. 2. Moscow: Izdat.
7. Bukarov, V.A. (2002) Technology of automatic gas-shielded arc welding. *Ibid.*, Vol. 1.
8. Poloskov, S.I., Bukarov, V.A., Ishchenko, Yu.S. (2000) Influence of deviations of parameter of position butt argon-arc welding on the quality of welded joints. In: *Proc. of All-Union Sci.-Techn. Conf. on Welding and Related Technologies* (Moscow, Sept. 2000). Moscow: MEI, 22-25.
9. (1989) *Unified procedure for control of base materials (semi-finished products), welded joints and surfacing of NPP equipment and pipelines. Visual and measuring control of PN AE G-7-016-89* (Goskonnadzor SSSR). Moscow: Energoatomizdat.
10. (1989) *Unified procedure for control of base materials (semi-finished products), welded joints and surfacing of NPP equipment and pipelines. Leakage test. Gas and liquid methods of PN AE G-7-019-89* (Goskonnadzor SSSR). Moscow: Energoatomizdat.

TWO-LAYER BIO-CERMET TITANIUM-HYDROXYAPATITE COATING

K.A. YUSHCHENKO, Yu.S. BORISOV, S.G. VOJNAROVICH, A.N. KISLITSA and E.K. KUZMICH-YANCHUK
E.O. Paton Electric Welding Institute, NASU, Kiev, Ukraine

It is suggested using two-layer bio-cermet (titanium-hydroxyapatite) coatings for titanium alloy endoprostheses. A combination of porous titanium with an external hydroxyapatite (HA) layer provides high strength of adhesion of such coatings to the surfaces of endoprostheses (24–25 MPa) and subsequent active growth of bone tissue into them. The microplasma spraying technology allows formation of the HA layer with the 88–98 % content of the crystalline phase, thus providing a high degree of utilisation of the powder (up to 90 %) in spraying and increasing the cost effectiveness of the process.

Keywords: *microplasma spraying, medical-application coatings, bio-compatible coatings, porous titanium, hydroxyapatite, endoprosthetics, hip joint*

Metal implants with bio-active ceramic coatings are widely applied now in medical practice. These implants are characterised by a triple positive effect: increased rate of formation of the bone tissue, possibility of formation of bond with the bone (osteointegration), and decrease in formation of metal corrosion products. This allows substantial reduction of the time of implantation of an endoprosthesis, provides the reliable bond with the bone and improves reliability of the implants. The most extensively used bio-active ceramics are ceramics based on calcium phosphate, i.e. hydroxyapatite (HA), or other calcium phosphates close to it in composition [1, 2].

Bio-ceramic coatings of HA are deposited by using different methods (magnetron sputtering, electrophoretic deposition, sol gel method, etc.), including plasma spraying, which has received a real practical application in production of coated endoprostheses [2–5].

The following main requirements to quality of the bio-ceramic coatings were worked out on the basis of clinical application of endoprostheses with such coatings: sufficiently high strength of adhesion to the endoprosthesis surface (15 MPa or more, according to standard ISO 13779-2), high content of the crystalline phase (not less than 70 %), and presence of developed porosity providing ingrowth of the bone tissue.

Phase composition of a coating (degree of crystallinity) has a considerable effect on the osteointegration process. During this process the amorphous HA phase has a higher rate of dissolution, thus reducing the time of recovery of a patient but, at the same time, decreasing reliability of fixation of an endoprosthesis in the bone.

A drawback of the conventional plasma spraying method is formation of coatings with a high content of the amorphous phase, which is caused by conditions of both heating of the HA particles (because of the

need to use working gases with increased thermal conductivity, i.e. Ar + H₂ and Ar + He mixtures) and their solidification on the substrate surface [6].

In the last years the E.O. Paton Electric Welding Institute has developed the microplasma spraying method and equipment, allowing spraying of ceramic coatings by using the laminar jet of argon plasma [7]. A low thermal conductivity of argon decreases the intensity of heating of the particles, thus decreasing the temperature gradient across their sections. In spraying of the HA coatings this allows avoidance of overheating of the melt of HA and formation of toxic products of its decomposition (CaO). Low velocities of the HA particles under conditions of the laminar jet lead to formation of coatings from the particles with a lower deformation degree and, hence, lower rate of hardening on the substrate, which provides the high content of the crystalline phase (up to 95–98 %).

In this connection, the E.O. Paton Electric Welding Institute completed a package of work on development of the compositions and technology for deposition of bio-ceramic coatings on endoprostheses by using microplasma spraying [8–10].

The technology for microplasma spraying of two-layer bio-cermet (Ti + HA) coatings on implant surfaces was developed to increase strength of adhesion of the coatings to the bone implant surfaces. This technology allows deposition of a titanium coating with regulated porosity by microplasma spraying using a variant of wire spraying.

The two-layer bio-cermet coatings are deposited by using microplasma spraying system MPN-004 (Figure 1), which comprises a power source with a cooling unit, control unit, plasmatron, as well as the interchangeable wire feed mechanism and powder feeder MPD-004 (Figure 2).

The spraying materials for the two-layer bio-cermet coatings are the 0.3 mm diameter titanium wire of the VT1-00 grade used for deposition of the titanium coating with developed porosity, as well as the HA powder used for deposition of the bio-active upper

layer, the phase composition of the HA powder produced by Scientific-and-Technical Service Centre «RAPID» being fully crystalline $\text{Ca}_{10}(\text{PO}_4)_6(\text{OH})_2$ with the Ca/P-1.67 ratio.

Appearance of the surface and structure of the bio-cermet coating are shown in Figure 3.

The costs of the HA coating deposition process depend on the consumption of the HA spraying powder, the price of the latter being very high. Experimental studies of the material utilisation factor (MUF) for HA in deposition of the two-layer bio-cermet coating show that in the case of microplasma spraying it is 1.5–2 times higher than in traditional plasma spraying. For instance, according to literature data, the maximal values of MUF in plasma spraying of HA on a plate are 50–62 %, whereas in microplasma spraying the maximal value of MUF amounts to 90 % [10]. Under conditions of microplasma spraying the spraying spot has a form of ellipse with an axes ratio of 1.1–1.3 and size of 8–15 mm (instead of 30–40 mm in conventional plasma spraying), depending on the spraying process parameters. The calculations of losses of the HA powder show that the total losses of the material (for recoil and spattering, and losses caused by geometric factor) in microplasma spraying on implants 8–10 mm in size (dental, intervertebral cages) are 20–40 %, whereas in traditional plasma spraying they amount to 85–90 %.



Figure 1. Appearance of microplasma spraying system MPN-004

The investigations conducted resulted in establishing the quantitative dependence of phase composition of the HA coating on such microplasma spraying parameters as current, plasma gas flow rate, spraying distance and powder consumption. Thus, the content of the crystalline phase of HA in a coating, as well as the content of the amorphous phase in it are most strongly affected by the spraying distance. The amount of tricalcium phosphate (β -TCP) in the coating greatly depends on the plasma gas flow rate and spraying distance. Therefore, by varying the microplasma

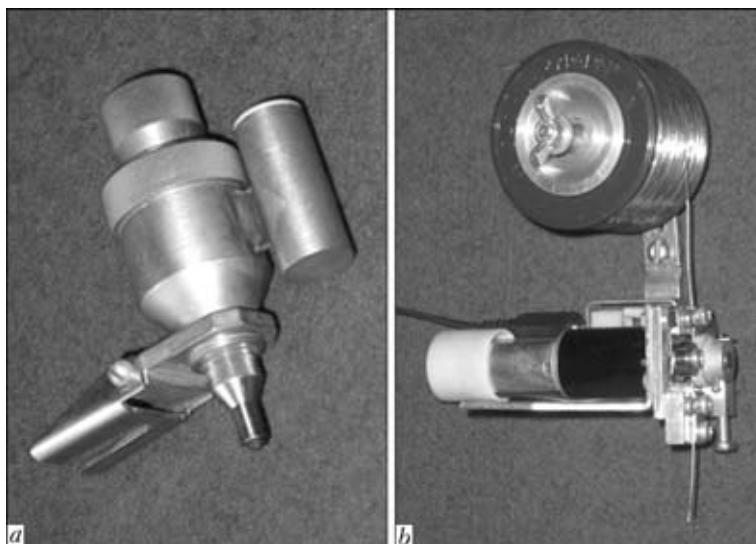


Figure 2. Appearance of powder feeder MPD-004 (a) and wire feed device MPP-04 (b)

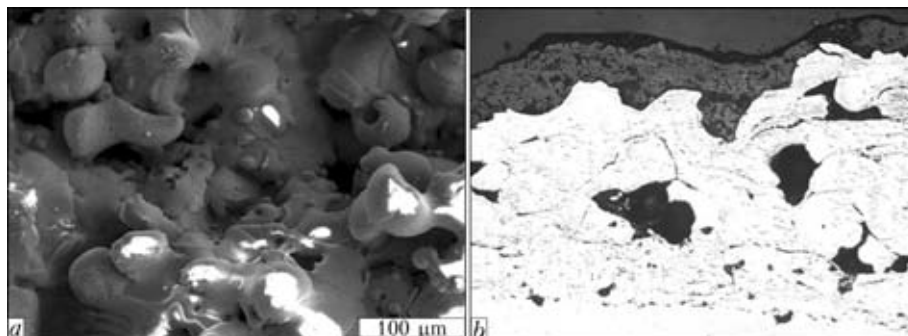


Figure 3. Appearance of surface (a) and microstructure (b – $\times 140$) of bio-cermet coating



Figure 4. Examples of items with bio-cermet coatings produced by microplasma spraying: *a* – hip joint endoprosthesis; *b* – cermet implant for interbody vertebral spondylosyndesis; *c* – dental implant

spraying parameters (current, plasma gas flow rate, spraying distance and powder consumption) it is possible to control phase composition of the HA coatings at a content of the HA crystalline phase ranging from 88 to 98 %, degree of amorphism in a range of 0 to 7 % and TCP content (degree of decomposition of HA) in a range of 0 to 6 %. Hence, it is possible to control formation of the HA coatings with the specified phase composition.

Strength properties of the two-layer bio-cermet coatings should provide their integrity and long-time reliable functioning in an organism. According to standard ISO 13779–2, sufficient strength of adhesion of the coatings to the substrate should be not less than 15 MPa. Spraying of the two-layer bio-cermet coatings by using a titanium coating with developed porosity (pores with a size of 100–150 μm) provides the adhesion strength equal to 25.2 ± 0.85 MPa.

Toxic-hygienic estimation of the bio-cermet coatings was carried out by the Institute of Macromolecular Chemistry of the NAS of Ukraine*. According to standard ISO 10993–2, samples of the coatings were implanted to white rats. Histological investigations of such tissues around the implanted coatings showed that the bio-cermet coatings of HA and titanium (Ti + HA) are non-toxic, bio-compatible with live tissues, and exert no irritating and sensitising effect.

The bio-medical investigations allowed a conclusion on the safety and bio-compatibility of endoprosthesis with the microplasma bio-cermet coatings (Ti + HA). Recommendations on deposition of the bio-cermet coatings by the microplasma spraying method were worked out on the basis the investigation results.

The developed microplasma spraying technology was applied for deposition of coatings on hip joint endoprosthesis, implants for interbody vertebral spondylosyndesis [11] and dental implants (Figure 4).

CONCLUSIONS

1. Microplasma spraying of bio-ceramic HA coating is characterised by the possibility of producing layers

with a high degree of crystallinity (88–98 %), which can be controlled by varying the spraying process parameters. Small size of the spraying spot (3–8 mm) provides substantial decrease (2–3 times) in powder consumption during spraying on small-size implants, compared to conventional plasma spraying.

2. The two-layer bio-cermet coating (porous titanium + HA) provides the strength of adhesion to endoprosthesis equal to 24–25 MPa and intensification of growth of the bone into the coating surface.

3. Toxic-hygienic examinations of the microplasma bio-cermet coatings proved their being non-toxic and bio-compatible with live tissues.

4. The bio-cermet coatings (Ti + HA) and technology for their microplasma spraying were used for coating of hip joint endoprosthesis, dental implants, intervertebral cages etc.

1. Kanazawa, T. (1998) *Inorganic phosphate materials*. Kiev: Nauka.
2. Shpak, A.P., Karbovsky, V.L., Grachevsky, V.V. (2002) *Apatites*. Kiev: Akadempriodika.
3. Kalita, V.I. (2000) Physics and chemistry of formation of bio-inert and bio-active surfaces on implants (Review). *Fizika i Khimiya Obrab. Materialov*, **5**, 28–45.
4. <http://www.biomet.co.uk>
5. <http://www.stryker.com>
6. Yang, C.Y., Wang, B.C., Chang, E. et al. (1995) The influences of plasma spraying parameters on the characteristics of hydroxyapatite coatings: a quantitative study. *J. Materials Sci.: Materials in Medicine*, **6**, 249–257.
7. Borisov, Yu.S., Vojnarovich, S.G., Fomakin, O.O. et al. *Plasmatron for spraying of coatings*. Pat. 2002076032 Ukraine. Int. Cl. B 23 K 10/00. Fil. 19.07.2002. Publ. 16.06.2003.
8. Borisov, Yu.S., Vojnarovich, S.G., Bobrik, V.G. et al. (2000) Microplasma spraying of bio-ceramic coatings. *The Paton Welding J.*, **12**, 62–66.
9. Borisov, Yu.S., Vojnarovich, S.G., Ulianchich, N.V. et al. (2002) Investigation of bio-ceramic coatings produced by microplasma spraying. *Ibid.*, **9**, 4–6.
10. Vojnarovich, S.G. (2010) Effect of microplasma spraying parameters on material utilisation factor in spraying of bio-ceramic coating. *Zbirka Nauk. Pr. Nats. Un-tu Korablebuduvannya*, 433(4), 58–61.
11. Brekhov, O.M., Eliseev, S.L., Ulianchich, N.V. et al. *Cermet implant for interbody vertebral spondylosyndesis*. Pat. 200112870 Ukraine. Int. Cl. B 23 K 10/10. Fil. 03.12.2001. Publ. 15.03.2002.

*The study was carried out under the leadership of Prof. N.A. Galatenko, Doctor of Biological Sciences.

ORGANIZATION AND TOPICS OF R&D IN THE FIELD OF JOINING TECHNOLOGIES CONDUCTED BY TWI AND DVS ASSOCIATION OF RESEARCHERS (Review)

O.K. MAKOVETSKAYA

E.O. Paton Electric Welding Institute, NASU, Kiev, Ukraine

The paper gives information on organization and topics of investigations in the field of joining technologies conducted by TWI and DVS Association of Researchers.

Keywords: *joining technologies, topics of R&D, TWI, DVS Association of Researchers*

Practice of «openness» of the investigation topics acquires a wide-accepted character under conditions of globalization of world economic development. The topics of planned scientific projects and programs of fundamental and applied investigations are published in the national editions as well as on the pages of web-sites by leading welding institutes, centers and welding societies of many countries, thus inviting to cooperation and mutual exchange of the scientific information.

The Institute Welding (TWI, Great Britain) and DVS Association of Researchers (DVS AR, Germany) are the leading European and world scientific centers in the field of joining technologies. Solution of specific and relevant tasks of the industry, i.e. development of new joining technologies, investigation of weldability of new structural materials, cut of industrial expenses in welding engineering, quality and safety of welding operations, increase of safety of welded structures, obtaining of scientific and experimental grounds to norm and standards etc. is the main direction of the investigation topics conducted in these scientific centers. High level of maturity of the developments sharply reducing time for technology transfer is provided for in the research programs of TWI and DVS.

TWI has been significantly growing its scientific and technical potential in the recent years. Number of researchers working in the Institute increased 1.3 times from 500 to 640 persons for the period from 2005 to 2010. A total gain from different areas of activities exceeded 53 mln GBP in 2010.

Researches on a plan of topics of Basic Investigation Program (CRP) make a basis of fundamental and applied scientific investigations in area of welding and related technologies of TWI. The budget of CRP Program made around 3.3 mln GBP for 2010–2012, and TWI income from results of the performed R&D was around 10 mln GBP in 2010.

TWI conducts significant volume of works on training, retraining and attestation of welding personnel, engineering and scientific stuff. A general fund for financing of this area of activity exceeded 14 mln GBP per year.

Membership fees from enterprises and individual persons from Great Britain as well as other countries of the world are the main source of financing of TWI scientific and production activities. Significant increase of a number of TWI members is observed in recent years. Thus, 110 companies became joint members in 2010 that allowed additionally obtaining around 1 mln GBP and the total gain from membership fees made around 7 mln GBP. Number of organizations and enterprises-joint members of TWI achieved 660 in 2010.

Industrial enterprises and firms (members of TWI) provide financial support at conductance of the specific topics and influence on direction of the performed investigations and developments. As a rule, the representatives of branches of industry reckon on obtaining of maximum benefit from the results of CRP Program for providing competitiveness of their production in the world market. Only commercial members of TWI which also can obtain additional information on CRP projects, including during the process of their execution, are provided with the final reports on results of R&D, performed in the range of CRP Program.

Organization of performance of the investigations in TWI is carried out on target projects. A scientific laboratory or department is organized for performance of works on that or another scientific direction for the time of conductance of R&D project and stops its existence after work on specific direction is finished.

TWI CRP Program for 2009–2012 includes 57 R&D projects which are grouped by five subject directions (strength of welded structures; metals and weldability; laser, arc and resistance welding; surface treatment; electron beam technologies and technologies of friction welding; plastics; glues, ceramics and electronics). Each research project is clearly oriented to one or several specific sectors of commercial production (airspace; motor car construction; welded structures and design; war industry; oil-, gas- and chemical industry; power engineering; railway transport; sensors and medicine; shipbuilding), where realization of obtained R&D results is supposed or which is a customer of given topic.

17 projects the topics of which can be divided on two main groups, i.e. mathematical modelling and visualization of physico-chemical and mechanical processes (6 projects) and methods for control of quality of welded joints (11 projects), have been performed/is performed in «Strength of Welded Struc-



tures» direction. The mathematical modelling and visualization find wider application in the investigations of welding processes replacing performance of multiple expensive experiments. A model for accurate forecasting of the residual stresses in circumferential welds of the pipelines is supposed to be developed and grounded in «Development of Progressive Methods for Evaluation of Circumferential Welds of the Pipelines» project. The project includes an investigation of changing of circumferential weld metal properties in the stress-strain state using stain-based failure assessment diagram, development and grounding of a model for accurate forecasting of the residual stresses in circumferential welds of the pipelines, development of a procedure for determination of influence of the residual stresses on crack formation for evaluation of crack resistance of circumferential weld. Development of a model for direct metal laser deposition using laser technologies that allows determining of the dependence between process parameters, material properties and resultant quality is the aim of «Progressive Methods of Modelling» project.

Large group of the projects is dedicated to development of methods of non-destructive testing of welded metal structures which, in particular, deal with evaluation of corrosion damage of steels in acid media, development of phased array ultrasonic testing, detection of small fatigue cracks. Computer X-ray tomography is interesting in application for testing and evaluation of porosity and undulation of black-reinforced plastic fiber.

Topics of the investigations in «Metals and Weldability» direction include 15 projects, aimed at investigation of weldability of structural, heat-resistant, stainless steels, nickel alloys and dissimilar materials using different welding technologies, i.e. electron beam, arc and TIG welding. In particular, the investigations are conducted on following R&D projects:

- Improvement of technology for welding of dissimilar materials — topic is relevant for nuclear-power engineering;
- Evaluation of weldability of ultrasupercritical materials for power units/power stations — for development of new structural materials designed for manufacture of turbogenerators of TPP with ultrasupercritical parameters of vapor;
- Repair of welded structures from heat-resistant steels with 9 % Cr without heat treatment — applicable to repair of turbosets and boiler units under conditions of TPP and NPP.

12 projects refer to the investigations in direction «Laser, Arc and Resistance Welding and Surface Engineering». They represent studies the topics of which are directed on development of new technologies, i.e. MIG/MAG, laser, hybrid laser-arc, welding of parts from carbon steel, corrosion-resistant alloys, dissimilar materials (steel and copper, steel and aluminum), heat-resistant steels, nickel, titanium and aluminum alloys.

The projects «Welding and Cutting Using New Generation Superpower Fiber Lasers and Single and Multipass Hybrid Laser Welding with Adaptive Control» are directly related with study of a peculiarity of interaction of laser and arc heating sources in hybrid

process; selection of alternative combinations of laser with arc or plasma heating sources, providing high efficiency of welding and quality of the joint; investigation and development of hybrid laser-arc technology of welding of thin sheets from aluminum alloys and combination of dissimilar materials.

Such investigation topics as «High-Efficiency Layer-by-layer Laser Surfacing of Metal and Laser Spraying and Cladding» reflect direction of TWI investigation in the field of creation and development of processes of surfacing and deposition of special and protective coatings as well as development of consumables of improved quality with special physico-mechanical and tribological properties designed for coating deposition.

There are seven projects on investigation topics directed to «Technologies of Electron Beam and Friction Welding». The projects connected with development of new technologies of EBW and FSW of ferrite and austenite steels and high-strength aluminum alloys were represented in the program.

Number of serious research investigations in the field of development of new types of FSW tool and technique has not been reduced in TWI regardless that the FSW process was developed and realized back in the 1990s including by means of selling of a license for technology and equipment. Thus, a technology of microFSW of aluminum alloys from 0.2–0.3 to 1.5–2.0 mm applicable to performance of the longitudinal and spot welds were developed and has been already widely implemented following the TWI plans.

Additive technologies find greater application in commercial production, in particular, replacing casting techniques in ferrous metallurgy. Possibility of application of this technology for the friction welding process, especially, for development of tool, is supposed to be investigated in «Additive Technologies Applicable to Friction Welding» project.

There are 9 projects in topic of the investigations in «Plastics, Glues, Ceramics and Electronics» direction. The projects aimed at investigation and development of a technology of welding (laser welding, fusion butt welding) and deposition of coatings on the parts from plastics and composites are represented in the Program, in particular:

- Investigation of polymeric materials reinforced by carbon nanotubes and designed for operation under extreme environment conditions;
- Improvement of quality of welding for fiber-reinforced thermoplastics;
- Technologies of joining in medicine [1].

DVS — federal society (association), realizing management and coordination of scientific and technical, industrial and educational activity of different enterprises of Germany, dealing with the problems of welding and related technologies. DVS is included into Otto von Herike Association of Industrial Research Associations (AiF) and includes 14 land and 94 regional departments, 9 welding training-experimental centers (SLV institutes) and more than 12 training-welding centers (SL).

Number of DVS members (collective and individual) in 2010 was 18456, including 597 collective members.

According to the basic functions of DVS the following organizations were formed in its composition:

- DVS Association of Researchers;
- DVS Publishing house;
- Certification center DVS-ZERT;
- Commission on professional training AfB and independent body DVS-PersZert;
- Technical committee on standardization TC;
- National delegation in IIW and EWF.

To activate engineering research and to increase the efficiency of professional education the Association of institutes of welding technology (GSI) is functioning in DVS since 1999, which combines the welding educational-experimental centers (institutes): SLV Duisburg, SLV Berlin-Brandenburg, SLV Halle, SLV Munchen, SLV Felbach, SLV Hannover, SLV Saabrucken, SLV Bilefeld.

The of DVS AR forms program of topics of DVS research works, meeting the interests of industry and general strategy of development of research directions; realizes the annual distribution of funds for their performance, coordinates the integral developments. The selection of projects for inclusion into the plan of R&D of DVS AR is performed within the frames of 15 expert commissions (committees): FA1 – metallurgy and metals science; FA2 – thermal spraying and autogenous technology; FA3 – arc welding; FA4 – resistance welding; FA5 – special welding methods; FA6 – beam processes; FA7 – brazing; FA8 – adhesion bonding; FA9 – designing and calculation; FA10 – microbonding technology; FA11 – joining of plastics; FA12 – modeling of welding processes; FA Q6 – safety instructions and environment protection; FA V4 – underwater welding; FA13 – manufacturing methods, production technology.

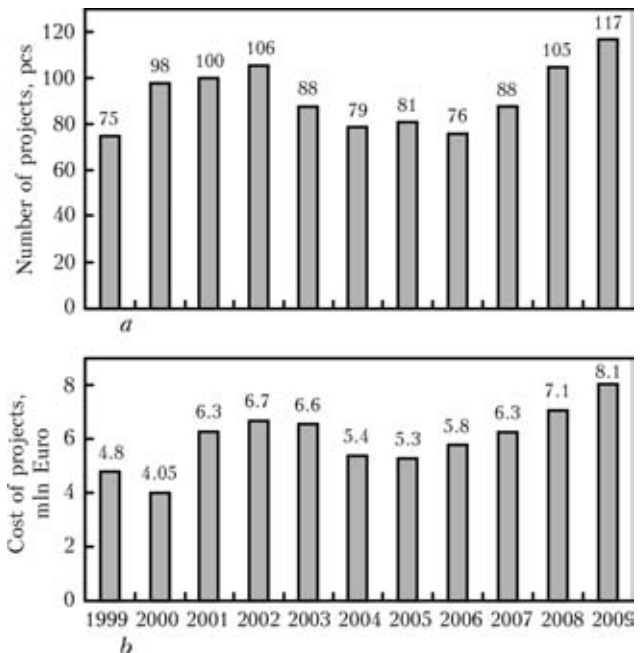
In 2010 the DVS AR performed R&D on 160 projects, with the total volume of financing of 11.5 mln Euro. The bulk of R&D projects is financed by AiF. In 2010 AiF financed 124 research projects at the sum of 8.8 mln Euro.

The Figure shows data on the number of R&D projects, performed by the DVS AR within the frames of financing of AiF in the period of 1999–2009 and their cost.

In 2009 the topics of DVS research works were distributed as follows: 86 % – research in the field of joining technologies and each 7 % – in the field of technology for spraying coatings and cutting technology.

The topics of DVS research works in the field of joining technology for different years are given in Table 1.

In the structure of topics of DVS research works the main part belongs to the research in the field of welding technologies, however their volume in the period of 2002–2009 decreased by 10 %. At the same period the volume of research on technologies of brazing joining increased practically by 3 times. The German scientists pay considerable attention to adhesion



Number (a) and total cost (b) of carried out DVS AR R&D projects

bonding technology, which is one of the most challenged at the technology market. It is predicted that along with the technology of laser welding the adhesion bonding will have the biggest growth. For example, in 2007 in EU countries more than 30 % of volume of production in the structure of production of welding equipment and rendering services belonged to adhesives and bonding equipment (about 6500 mln Euro).

The topics of DVS research works in the field of welding technology for different years are given in Table 2. As is seen from the Table, the arc fusion welding preserves the positions of basic welding technology. The volume of topics of research works in this field is high and amounts nearly 40 %. In the structure of DVS research works the volume of laser and hybrid technologies is growing.

The main material for welded structures remains steel (Table 3). After growth of volume of research works in the field of technologies of aluminium welding in 2002, 2007, 2009 the decrease of works in this direction is observed. In connection with increasing application of new materials, such as ceramics, composites in many fields of industry (transport, aircraft industry, etc.) and also increase in need in joining of dissimilar materials the volume of research works in these directions is increased.

Table 1. Topics of DVS research works in the field of joining technology, %

Type of joint	2002	2007	2009
Welding	73	62	64
Microjoints	11	14	12
Adhesion bonding	11	16	8
Brazing	5	8	16

Table 2. Distribution of DVS research directions in the field of welding technology, %

Joining technology	2002	2007	2009
Arc welding in shielding gas	45	37	38
Resistance welding	18	12	13
Electron beam welding	7	5	5
Hybrid welding	8	13	13
Laser welding	17	22	19
Other	5	11	12

Table 3. Structure of research works in the field of joining of weldable materials, %

Material	2002	2007	2009
Steel	40	28	34
Aluminium	28	36	21
Plastics	6	7	14
Glass/ceramics	5	5	7
Dissimilar materials	14	16	10
Magnesium	5	5	–
Other	2	2	14

Table 4. DVS R&D projects on separate topic directions

Topic direction	Name of the project
Metallurgy and materials science	Systems of alloying of flux-cored wires for shielded-gas welding of wrought aluminium alloys and alloys produced using die casting Improvement of weldability of aluminium by grain refining Investigation of prevention of hot cracks in austenite Cr–Ni steels and Ni-based alloys using optimization of temperature field
Thermal spraying and autogenous technology	Development of express-methods of NDT for measuring mechanic characteristics and porosity of thermal-sprayed coatings Thermographic methods of NDT for evaluation of thermal-sprayed coatings Improvement of quality of coatings deposited using arc method applying modified autogenous technology and high-velocity gas flows
Arc welding	Increase of stability of welding process in shielding gas using modified shielding gas flow Development of system of control of welding torch for automatic welding of steel and aluminium alloys in shielding gas Evaluation of efficiency of welding in shielding gas
Special welding methods	Investigation of FSW of steel and aluminium Development of conception of evaluation of fitness of installations for FSW and also determination of welding parameters Development of on-line control for FSW on the basis of sensors integrated into the tool
Beam welding methods	Application of multi-beam technology for decrease of internal stresses in the EB- and laser-welded parts Hybrid laser-arc welding of thick-wall precision pipes Hybrid laser-arc welding using low power arc methods
Designing and calculation	Experimental research and numerical modeling of deformation process of aluminium welded joints subjected to impact Calculation of micromagnetic characteristics of internal stresses in steels welded
Joining of plastics	Welding of plastics with heating by infrared radiation Laser welding of optically transparent plastics without using of absorber Automatic optimization and providing of quality on the basis of a new concept of machines for welding using a heating element
Modeling of welding processes	Rapid automatic reproduction of temperature field for modeling of welding deformations Digital diagnostics of cold cracks of parts of laser-welded high-strength steels Applying of modeling welding for calculation of load-carrying capacity of light steel structures of irregular shape

Quantitatively the topics of DVS research works on basic directions of R&D was divided in the following way: joining technologies, respectively, in 2007 – 42; 2009 – 38; materials – 27 and 17; calculation, designing, modeling – 13 and 28; automation – 10 and 7; safety regulations – 8 and 10 %.

The development of new technologies of joining occupies the major part (about 40 %) in the topics of DVS research works. However ever more attention is paid to studying of visualization of welding processes, including calculations, designing and computer modeling. The volume of research works, connected with safety regulations and environment protection, is increased (Table 4).

In conclusion it is necessary to note that familiarization with topics of R&D works carried out by leading world welding institutes, its analysis allows determination of scientific priorities in research works, clear out the problems at which the scientists are working by the orders of industry, personify the topics of research works, find possible partners, etc. The transparency of research topics gives possibility to realize the international coordination in the development of actual scientific trends [2].

1. Core research programme 2010–2012: Project summaries. TWI world centre for materials joining technology. *www.twi.co.uk*
2. Geschäftsbericht 2010. Innovationen für die Wirtschaft. Forschung in der Füge-technik. DVS. *www.dvs-ev.de*

INDEX OF ARTICLES FOR TPWJ'2011, Nos. 1–12

Unique technology developed by Ukrainian scientists for elimination of underwater accidents in oil and gas pipelines

BRIEF INFORMATION

Abstracts of works on innovation projects of the NAS of Ukraine

Developed at PWI

Development of the methods for elimination of deformation of crankshafts in wide-layer hardfacing (Krivchikov S.Yu.)

Development of versatile transport ships and ocean engineering facilities (Ryzhkov S.S., Blintsov V.S., Egorov G.V., Zhukov Yu.D., Kvasnitsky V.F., Koshkin K.V., Krivtsun I.V., Nekrasov V.A., Sevryukov V.V. and Solonichenko Yu.V.)

Experience of application of S355 J2 steel in metal structures of the roofing over NSC «Olimpijsky» (Kiev) (Poznyakov V.D., Zhdanov S.L., Sineok A.G. and Maksimenko A.A.)

Information-calculation system for hygienic characteristics of welding electrodes (Levchenko O.G., Savitsky V.V. and Lukianenko A.O.)

International Scientific-Practical Seminar in Kiev

New Book

New information on «old» electrodes (Yavdoshchin I.R. and Folbort O.I.)

News

System of video observation of the process of TIG welding of titanium structures (Kolyada V.A.)

Theses for a scientific degree

Upgrading of electric circuit of A-1150 machine for vertical welding (Stepakhno V.I., Kopylov L.N. and Zelenchenok G.S.)

INDUSTRIAL

All-purpose power source for arc welding and plasma cutting (Vladimirov A.V., Khabuzov V.A., Lebedev V.A., Maksimov S.Yu. and Galyshev A.A.)

Application of automatic orbital welding to fabricate absorbing inserts for spent nuclear fuel storage containers (Bogdanovsky V.A., Gavva V.M., Makhlin N.M., Cherednik A.D., Tkachenko A.V., Kudryashev V.B., Kulikov A.P. and Kovalyuk A.V.)

Assessment of the effectiveness of composite bands for reconditioning of defective sections of pipelines (Garf E.F., Nekhotyashchy V.A., Dmitrienko R.I., Banakhevich Yu.V., Savenko A.V. and Olejnik I.N.)

Automatic control drive of electrode movement trajectory for the arc surfacing machines (Gulakov S.V. and Burlaka V.V.)

Capabilities of application of high-strength low-alloy pipe steels for manufacture of high-pressure vessels (Kulik V.M., Savitsky M.M., Elagin V.P. and Demchenko E.L.)

Chambers for explosion welding of metals (Review) (Shlensky P.S., Dobrushin L.D., Fadeenko Yu.I. and Ventsev S.D.)

Control of arc ignition during excitation of electroslag process (Lankin Yu.N., Moskalenko A.A., Tyukalov V.G. and Semikin V.F.)	1	3
Current consumables and methods of fusion arc welding (Review) (Shlepakov V.N.)	3	10
Development of a sensor for estimation of the rate of corrosion of welded metal structure under atmospheric conditions (Osadchuk S.A., Nyrkova L.I., Polyakov S.G., Melnichuk S.L. and Gapula N.A.)	3	7
Devices for impact treatment of a weld in the process of resistance spot welding (Pismenny A.S., Pentegov I.V., Kislitsyn V.M., Stemkovsky E.M. and Shejkovsky D.A.)	8	1
Efficiency of melting of electrode wire in submerged-arc surfacing with influence of transverse magnetic field (Razmyshlyayev A.D., Mironova M.V., Kuzmenko K.G. and Vydmysh P.A.)	9	5
Electron beam welding in production of steel-aluminium joints of transition pieces of dissimilar metals (Bondarev A.A., Nesterenkov V.M. and Arkhangelsky Yu.A.)	6	7
Electron beam welding of bodies of drill bits with modifying of weld metal by zirconium (Nesterenkov V.M., Bondarev A.A., Arkhangelsky Yu.A. and Zagornikov V.I.)	2	9
Electron beam welding of measuring chamber of magnetic pneumatic gas analyser (Nesterenkov V.M. and Kravchuk L.A.)	5	10
Electron beam welding of thin-sheet three-dimensional structures of aluminium alloys (Bondarev A.A. and Nesterenkov V.M.)	5	6
Evaluation of stability of the flashing process in flash butt welding (Skachkov I.O. and Chvertko E.P.)	11	3
Experience of manufacture and application of seamless flux-cored wire for electric arc welding (Shlepakov V.N. and Kotelchuk A.S.)	2	2
Flux-cored wires of FMI series for coating deposition by electric arc spraying (Review) (Pokhmursky V.I., Student M.M., Gvozdetsky V.M. and Pokhmurskaya A.V.)	4	9
Improvement of the quality of welded assembly for branch-pipe cutting into the wall of oil storage tank (Barvinko A.Yu. and Barvinko Yu.P.)	1	3
Influence of preliminary cyclic loading on effectiveness of welded joint strengthening by high-frequency peening (Knysh V.V., Solovej S.A. and Kuzmenko A.Z.)	12	10
Influence of surface strengthening and argon-arc treatment on fatigue of welded joints of structures of metallurgical production (Kolomijtsev E.V. and Serenko A.N.)	7	4
Influence of welding power sources on three-phase mains (Rymar S.V., Zhernosekov A.M. and Sydorets V.N.)	2	10
Laser based girth welding technologies for pipeline construction (Keitel S. and Neubert J.)	2	2
Laser welding of thin-sheet stainless steel (Shelyagin V.D., Lukashenko A.G., Lukashenko D.A., Bernatsky A.V., Garashchuk V.P. and Lutsenko V.I.)	2	4

Level of effect of preparation and assembly for welding on quality of welded joints for industrial pipelines (Zankovets P.V.)

Limitation of overvoltages in high-voltage circuits after discharges in welding gun (Nazarenko O.K. and Matvejchuk V.A.)

Manufacture of outstanding thick-walled constructions (Engindeniz E., Kaplan E., Ganioglu E., Yuksel F., Bayezid N. and Rosert R.)

Method for estimation of welding properties of power sources for arc welding (Shevchenko N.V., Skachkov I.O. and Ponomarev V.E.)

Modern market of welding equipment and materials (Makovetskaya O.K.)

Organization and topics of R&D in the field of joining technologies conducted by TWI and DVS Association of Researchers (Review) (Makovetskaya O.K.)

Selection of the groove shape for repair of through cracks by multilayer electroslag welding (Kozulin S.M.)

Shielding materials and personal gear for welder protection from magnetic fields (Levchenko O.G., Levchuk V.K. and Timoshenko O.N.)

Single- and multioperator systems for automatic welding of position butt joints of nuclear power plant piping (Makhlin N.M., Korotynsky A.E., Bogdanovsky V.A., Omelchenko I.A. and Sviridenko A.A.)

State-of-the-art and prospects of market of steel and welding equipment in China (Review) (Makovetskaya O.K.)

State-of-the-art of development and manufacture of low-hydrogen electrodes with double-layer coating in CIS countries (Review) (Marchenko A.E., Skorina N.V. and Kostyuchenko V.P.)

System for automatic regulation of position of tungsten electrode in narrow-gap magnetically controlled arc welding of titanium (Belous V.Yu. and Akhonin S.V.)

Transformable structures (Review) (Paton B.E., Lobanov L.M. and Volkov V.S.)

Technological capabilities for improvement of reliability of welded joints on aluminium-lithium alloys (Labur T.M.)

Technological peculiarities of cladding of high alloys (Bartenev I.A.)

To 130th anniversary of the first method of arc electric welding

Two-layer bio-cermet titanium-hydroxyapatite coating (Yushchenko K.A., Borisov Yu.S., Vojnarovich S.G., Kislitsa A.N. and Kuzmich-Yanchuk E.K.)

Welded electric contacts of dissimilar conductors (Paton B.E., Lakomsky V.I. and Braginets V.I.)

Welding fume – factors of influence, physical properties and methods of analysis (Review) (Pokhodnya I.K., Yavdoshchin I.R. and Gubenya I.P.)

Ways of increasing the technological efficiency of rectifiers for mechanized welding and surfacing (Review) (Zaruba I.I., Andreev V.V., Stepakhno V.I. and Koritsky V.A.)

INFORMATION

Abstracts of works on innovation projects of the NAS of Ukraine

Flash-butt welding of rod reinforcement in reconstruction of Olympic NSC (Kiev)

NEWS

Branch meeting-conference «Status and Main Directions of Development of Welding Production in OJSC «Gazprom»

5th International Seminar «New research areas in the field of welding live soft tissues»

First Meeting of Council of Chinese-Ukrainian E.O. Paton Welding Institute

Foundation of the E.O. Paton Chinese-Ukrainian Welding Institute

Industrial Exhibition «Paton Expo-2011»

International Conference «Surface Engineering and Renovation of Parts»

International Conference «Titanium-2011 in CIS»

International Specialized Exhibition «Welding, Cutting, Surfacing»

Laser Technology Conference in Ukraine

News

Plasma-arc welding of large-sized products from carbon materials to metals

Report-and-Election Conference of the Ukrainian Welding Society

Seminar of the Society of Welders of Ukraine

Technical Seminar on Welding Consumables

The 3rd Paton Readings-2010

Ukrainian-Polish Scientific-Technical Conference

SCIENTIFIC AND TECHNICAL

Admissible pressure for filler of sealed sleeves used to repair main pipelines (Makhnenko V.I., Velikoivanenko E.A., Milenin A.S., Olejnik O.I., Rozyinka G.F. and Pivtorak N.I.)

Analysis of spectrum of the welding arc light for monitoring of arc welding (Review) (Lazorenko Ya.P., Shapovalov E.V. and Kolyada V.A.)

Application of nanopowders of metals in diffusion welding of dissimilar materials (Lyushinsky A.V.)

Application of nanostructured interlayers in joints of difficult-to-weld aluminium-base materials (Review) (Ishchenko D.A.)

Assessment of deformability of pipe steel joints made by automatic continuous flash-butt welding (Kuchuk-Yatsenko S.I., Kyrian V.I., Kazymov B.I. and Khomenko V.I.)

Cause of secondary hardening in Cr–Mo–V weld metal during long-term heat exposure (Mohyla P., Hlavaty I. and Tomcik P.)

¹³⁷Cs and ⁹⁰Sr phase transitions in surfacing of radioactively contaminated metal structures (Ennan A.A., Kiro S.A., Oprya M.V., Khan V.E., Ogorodnikov B.I., Krasnov V.A., A. de Meyer-Vorobets, Darchuk L. and Horemence B.)

Comparative evaluation of sensitivity of welded joints on alloy Inconel 690 to hot cracking (Yushchenko K.A., Savchenko V.S., Chervyakov N.O., Zvyagintseva A.V., Monko G.G. and Pestov V.A.)

Concentrations of carbon oxide and nitrogen dioxide in air of a working zone in covered-electrode welding (Levchenko O.G., Lukianenko A.O. and Polukarov Yu.O.)	1	Experimental evaluation of δ_{1c} -curve temperature shift and brittle-tough transition of structural steels and welded joints by the results of standard tests (Dyadin V.P. and Yurko L.Ya.)	2
Conditions for formation of defect-free welds in narrow-gap magnetically controlled arc welding of low titanium alloys (Belous V.Yu.)	3	Experimental investigation of hot cracking susceptibility of wrought aluminum alloys (Kah P., Hiltunen E. and Martikainen J.)	9
Conditions of propagation of the SHS reaction front in nanolayered foils in contact with heat-conducting material (Zaporozhets T.V., Gusak A.M. and Ustinov A.I.)	8	Features of formation of dissimilar metal joints in hot roll welding in vacuum (Neklyudov I.M., Bortz B.V. and Tkachenko V.I.)	8
Control of properties of the weld metal by regulating the level of oxidation of the weld pool in gas-shielded welding (Rimsky S.T.)	12	Flash-butt welding of high-temperature nickel alloy using nano-structured foils (Kuchuk-Yatsenko V.S.)	11
Damping of welding current fluctuations in robotic arc welding (Tsybulkin G.A.)	7	Force effect on welded surfaces initiated by running of SHS reaction in nanolayered interlayer (Velikoivanenko E.A., Ustinov A.I., Kharchenko G.K., Falchenko Yu.V., Petrushinets L.V. and Rozyinka G.F.)	7
Deformations of welded joints in multilayer electroslag welding (Kozulin S.M. and Lychko I.I.)	1	Forecasting the content of σ -phase in the HAZ of welded joints of duplex steels in arc welding (Makhnenko V.I., Kozlitina S.S. and Dzyubak L.I.)	6
Deposition of titanium-based graded coatings by laser cladding (Narva V.K. and Marants A.V.)	4	Formation of liquid metal film at the tip of wire-anode in plasma-arc spraying (Kharlamov M.Yu., Krivtsun I.V., Korzhik V.N. and Petrov S.V.)	12
Detachability of slag crust in arc welding (Review). Part 1. Mechanism of chemical adhesion of slag crust to weld metal (Moravetsky S.I.)	1	Formation of narrow-gap welded joints on titanium using the controlling magnetic field (Belous V.Yu. and Akhonin S.V.)	4
Detachability of slag crust in arc welding (Review). Part 2. Character of the effect of main factors on detachability of slag crust (Moravetsky S.I.)	2	Fracture surface morphology at fatigue of MIG-welded joints of AMg6 alloy (Labur T.M., Shonin V.A., Taranova T.G., Kostin V.A., Mashin V.S. and Klochkov I.N.)	3
Development of a procedure for selection of parameters of strip electrode surfacing with mechanical forced transfer of liquid metal (Nosovsky B.I. and Lavrova E.V.)	3	Friction stir welding of composite, granulated and quasi-crystalline aluminium alloys (Poklyatsky A.G., Ishchenko A.Ya. and Fedorchuk V.E.)	7
Development of flux-cored wire for arc welding of high-strength steel of bainite class (Shlepakov V.N., Gavrilyuk Yu.A. and Naumejko S.M.)	11	Heating and melting of anode wire in plasma arc spraying (Kharlamov M.Yu., Krivtsun I.V., Korzhik V.N. and Petrov S.V.)	5
Development of the technology and equipment for laser and laser-arc welding of aluminium alloys (Turichin G.A., Tsybulsky I.A., Zemlyakov E.V., Valdajtseva E.A. and Kuznetsov M.V.)	9	Hydrogen behaviour in repair welding of the main pipelines under pressure (Makhnenko V.I., Olejnik O.I. and Paltsevich A.P.)	9
Diffusion bonding of γ -TiAl base alloy in vacuum by using nanolayered interlayers (Kharchenko G.K., Ustinov A.I., Falchenko Yu.V., Muravejnik A.N., Melnichenko T.V. and Petrushinets L.V.)	3	Hygroscopicity of high-basicity synthetic flux (Moravetsky S.I.)	12
Effect of alloying of the welds on structure and properties of welded joints on steel 17Kh2M (Markashova L.I., Poznyakov V.D., Alekseenko T.A., Berdnikova E.N., Zhdanov S.L., Kushnaryova O.S. and Maksimenko A.A.)	4	Indicators of stability of the GMAW process (Lankin Yu.N.)	1
Effect of ductile sub-layer on heat resistance of multilayer deposited metal (Ryabtsev I.A., Babinets A.A. and Ryabtsev I.I.)	10	Induction system for local treatment of surfaces by liquid metal flows (Pismenny A.S., Baglaj V.M., Pismenny A.A. and Rymar S.V.)	6
Effect of low-frequency resonance oscillations on structure and crack resistance of deposited high-chromium cast iron (Tyurin Yu.N., Kuskov Yu.M., Markashova L.I., Chernyak Ya.P., Berdnikova E.N., Popko V.I., Kashnaryova O.S. and Alekseenko T.A.)	2	Influence of repeated loading on the efficiency of electrodynamic treatment of aluminium alloy AMg6 and its welded joints (Lobanov L.M., Pashchin N.A., Loginov V.P. and Mikhoduj O.L.)	4
Effect of single-phase power sources of welding arc on electric mains (Rymar S.V., Zhernosekov A.M. and Sidoretz V.N.)	12	Influence of technological factors on resistance to delayed fracture of butt joints of rail steel in arc welding (Poznyakov V.D., Kiriakov V.M., Gajvoronsky A.A., Kasatkin S.B., Klapatyuk A.V., Taranenko S.D. and Proshchenko V.A.)	11
Electric arc spraying of cermet and metal-glass coatings (Karpechenko A.A.)	4	In-process quality control of welded panels of alloy VT20 using method of electron shearography (Lobanov L.M., Pivtorak V.A., Savitskaya E.M., Kiyanyets I.V. and Lysak V.V.)	11
Electron beam welding of heat exchangers with single or double refraction of the electron beam (Kravchuk L.A., Zagornikov V.I. and Kuleshov I.A.)	1	Investigation of thermochemical characteristics of mixtures of dispersed materials by differential thermal analysis methods (Shlepakov V.N. and Kotelchuk A.S.)	12

Methods for assessment of strengthening of HSLA steel weld metal (Kostin V.A., Golovko V.V. and Grigorenko G.M.)	10	Properties and structure of circumferential joints of tubes made by orbital electron beam welding (Ternovoj E.G., Shulym V.F., Bulatsev A.R., Solomijchuk T.G. and Kostin V.A.)	1
Monitoring of corrosion of pipelines of cooling system of automobile gas-filling compressor stations (Osadchuk S.A., Kotlyar O.V., Nyrkova L.I. and Polyakov S.G.)	3	Properties of iron-base alloys for plasma powder hard-facing of sealing surfaces of fittings (Pereplyotchikov E.F. and Ryabtsev I.A.)	9
On the subject of electric submerged-arc welding (Kuzmenko V.G.)	5	Resistance of welds on thin-sheet aluminium alloys to initiation and propagation of service cracks (Poklyatsky A.G.)	10
Optimization of conditions of reduction heat treatment of blades of alloy KhN65VMTYu after long-term service (Tarasenko Yu.P., Berdnik O.B. and Tsaryova I.N.)	9	Role of non-metallic inclusions in cracking during arc cladding (Kuskov Yu.M., Novikova D.P. and Bogajchuk I.L.)	10
Optimisation of the process of strengthening of welded joints of 09G2S steel by high-frequency mechanical peening (Knysh V.V., Solovej S.A. and Bogajchuk I.L.)	5	Simulation of electric circuit as a stage in development of power source with controllable shape of alternating current (Andreev V.V., Efremenko E.M. and Moskovich G.N.)	2
Particle dispersity and manganese valence in welding aerosol (Pokhodnya I.K., Karmanov V.I., Yavdoshchin I.R., Gubnya I.P., Khizhun O.Yu. and Khobta I.V.)	9	Simulation of the effect of high-voltage cables on current ripple in welding guns with automatic bias (Nazarenko O.K., Matvejchuk V.A. and Galushka V.V.)	5
Peculiarities of formation of structure in the transition zone of the Cu-Ta joint made by explosion welding (Grinberg B.A., Elkina O.A., Antonova O.V., Inozemtsev A.V., Ivanov M.A., Rybin V.V. and Kozhevnikov V.E.)	7	Strength and features of fracture of welded joints on high-strength aluminium alloys at low temperature (Labur T.M.)	5
Peculiarities of influence of defects in cast billets of steel 110G13L on mechanical properties of joints during flash-butt welding (Kuchuk-Yatsenko S.I., Shvets Yu.V., Kavunichenko A.V., Shvets V.I., Taranenko S.D. and Proshchenko V.A.)	6	Studying the features of mass transfer in the process of friction stir welding using physical modelling (Poklyatsky A.G.)	6
Peculiarities of intergranular mass transfer of gallium in aluminium alloy during solid phase activation of surfaces being joined (Khokhlova Yu.A., Fedorchuk V.E. and Khokhlov M.A.)	3	Wear- and heat resistance of deposited metal of graphitized steel type (Ryabtsev I.A., Kondratiev I.A., Osin V.V. and Gordan G.N.)	8
Peculiarities of resistance welding of copper with aluminium alloys using nanostructured foil of Al-Cu system (Kuchuk-Yatsenko V.S.)	5	WELDING FACULTY of PSTU is 40	
Peculiarities of temperature distribution in thin-sheet aluminium alloy AMg5M in friction stir welding (Poklyatsky A.G.)	8	Effect of manganese on structure and wear resistance of deposited metal of the low-carbon steel type (Malinov V.L.)	8
Peculiarities of the influence of complex alloying on structure formation and mechanical properties of welds on low-alloyed high-strength steels (Golovko V.V., Kostin V.A. and Grigorenko G.M.)	7	Influence of hardfacing technology and heat treatment on structure and properties of metal deposited on carbon steel by LN-02Kh25N22AG4M2 strip electrode (Ivanov V.P. and Ivashchenko V.Yu.)	8
Peculiarities of thermal spraying of coatings using flux-cored wire (Review) (Wielage B., Rupprecht C. and Pokhmurska H.)	10	Modification of medium-chromium deposited metal (Stepnov K.K., Matvienko V.N. and Oldakovsky A.I.)	8
Prediction of thermodynamic properties of melts of MgO-Al ₂ O ₃ -SiO ₂ -CaF ₂ system (Goncharov I.A., Galinich V.I., Mishchenko D.D., Shevchenko M.A. and Sudavtsova V.S.)	10	Specialist training at PSTU Welding Faculty (Gulakov S.V. and Shaferovsky V.A.)	8
		Structure and properties of deposited wear-resistant Fe-Cr-Mn steel with a controllable content of metastable austenite (Chejlyakh Ya.A. and Chigarev V.V.)	8
		To the 65th Anniversary of the welding equipment and technology chair of the Priazovsky State Technical University (Royanov V.A.)	8
		Index of articles for TPWJ'2011, Nos. 1-12	12
		List of authors	12

LIST OF AUTHORS

Akhonin S.V. No.4, 6, 7
Alekseenko T.A. No.2, 4
Andreev V.V. No.2, 6, 11
Antonova O.V. No.7
Arkhangelsky Yu.A. No.7, 9

Babinets A.A. No.10
Baglaj V.M. No.6
Bakumtsev N.I. No.1
Banakhevich Yu.V. No.7
Bartenev I.A. No.5
Barvinko A.Yu. No.3
Barvinko Yu.P. No.3
Bayezid N. No.5
Belous V.Yu. No.3, 4, 7
Berdnik O.B. No.9
Berdnikova E.N. No.2, 4
Bernatsky A.V. No.4
Blintsov V.S. No.9
Bogajchuk I.L. No.5, 10
Bogdanovsky V.A. No.11, 12
Bondarev A.A. No.6, 7, 9
Borisov Yu.S. No.12
Bortz B.V. No.8
Braginets V.I. No.9
Burlaka V.V. No.2
Bulatsev A.R. No.1

Chejlyakh Ya.A. No.8
Cherednik A.D. No.12
Chernyak Ya.P. No.2
Chervyakov N.O. No.11
Chigarev V.V. No.8
Chvertko E.P. No.3

Darchuk L. No.7
Demchenko E.L. No.2
Didkovsky A.V. No.8
Dmitrienko R.I. No.7
Dobrushin L.D. No.5
Dyadin V.P. No.2
Dzyubak L.I. No.6

Efremenko E.M. No.2
Egorov G.V. No.9
Elagin V.P. No.2
Elkina O.A. No.7
Engindeniz E. No.5
Ennan A.A. No.7

Fadeenko Yu.I. No.5
Falchenko Yu.V. No.3, 7
Fedorchuk V.E. No.3, 7
Folbort O.I. No.1

Gajvoronsky A.A. No.11
Galinich V.I. No.10

Galushka V.V. No.5
Galyshev A.A. No.1
Ganioglu E. No.5
Gapula N.A. No.7
Garashchuk V.P. No.4
Garf E.F. No.7
Gavrilyuk Yu.A. No.11
Gavva V.M. No.12
Golovko V.V. No.7, 10
Goncharov I.A. No.10
Gordan G.N. No.8
Grigorenko G.M. No.7, 10
Grinberg B.A. No.7
Gubnya I.P. No.6, 9
Gulakov S.V. No.2, 8
Gusak A.M. No.8
Gvozdetsky V.M. No.9

Hiltunen E. No.9
Hlavaty I. No.2
Horemence B. No.7

Ilyushenko V.M. No.1
Inozemtsev A.V. No.7
Ishchenko A.Ya. No.7
Ishchenko D.A. No.4
Ivanov M.A. No.7
Ivanov V.P. No.8
Ivanova O.N. No.1
Ivashchenko V.Yu. No.8

Kah P. No.9
Kajdalov A.A. No.8
Kaplan E. No.5
Karmanov V.I. No.9
Karpechenko A.A. No.4
Kasatkin S.B. No.11
Kashnaryova O.S. No.2
Kavunichenko A.V. No.6
Kazymov B.I. No.2
Keitel S. No.2
Khabuzov V.A. No.1
Khan V.E. No.7
Kharchenko G.K. No.3, 7
Kharlamov M.Yu. No.5, 12
Khizhun O.Yu. No.9
Khobta I.V. No.9
Khokhlov M.A. No.3
Khokhlova Yu.A. No.3
Khomenko V.I. No.2
Kiriakov V.M. No.11
Kiro S.A. No.7
Kislitsa A.N. No.12
Kislitsyn V.M. No.1
Kiyans I.V. No.11
Klapatyuk A.V. No.11

Klimenko S.A. No.7
Klochkov I.N. No.3
Knysh V.V. No.5, 10
Kolomijtsev E.V. No.4
Kolyada V.A. No.11(2)
Kondratiev I.A. No.8
Kopeikina M.Yu. No.7
Kopylov L.N. No.4
Koritsky A.V. No.6
Koritsky V.A. No.11
Kornienko A.N. No.5
Korotynsky A.E. No.11
Korzhih V.N. No.5, 9(2), 12
Koshkin K.V. No.9
Kostin V.A. No.1, 3, 7, 10
Kostyuchenko V.P. No.1
Kotelchuk A.S. No.2, 12
Kotlyar O.V. No.3
Kovalenko V.S. No.7
Kovalyuk A.V. No.12
Kozhevnikov V.E. No.7
Kozlitina S.S. No.6
Kozulin S.M. No.1, 3
Krasnov V.A. No.7
Kravchuk L.A. No.1, 10
Krivchikov S.Yu. No.8
Krivtsun I.V. No.5, 9, 12
Kuchuk-Yatsenko S.I. No.2, 6
Kuchuk-Yatsenko V.S. No.5, 11
Kudryashev V.B. No.12
Kuleshov I.A. No.1
Kulik V.M. No.2
Kulikov A.P. No.12
Kunkin D.D. No.1
Kushnaryova O.S. No.4
Kuskov Yu.M. No.2, 10
Kuzmenko A.Z. No.10
Kuzmenko K.G. No.5
Kuzmenko V.G. No.5
Kuzmich-Yanchuk E.K. No.12
Kuznetsov M.V. No.9
Kvasnitsky V.F. No.9
Kyrian V.I. No.1, 2

Labur T.M. No.3, 4, 5
Lakomsky V.I. No.9
Lankin Yu.N. No.1, 3
Lavrova E.V. No.3
Lazorenko Ya.P. No.11
Lebedev V.A. No.1
Levchenko O.G. No.1, 2, 3
Levchuk V.K. No.3
Lipodaev V.N. No.6(2), 7, 8
Lobanov L.M. No.4, 11, 12
Loginov V.P. No.4
Lukashenko A.G. No.4
Lukashenko D.A. No.4
Lukianenko A.O. No.1, 2
Lutsenko V.I. No.4
Lychko I.I. No.1
Lysak V.V. No.11

Lyushinsky A.V. No.5

Makhlin N.M. No.11, 12
Makhnenko V.I. No.6, 8, 9
Makovetskaya O.K. No.6, 11, 12
Maksimenko A.A. No.4, 6
Maksimov S.Yu. No.1
Malinov V.L. No.8
Marants A.V. No.4
Marchenko A.E. No.1
Markashova L.I. No.2, 4
Martikainen J. No.9
Mashin V.S. No.3
Matvejchuk V.A. No.5, 10
Matvienko V.N. No.8
Melnichenko T.V. No.3
Melnichuk S.L. No.7
de Meyer-Vorobets A. No.7
Mikhoduj O.L. No.4
Mikitin Ya.M. No.8
Milenin A.S. No.8
Mironova M.V. No.5
Mishchenko D.D. No.10
Mohyla P. No.2
Monko G.G. No.11
Moravetsky S.I. No.1, 2, 12
Moskalenko A.A. No.3
Moskovich G.N. No.2
Muravejnik A.N. No.3

Narva V.K. No.4
Naumejko S.M. No.11
Nazarenko O.K. No.5, 10
Nekhotyashchy V.A. No.7
Neklyudov I.M. No.8
Nekrasov V.A. No.9
Nesterenkov V.M. No.6, 7, 9, 10
Neubert J. No.2
Nosovsky B.I. No.3
Novikova D.P. No.10
Nyrkova L.I. No.3, 7

Ogorodnikov B.I. No.7
Oldakovsky A.I. No.8
Olejnik I.N. No.7
Olejnik O.I. No.8, 9
Omelchenko I.A. No.11
Oprya M.V. No.7
Osadchuk S.A. No.3, 7
Osin V.V. No.8

Paltsevich A.P. No.9
Pashchin N.A. No.4
Paton B.E. No.9, 12
Pentegov I.V. No.1
Pereplyotchikov E.F. No.9
Pestov V.A. No.11
Petrov S.V. No.5, 12
Petrushinets L.V. No.3, 7
Pismenny A.A. No.6
Pismenny A.S. No.1, 6
Pivtorak N.I. No.8

Pivtorak V.A. No.11
Pokhmurska H. No.10
Pokhmurskaya A.V. No.9
Pokhmursky V.I. No.9
Pokhodnya I.K. No.6, 9
Poklyatsky A.G. No.6, 7, 8, 10
Polukarov Yu.O. No.1
Polyakov S.G. No.3, 7
Ponomarev V.E. No.4
Popko V.I. No.2
Poznyakov V.D. No.4, 6, 11
Proshchenko V.A. No.6, 11

Razmyshlyayev A.D. No.5
Rimsky S.T. No.12
Rosert R. No.5
Royanov V.A. No.8
Rozyinka G.F. No.7, 8
Rupprecht C. No.10
Ryabtsev I.A. No.8(2), 9, 10
Ryabtsev I.I. No.10
Rybin V.V. No.7
Rymar S.V. No.6, 10, 12
Ryzhkov S.S. No.9

Savchenko V.S. No.11
Savenko A.V. No.7
Savitskaya E.M. No.11
Savitsky M.M. No.2
Savitsky V.V. No.2
Semikin V.F. No.3
Serenko A.N. No.4
Sevryukov V.V. No.9
Shaferovsky V.A. No.8
Shapovalov E.V. No.11
Shejkovsky D.A. No.1
Shelyagin V.D. No.4
Shevchenko M.A. No.10
Shevchenko N.V. No.4
Shlensky P.S. No.5
Shlepakov V.N. No.2, 10, 11, 12
Shonin V.A. No.3
Shulym V.F. No.1
Shvets V.I. No.6
Shvets Yu.V. No.6
Sidorets V.N. No.12
Sineok A.G. No.6
Skachkov I.O. No.3, 4
Skorina N.V. No.1
Solomijchuk T.G. No.1
Solonichenko Yu.V. No.9

Solovej S.A. No.5, 10
Stemkovsky E.M. No.1
Stepakhno V.I. No.4, 11
Stepnov K.K. No.8
Student M.M. No.9
Sudavtsova V.S. No.10
Sviridenko A.A. No.11
Sydorets V.N. No.10

Taranenko S.D. No.6, 11
Taranova T.G. No.3
Tarasenko Yu.P. No.9
Ternovoj E.G. No.1
Timoshenko O.N. No.3
Tkachenko A.V. No.12
Tkachenko V.I. No.8
Tomcik P. No.2
Tsaryova I.N. No.9
Tsybulkin G.A. No.7
Tsybulsky I.A. No.9
Turichin G.A. No.9
Tyukalov V.G. No.3
Tyurin Yu.N. No.2

Ustinov A.I. No.3, 7, 8

Valdajtseva E.A. No.9
Velikoivanenko E.A. No.7, 8
Ventsev S.D. No.5
Vladimirov A.V. No.1
Vojnarovich S.G. No.12
Volkov V.S. No.12
Vydmysh P.A. No.5

Wielage B. No.10

Yavdoshchin I.R. No.1, 6, 9
Yuksel F. No.5
Yurko L.Ya. No.2
Yushchenko K.A. No.11, 12

Zagornikov V.I. No.1, 9
Zankovets P.V. No.6
Zaporozhets T.V. No.8
Zaruba I.I. No.11
Zelenchenok G.S. No.4
Zemlyakov E.V. No.9
Zhdanov S.L. No.4, 6
Zhernosekov A.M. No.10, 12
Zhukov Yu.D. No.9
Zvyagintseva A.V. No.11
Zyakhor I.V. No.5

SUBSCRIPTION FOR «THE PATON WELDING JOURNAL»

If You are interested in making subscription directly via Editorial Board, fill, please, the coupon and send application by fax or e-mail.

The cost of annual subscription via Editorial Board is \$324.

Telephones and faxes of Editorial Board of «The Paton Welding Journal»:

Tel.: (38044) 200 82 77, 200 81 45

Fax: (38044) 200 82 77, 200 81 45.

«The Paton Welding Journal» can be also subscribed worldwide from catalogues of subscription agency EBSO.

SUBSCRIPTION COUPON	
Address for journal delivery	_____
Term of subscription since	20 till 20
Name, initials	_____
Affiliation	_____
Position	_____
Tel., Fax, E-mail	_____

Subscription to the electronic version of «The Paton Welding Journal»
can be done at site: www.rucont.ru



We offer for the subscription all issues of the Journal in pdf format, starting from 2009. You can subscribe to individual issues or to the entire archive including all issues over a period of 2009–2011. The subscription is available for natural persons and legal entities.



ADVERTISEMENT IN «THE PATON WELDING JOURNAL»

External cover, fully-colored:

First page of cover (190×190 mm) – \$700
Second page of cover (200×290 mm) – \$550
Third page of cover (200×290 mm) – \$500
Fourth page of cover (200×290 mm) – \$600

Internal cover, fully-colored:

First page of cover (200×290 mm) – \$350
Second page of cover (200×290 mm) – \$350
Third page of cover (200×290 mm) – \$350
Fourth page of cover (200×290 mm) – \$350

Internal insert:

Fully-colored (200×290 mm) – \$300
Fully-colored (double page A3) (400×290 mm) – \$500
Fully-colored (200×145 mm) – \$150
Black-and-white (170×250 mm) – \$80
Black-and-white (170×125 mm) – \$50
Black-and-white (80×80 mm) – \$15

- Article in the form of advertising is 50 % of the cost of advertising area
- When the sum of advertising contracts exceeds \$1000, a flexible system of discounts is envisaged

Technical requirement for the advertising materials:

- Size of journal after cutting is 200×290 mm
- In advertising layouts, the texts, logotypes and other elements should be located 5 mm from the module edge to prevent the loss of a part of information

All files in format IBM PC:

- Corell Draw, version up to 10.0
- Adobe Photoshop, version up to 7.0
- Quark, version up to 5.0
- Representations in format TIFF, color model CMYK, resolution 300 dpi
- Files should be added with a printed copy (makeups in WORD for are not accepted)